THE UNIVERSITY
of EDINBURGH

Growth influences the single cell variability of the DNA damage response in *Escherichia coli*

Sebastián Jaramillo-Riveri

Doctor of Philosophy

School of Biological Sciences
University of Edinburgh

2018

Abstract

The resilience of bacteria depends upon their capacity to proliferate and survive under different conditions, including in the human body where some bacterial infections can be fatal. Many antibiotics used to treat infections cause direct and indirect DNA damage, in particular DNA double-strand breaks, which can lead to bacterial cell death. Bacteria respond to DNA damage by inducing the SOS response, which is an important process in the repair and tolerance of DNA damage. Additional consequences of SOS induction by antibiotic exposure, is the potential increase of mutagenesis, horizontal gene transfer, and tolerance to other antibiotics. Therefore, identifying the factors involved in SOS induction is essential to understanding the dynamics of bacterial infections.

Previous studies have indicated that bacterial susceptibility to DNA damaging agents is dependent on growth conditions, but the mechanisms involved are not well understood. Many physiological changes are associated with growth rate, including DNA replication (a major mechanism leading to DNA damage), and reallocation of resources towards growth-limiting processes, which could impair the capacity of cells to induce the SOS response. In addition, previous reports indicate that SOS expression is variable in single cells, and the effect of growth conditions in variability has not been evaluated.

In order to evaluate how changes in growth conditions influence the SOS response, we have quantified the levels of SOS induction by DNA damage in single cells using *E. coli* as a model organism. Our results show that cells with very high levels of SOS expression are more abundant in slow-growing conditions, that is under spontaneous DNA damage, under damage induced by the antibiotic ciprofloxacin, and under replication-dependent chronic double-strand breaks. We explain these observations as a combination of population dynamics, that contributes to enriching for slow dividing cells (high SOS) in slow-growing populations, and an influence of growth conditions in the variability of SOS induction, possibly because of influences in the DNA-repair process via an unknown mechanism. The population dynamics arguments presented here may be relevant to other antibiotics, and argue to the significance of studying the response to antibiotics in single cells. We believe the observations on variability in SOS-expression may open new avenues for understanding the limiting factors for DNA repair.

Lay Summary

In the past few decades, there has been a rise in the frequency of bacteria resistant to antibiotics, with very worrying implications for the treatment of infections in the near future. Most antibiotics' toxic effect is mediated by disrupting processes essential for bacterial growth and survival, such as DNA replication, indirectly leading to lethal forms of DNA damage.

Bacteria possess dedicated pathways that are activated in stressful conditions such as DNA damage, which help them to repair and tolerate the damage. In addition to adapting to stressful conditions, bacteria can adapt to different nutrient conditions by modulating how much of their internal resources are allocated to growth related processes. These adaptations to nutrient conditions could affect the sensitivity of bacteria to antibiotic stress, as well as their capacity to induce dedicated stress response. These considerations are clinically relevant when comparing bacterial infections in different organs, for example between the human bladder and the gut. Understanding the fundamental principles of how bacteria respond to stress may provide useful insights for the prevention of antibiotic resistance.

In this thesis, we have used the model bacteria *E. coli* to interrogate how the capacity to induce DNA damage stress response depends on growth conditions. We found that under different conditions of DNA damage, cells that induce very high levels of the DNA damage response are enriched in slow growing conditions. We also observed that cells with higher response also slow down in growth and remain in this state for a long time. This results in increasing the probability of observing cells with higher induction in slow-growing conditions, and it partially explains our observations. Furthermore, we provide evidence that the molecular mechanisms involved in the repair of DNA damage may be influenced by growth conditions. This study highlights the relevance of studying how bacteria respond to antibiotics in individual cells.

Acknowledgements

My gratitude to my supervisor Meriem El Karoui, for her guidance and support both in scientifically and personally, as well as the trust she placed in me.

My gratitude to Matthew Scott sharing his knowledge on physiology and gene expression, Vincent Danos for sharing his creativity and curiosity in mathematical modelling, and Teuta Pilizota for critical comments on quantitative biology.

My gratitude to David Leach and the members of his lab, Benura Azeroglu and Elise Darmon, for their help with genetics and molecular biology techniques, and insightful discussions regarding double-strand break repair.

My gratitude to the members of El Karoui lab for their support, help, and great company: Alessia Lepore, Lorna McLaren, Hannah Taylor, Irina Kalita, and Xavier Zaoui. Also, to our visiting students, Aleksandra Jartseva and Karolina Gaebe, who contributed this project and I had the pleasure to supervise.

My gratitude to those whose help was indispensable for implementing the microfluidics setup, in particular to Juan Carlos Arias Castro, Alex McVey, Jean-Baptiste Lugagne, and Lloyd Mitchel.

My gratitude to the many people that have taught and trusted me over the years, specially to Ricardo Santelices, Juan Carlos Letelier, Jorge Soto-Andrade, William R. Cannon, and Vincent Danos.

My gratitude to the support and advice of very good friends: Ricardo Honorato, Alejandro Granados, Philpp Thomas, Guillaume Terradot, and Matthew Deyell.

My gratitude also to my family Giovanna, Alfonso and Tomás, whose company and trust I felt present despite of the distance.

My gratitude specially to Benura Azeroglu, my best friend for her unconditional trust and loving care.

Finally, I would like to thank the Darwin Trust of Edinburgh for funding my degree.

Declaration

I declare that this thesis was composed by myself, that the work contained herein is my own except where explicitly stated otherwise in the text, and that this work has not been submitted for any other degree or professional qualification except as specified.

(*Sebastián Jaramillo-Riveri*)

Table of Contents

List of Figures

List of Tables

Chapter 1

Introduction

1.1 Growth and stress tolerance in bacteria

Bacteria are unicellular organisms that have been around the earth for billions of years. They have colonised almost every possible environmental condition imaginable, within the constraints imposed by physics and chemistry, including humans, where some bacteria cause potentially lethal infectious diseases. The evolutionary success of bacteria is partially explained by their capacity to grow and proliferate, together with their ability to respond favourably to different enviromental conditions. This includes changes in nutrient availability and the perturbation from stressful agents, such antibiotics used in medical treatments. Understanding the fundamental principles of how cellular responses to different environmental conditions influence eachother, may provide relevant understanding on how bacteria respond to antibiotics.

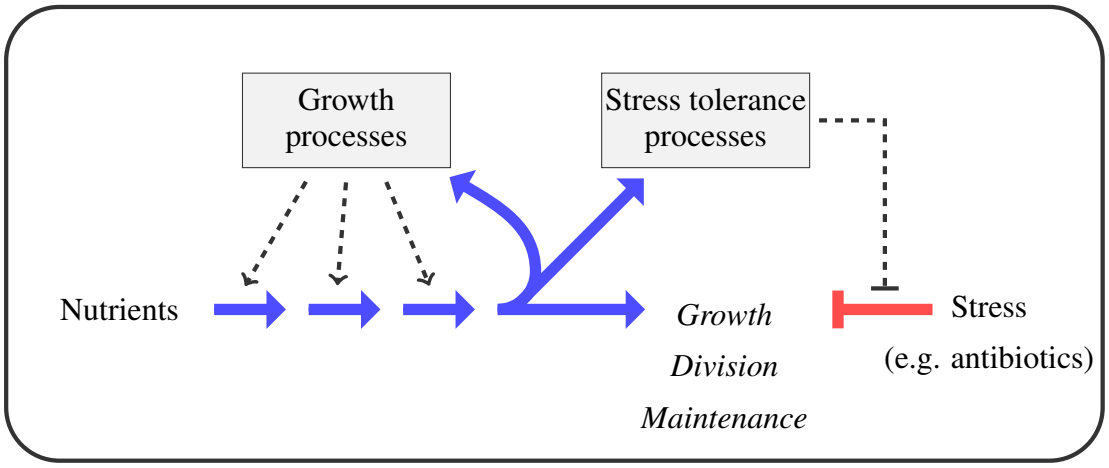

Figure 1.1: **The stability of a cell lineage depends on its capacity to grow and tolerate stress**. Schematic diagram illustrating how populations of bacteria remain stable in time. Nutrients are diverted towards processes that catalyses growth, proliferation, and maintenance of cellular processes. In addition, part of these resources are diverted towards processes whose role is to tolerate stressful conditions, which would otherwise be toxic for growth and maintenance. The overall motivation for this thesis is to evaluate whether the fact that resources are finite within cell leads to trade-offs between growth and stress tolerance.

1.1.1 Cell physiology in a nutshell

Cellular metabolism can be summarised as the spontaneous conversion of relatively high-energy sources into lower-energy molecules and/or heat (Chubukov et al., 2014; von Stockar and Liu, 1999); and in the process synthesise their own constituents, allowing them to grow and reproduce themselves (Maturana and Varela, 1980; Ganti, 2003). The components that catalyse and coordinate these processes are macro-molecules, coupled with high energy carriers like ATP (Demirel, 2014). DNA stores the genetic information for coding RNAs and proteins (Washburn and Gottesman, 2015; Rodnina, 2018), so faithful duplication and segregation of the genome into daughter cells is essential for stability Haeusser and Levin (2008). Coordination of cellular processes is important for cells to proliferate and survive efficiently, and takes place at many levels (Pugatch, 2015). General examples are the coordination of DNA replication with cell division (Bremer and Churchward, 1991; Willis and Huang, 2017), and diverting resources towards rate-limiting processes, such as translation-related processes to support faster cellular growth (Marr, 1991). Coordination of cellular processes needs to be coupled with changes in environmental conditions, which is often achieved by changes in gene expression. Many factors can directly modulate transcription, e.g. transcription factors, influence the stability of RNAs, e.g. small RNAs (Duval et al., 2015; Browning and Busby, 2016; Hui et al., 2014). Combined, these factors permit bacteria to coordinate gene expression in response to environmental perturbations (Guo and Gross, 2014).

1.1.2 Stress responses in bacteria

Several internal and external agents can be toxic for cellular growth, and if the cell does not change their state, its survival can be compromised. Therefore, we find in bacteria molecular mechanism devoted to mitigate or avoid different toxic elements. The molecular pathways devoted to tolerate stress are called stress responses and are classified by their master regulators and stress signals. Examples include the SOS response controlled by the repressor LexA, and triggered by DNA-damage (Kreuzer, 2013); the heat-shock response controlled by the transcription factor RpoH, and triggered by the accumulation of misfolded proteins (Roncarati and Scarlato, 2017); the stringent response controlled by the small molecule ppGpp in response to starvation (Bouveret and Battesti, 2011), the oxidative damage response controlled by OxyR and SoxRS, and

triggered by the accumulation of superoxide radicals (Chiang and Schellhorn, 2012); and the general stress response controlled by the transcription factor RpoS, and triggered by different sources of stress (Battesti et al., 2011). It is worth mentioning that these classifications are useful, but the regulatory targets can overlap, and also some external stress agents may trigger several stress responses.

1.1.3 Antibiotics target growth related processes and cause stress

Antibiotics are natural and synthetic compounds used clinically to treat bacterial infections. The mode of action for most antibiotics is by compromising growth-related processes, and therefore it is not surprising that survival to antibiotics has been linked to the activation of stress responses (Laureti et al., 2013; Mitosch et al., 2017). Antibiotics are classified as: bacteriostatic, if they simply arrest cellular proliferation (e.g. inhibiting translation); or bactericidal if they lead to cell death (e.g. targeting the cell wall, or causing DNA damage). Bactericidal activity is defined by testing whether cells resume growth after removing the antibiotic. Cell death typically occurs from irreversible disruption of cell integrity, such as damage to the cell envelope or irreparable degradation of the chromosome following DNA damage (Kohanski et al., 2010).

As growth processes are common targets for antibiotics, slow growing cells take longer to die under lethal exposure to antibiotics. Thus, a convenient definition is the one of “antibiotic tolerance”, and that that is the rate at which bactericidal antibiotics kills cells (Brauner et al., 2016). Given that populations can be heterogeneous (see subsection 1.1.4), it is possible to find subpopulations with various degree of tolerance, which are referred to as persisters, typically subpopulations of slow-growing cells. Persisters are classified into two categories depending on their origin: type I, if they are stationary cells which have not begun to grow; or type II, if they arise spontaneously from a previously growing cell (Brauner et al., 2016). Given the broad definition of tolerance and persistence, several cellular processes have been shown to be involved, which typically involved reduction of metabolism in single cells, or activation of efflux transporters reducing the internal cellular concentration of antibiotics (multiple drug resistance). (Brauner et al., 2016; Radzikowski et al., 2017; Erickson et al., 2017b). Recently it has been demonstrated that acquisition of mutations with tolerance can accelerate the probability of observing full antibiotic resistance in bacteria populations (Levin-Reisman et al., 2017). Another important contribution to the spread of antibiotic resistance is horizontal gene transfer, which can be enhanced in

some stressful conditions like DNA damage (Baharoglu et al., 2010).

In the past few decades, there has been an increasing rise in the frequency of resistant strains, with very worrying implications for the treatment of infections in the near future (Levy and Marshall, 2004; Andersson and Hughes, 2011). In order to prevent this crisis, part of the strategy is to push the discovery of new antibiotics (Wohlleben et al., 2016), evaluate the use of antibiotics in combination (Chevereau and Bollenbach, 2015), and in the long term, understand the fundamental principles of how bacteria respond to stress and how this impacts on the evolution and spread of resistance.

1.1.4 Single cell variability

Phenomena like antibiotic persistence show that it is important to understand how cells respond to stress at the single cell level. Bulk population measurements can sometimes mask relevant heterogeneity in the physiology of single cells. The concept of bet-hedging is often used to explain the evolutionary benefit of single cell variability (Veening et al., 2008). Indeed, fluctuations in gene expression can be useful in conditions when environments change in time, and can also lead to spontaneous diversification of functions within a population (Kussell, 2013). However in the context of stress responses, selecting against single cell variability may be masked by the fact that sub-populations that respond "optimally" may proliferate more, therefore casting a "selection shadow" (Haldane, 1941; Medawar, 1952) on sub-populations with "sub-optimal" responses[1]. Thus, the prevalence of single cell variability could be explained by bet-hedging in some cases, and more generally by the difficulty of selecting against single cell variability because of a "selection shadow".

Heterogeneous populations are ultimately an unavoidable consequence of fluctuations in the dynamics of chemical processes (Van Kampen, 2007). It is useful to distinguish two main sources of variability in single-cells: one unavoidable resulting from the stochastic fluctuation in molecular kinetics, called "intrinsic noise", and a second component collecting the influence of the extracellular environment and different stages in the cell cycle, called "extrinsic noise" (Thomas, 2019). Intrinsic noise becomes more relevant in cells where relevant molecules are in low numbers. It is worth mentioning that many regulatory species within the cell are relatively low abundant

[1]This argument was taken from a presentation by Thomas Julou from the University of Basel, Switzerland (unpublished)

(Li et al., 2014). Regulatory feedbacks can either amplify or reduce intrinsic noise depending on their configuration (Shinar et al., 2007; Szekely et al., 2013; Ferrell, 2002; Iyer-Biswas and Zilman, 2016).

Efforts to characterise single cells behaviour have been driven by important developments in technical capabilities. In particular advances in microscopy techniques, together with the popularisation of microfluidic devices for controlled growth conditions, with number studies observing the behaviour of single cells (Taheri-Araghi et al., 2015; Rosenthal et al., 2017). A common strategy is the use of fluorescent microscopy to quantify elements of interest; for example, fusing proteins to fluorescent tags where protein levels in single cells can be quantified, or by placing fluorescent protein genes under the transcriptional control of promoters of interest, which allows indirect quantification of expression from such promoters (transcriptional fusions).

1.1.5 *E. coli* as a model organism

Escherichia coli is the best characterised microbial organism. The study of this bacteria began in 1885, with the work of Theodor Escherich characterizing a common bacteria found in the human intestine and soil samples (Friedmann, 2014). The rise of *E. coli* as a model organism can be explained partially by three main observations: i) its relevance to infectious deceases; ii) its fast proliferation and facility to culture in laboratory settings; iii) and because it became the epicentre in discoveries that lead to molecular biology as a discipline. Yet, the *E. coli* classification consists of a fairly diverse group of bacteria with important differences (Touchon et al., 2009). Among *E. coli* model lineages, the best documented are K-12 derivatives (e.g. MG1655), originating from a stool sample collected in 1922 (Bachmann, 1972).

E. coli is common to many warm-blooded animals, particularly in the intestine tract. In human intestines, it has been estimated that *E. coli* comprises about 1% of the microbial biomass (Eckburg et al., 2005). Some *E. coli* variants are harmless for the host (commensal strains), and others can lead to infectious disease (pathogenic strains). *E. coli* is the most common gram-negative bacteria to cause of urinary tract infections, genital infections in women, and neonatal infections (Dubreuil et al., 2016; Bryce et al., 2016). The difference between commensal and pathogenic is due to the production of toxic products (virulence factors) and adaptions that promote colonisation (e.g. outcompeting other bacteria by growth). Similar to other pathogenic bacteria, an increase

in the frequency of *E. coli* strains resistant to antibiotics has been observed during the past few decades, in particular, those targeting cell wall synthesis (β-lactams), and those whose target is to damage DNA (e.g. trimethoprim, and Quinolones).

1.2 DNA damage threatens the stability of cell lineages

The DNA sequence of the chromosome has a crucial role in the stability of cell lineages over successive generations. Therefore, failures in its faithful replication or in its segregation to daughter cells can have lethal consequences. Through evolution, bacteria have acquired specialised molecular mechanisms to repair DNA lesions. These are dedicated enzymes operating on DNA, whose role is to restore the DNA sequence to its original state or mitigate the toxic effects from DNA damage. DNA is a dynamic molecule, constantly being manipulated and probed by different enzymes. The most common internal source of DNA damage arises from conflicts in the DNA manipulating process, in particular when lesions are confronted during DNA replication.

There are many forms of DNA lesions that can be problematic for the survival and proliferation of bacteria, for example chemical modifications of single nucleotides which can block DNA replication (Bichara et al., 2011); loss of a single phosphate bond (called “nick”) and larger discontinuities in the backbone of one strand expanding more than one nucleotide called “single-strand gaps”, which if replicated will lead to the formation of a free double-strand end (Michel et al., 2018). For the purpose of this introduction, we should focus our attention to double-strand breaks, how they can arise spontaneously and by antibiotics, and finally how they can be repaired.

1.2.1 Double-strand breaks can originate from various sources

Double-strand breaks (DSBs) refers to hydrolysis of phosphate bonds in both complementary strands. This type of DNA lesion is particularly problematic to cells for two main reasons. Firstly, DSBs can prevent cells from using DNA sequences as template for DNA and RNA synthesis. Secondly, exposed double-strand ends can be substrate for exonucleases which can lead to degrading part of the chromosome. In *E. coli*, these breaks are repaired by homologous recombination. Less frequent in bacteria is the presence of an additional mechanism for repair called non-homologous end-joining (Rocha et al., 2005). To date, the best estimation for spontaneous frequency of double-strand breaks is from the viability of mutants unable to repair breaks, suggest-

ing approximately a 25% chance of generating a double-strand break per generation (Kuzminov, 1999).

1.2.1.1 DNA replication of DNA lesions can lead to double-strand ends

Conflicts arising from replicating DNA in certain context are the main endogenous source for double-strand ends. These mechanisms can be classified in three main categories. The first and most obvious, is via DNA replication of a region with a nick or a single-strand gap (called "fork collapse"). Unwinding and DNA synthesis of this region will lead the replisome falling from DNA, resulting in the generation of a double-strand end. A second way to generate double-strand ends is via a mechanism called "fork reversal". This process occurs when the replisome becomes stalled, leaving the possibility for the newly-synthesised strands to anneal with each other, forming a double-strand end. This could result from other proteins operating on DNA, for example, RNA polymerase operating in the reverse direction, and/or adducts blocking DNA replication (Michel et al., 2018). A particular case of replication stalling leading to double-strand breaks is called "fork collision". This occurs when two replication forks traveling in the same direction are blocked at the same place, leading to two exposed double-strand ends. Naturally-occurring blockages for replisomes are Tus proteins, which bind specific DNA sequences called *ter* sites. The role of Tus-ter is to prevent DNA replication of one arm proceeding towards the other replicative arm (Bidnenko et al., 2002). Diagrams illustrating these different mechanisms are presented in figure 1.2.

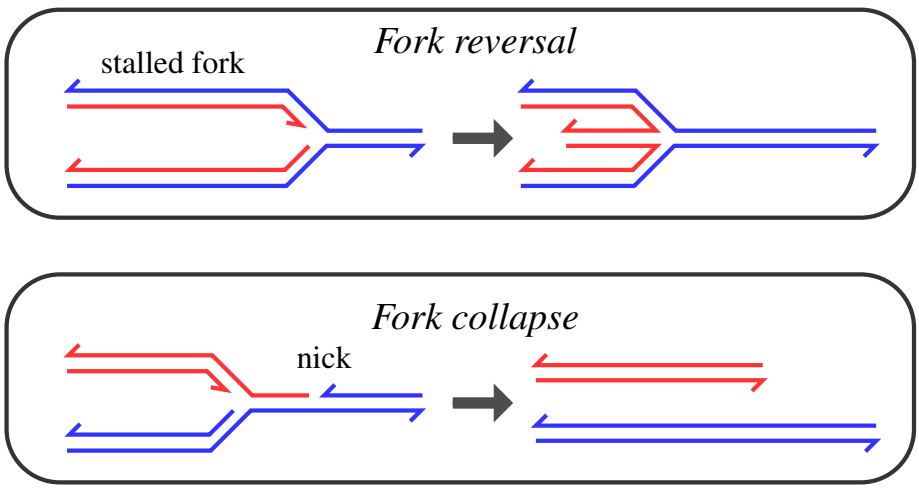

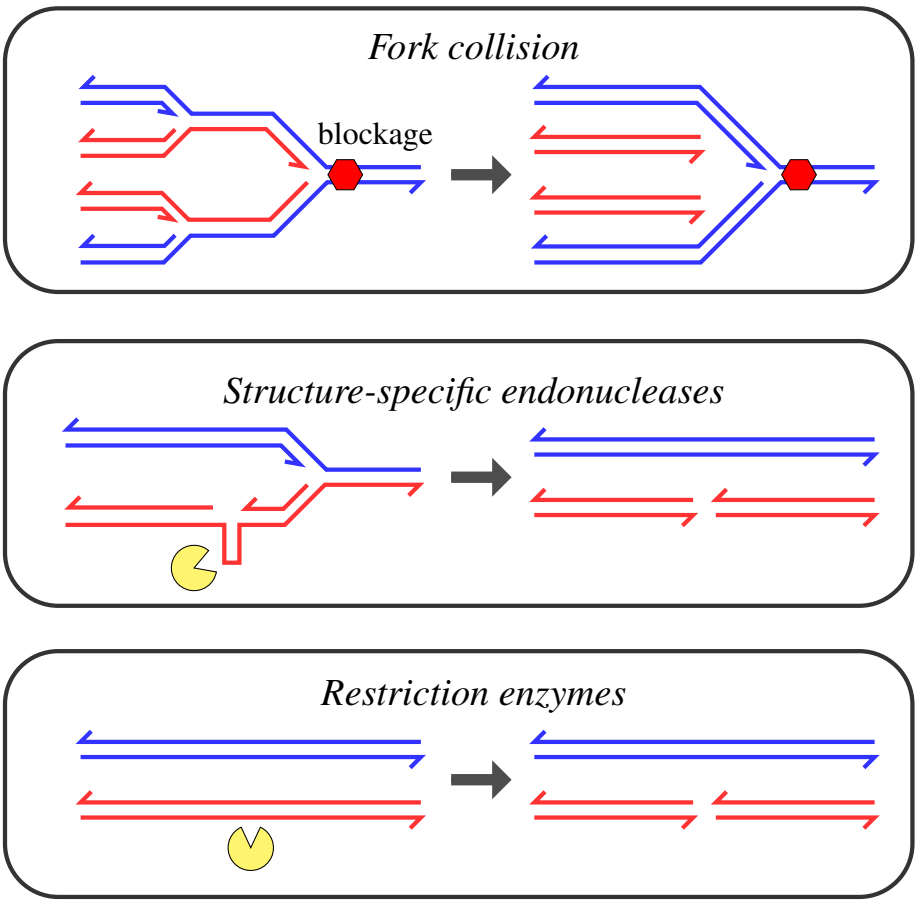

Figure 1.2: **Mechanisms that can lead to double-strand ends**. Double-strand ends can be generated by diverse mechanisms. When progression of the replication fork is interrupted, it can lead to the annealing of newly-synthesised strands forming a double-strand end (fork reversal). When the replication fork encounters a nick, it would naturally lead to a double-strand break (fork collapse). When two replication forks are stalled it is possible for them to fall, leading to two double-strand ends (fork collapse). Special cases are endonuleases that are able to cleave both strands of DNA. Strands that will serve as a template for repair by homologous recombination are in blue. Diagrams were adapted from Michel and Leach (2012).

1.2.1.2 Formation of double-strand breaks by endonucleases

The final and most direct way to generate double-strand breaks is cleavage from endonucleases. Most of the endogenous endonucleases in *E. coli* cleave DNA on one strand (forming a nick), which is unlikely to form a DSB. Some site-specific endonucleases, such as restriction enzymes, are able to cleave both strands. These have

been used to study double-strand breaks in bacteria, by introducing the corresponding recognition site into the genome of *E. coli* (Lesterlin et al., 2014). Another endonuclease that has been used to study double-strand break repair is the SbcCD complex, endogenous to *E. coli*. Instead of recognising a particular sequence, SbcCD cleaves double-stranded DNA in a structure-dependent manner. SbcCD recognises hairpin-like structures cleaving both strands of DNA, leading to a double-strand break (Eykelenboom et al., 2008). Diagrams illustrating these different mechanisms are presented in figure 1.2.

1.2.2 DNA damage induced by antibiotics

1.2.2.1 DNA damage by antibiotics targeting topoisomerases

Quinolones are a class of common antibiotics whose primary target is DNA type II topoisomerases: Gyrase and Topo IV (Drlica et al., 2008; Cheng et al., 2013; Aldred et al., 2014). The function of these enzymes is to relieve positive and negative DNA supercoiling caused by the action of helicases during DNA replication and transcription (Bush et al., 2015). Type II topoisomerases, e.g. Gyrase and Topo IV, are able to bind to DNA and modify its topology by inducing a transient double-strand break (Ashley et al., 2017). Covalent binding to double-strand ends (cleavage complex) prevents the generation of naked double-strand ends during this process. Gyrase and Topo IV differ on their molecular mechanism and preferred supercoiled substrate (Ashley et al., 2017). Gyrase is believed to operate mostly ahead of the replication fork, removing positive super coiling. The activity of Gyrase has been shown to be important in allowing RNA polymerase elongation during transcription (Rovinskiy et al., 2012). Gyrase may not be randomly distributed in the chromosome, but biased towards regions near the origin of replication (Jeong et al., 2004). Topo IV is believed to operate mostly behind the replication fork removing knots that accumulate during DNA synthesis, and decatenating daughter chromosomes at the end of DNA replication (El Sayyed et al., 2016).

Quinolones trap type II topoisomerases on DNA leading directly and indirectly to the formation of double-strand breaks. Quinolone-bound complexes can prevent progression of DNA replication and RNA polymerase, leading to stalled replication forks and fork reversal, and potentially other conflicts (Wentzell and Maxwell, 2000; Pohlhaus and Kreuzer, 2005). There is additional evidence suggesting DSBs may be

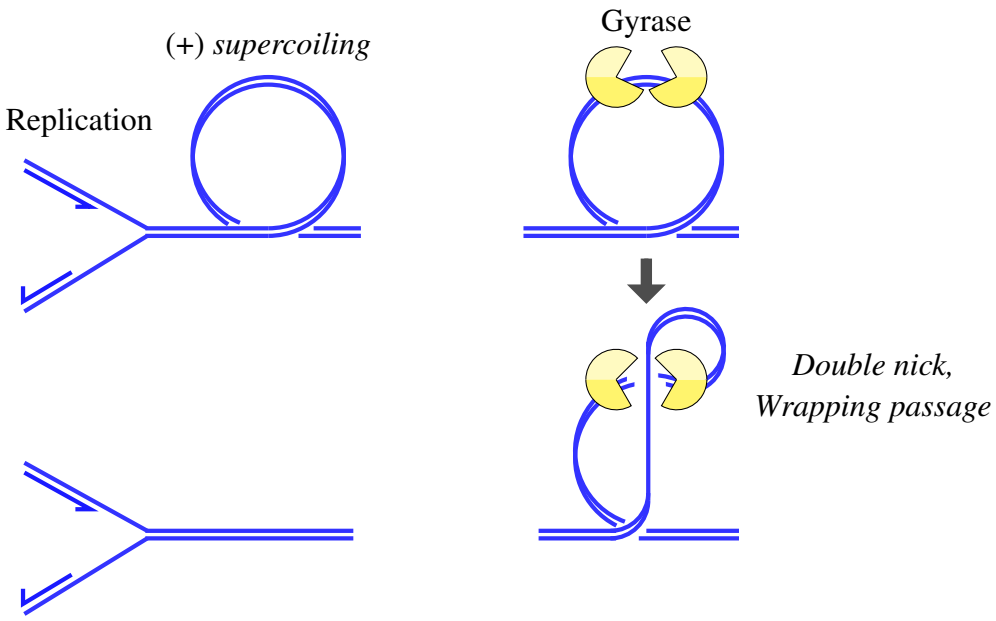

Figure 1.3: **Relaxation of positive super-coiling by Gyrase**. The action of helicases from DNA replication and transcription create positive super-coiling. Gyrase complex binds to DNA and creates two nicks. During this step, Gyrase is covalently bound to both the 5' end of each strand ("cleavage complex"). One of the ends is wrapped around Gyrase, which is passed through the middle, resulting in relaxation of positive super-coiling ("Wrapping passage"). Schematic was based on Gore et al. (2006); Basu et al. (2016); Ashley et al. (2017)

formed independently of DNA replication, as inhibiting DNA synthesis using thermosensitive *dnaB* mutants does not increase survival to quinolones (Zhao et al., 2006; Drlica et al., 2008). Studies have suggested that bactericidal effects from quinolones may be related to oxidative stress induced by quinolones (Dwyer et al., 2007, 2015; Machuca et al., 2017), which could provide an alternative interpretation of why preventing DNA replication fails to rescue cells from quinolone toxicity, although this interpretation has been challenged by other studies (Liu and Imlay, 2013).

1.2.2.2 DNA damage by antibiotics targeting DNA synthesis

One way antibiotics may lead to DNA damage is by preventing the synthesis of DNA nucleotides. Trimethoprim and sulfamethoxazole antibiotics are relatively common for treating bladder infections, although their usage has decreased given the appearance of strains resistant to these drugs (Eliopoulos and Huovinen, 2001). Their mode of action

is by inhibiting thymidine synthesis and, therefore, DNA replication. Trimethoprim inhibits dihydrofolate reductase, and sulfamethoxazole inhibits dihydropteroate synthase, two enzymes important for the synthesis of thymidine precursors (Green and Matthews, 2007). DNA-synthesis inhibition by these drugs can lead to DSBs because of stalled replication forks, however, it appears that incorporation of damaged or wrong DNA bases is largely responsible for trimetroprim toxicity (Lewin and Amyes, 1991; Giroux et al., 2017).

1.2.2.3 DNA damage by antibiotics targeting cell wall synthesis

Antibiotics targeting cell wall synthesis (β-lactams) can lead to DNA damage via an indirect route. Inhibition of FtsI (septum cell wall synthesis) caused by the β-lactam ampicillin, has been shown to activate the transcriptional regulator DpiA involved in anaerobic citrate catabolism, indirectly leading to DNA damage (Miller et al., 2004). DpiA binds to the origin of replication competing with DnaA, which is responsible for DNA damage under high levels of DpiA expression (Miller et al., 2003). It is unclear how FtsI inhibition leads to DpiA activation. However, DNA damage is not the main mechanism for killing cells by β-lactams, as *recA* mutants (unable to repair breaks) are slightly more senstive than wild-type to low doses of ampicillin (1-2 μg/ml), but are not more sensitive to higher doses (Liu and Imlay, 2013; Mo et al., 2016).

1.2.3 Palindromic sequences as a tool for chronic double-strand breaks

Hairpins formed by palindromic sequences can be cleaved by the SbcCD complex, which makes it a useful tool to study double-strand break repair (DSB repair) (Eykelenboom et al., 2008). Palindromic sequences are composed of two identical repeat units. The most commonly used palindrome is 246 base-pairs long, interrupted by a few nucleotides, and located at the *lacZ* locus (Eykelenboom et al., 2008). During DNA replication, this palindrome forms a hairpin in one of the strands (presumably the lagging strand), which is recognised by the structure-dependent endonuclease SbcCD, leading to a double-strand break (see figure 1.4). Formation of the hairpin appears to happen only during *oriC*-dependent DNA replication, and not during DNA synthesis after homologous recombination, as cells survive chronic palindrome cleavage (Eykelenboom et al., 2008). Estimates indicate that palindrome locus is cleaved with an

approximate 70% chance per DNA replication event (Eykelenboom et al., 2008).

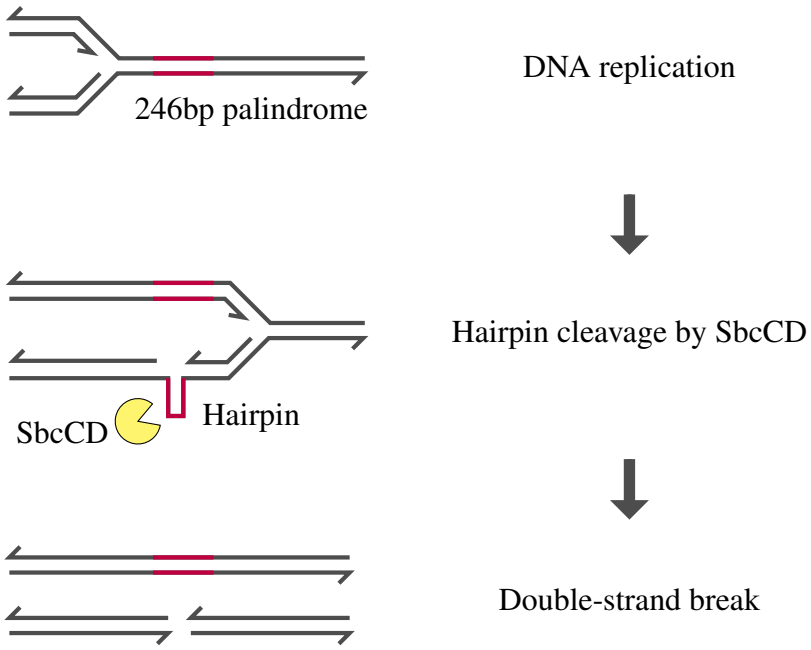

Figure 1.4: **Genetic system for generating replication-dependent chronic site-specific double-strand breaks**. Palindrome inserted in *E. coli*'s genome leads to the formation of a hairpin upon DNA replication, which is recognised and then cleaved by SbcCD. Given that only one copy is cleaved, the intact copy can serve as template for repair by homologous recombination. Diagram modified from (Eykelenboom et al., 2008)

1.2.4 DNA repair by homologous recombination

Homologous recombination is the only pathway for repairing double-strand breaks in *E. coli* and many bacteria, and also can serve to repair single-strand gaps (Rocha et al., 2005). During homologous recombination, the damaged DNA molecule is paired with a homologous sequence, which serves as the template for repair.

Homologous recombination can be divided into 3 stages: (1) loading of the recombination machinery (pre-synapsis); (2) search for the homologous partner and strand invasion (synapsis) and; (3) re-synthesis of DNA and resolution of the two joint molecules (post-synapsis) (Cromie et al., 2001). The ability of cells to use homologous recombination for DNA repair depends on their capacity to load RecA forming a

nucleoprotein filament. *E. coli* has two different pathways to load RecA protein into DNA, one that recognises double-strand breaks (RecBCD pathway), and a second that recognises single-strand gaps (RecFOR pathway) (Michel and Leach, 2012).

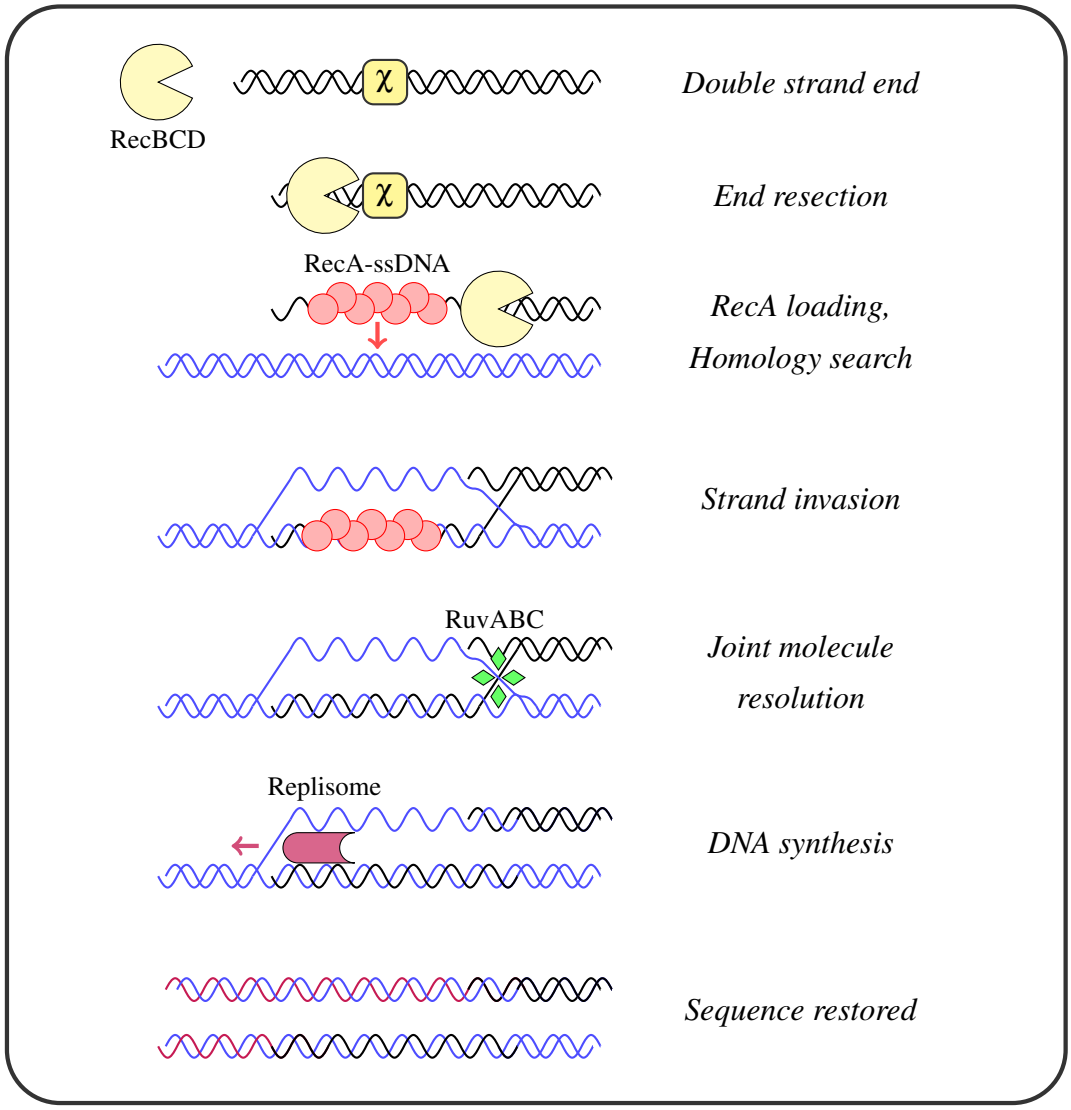

Figure 1.5: **Double-strand break repair via homologous recombination**. Schematic of double-strand break repair pathway by homologous recombination in *E. coli*. The DSB is processed by RecBCD until recognition of a χ-site, from which it promotes the loading of RecA. RecA forms a nucleofilament and catalizes the search for a homologous sequence and subsequent strand invasion. From there, the two joint molecules are resolved by RuvABC, and the full double-stranded DNA is restored to loading the replisome and synthesising the missing sequence.

1.2.4.1 RecBCD complex initiate double-strand break repair

Bacteria, such as *E. coli* have a single pathway to repair double-strand breaks, and is initiated by the RecBCD complex. Eukaryotes and other bacteria have an alternative mechanism called non-homologous end joining, which involves the rejoining of the broken ends, but can potentially result in some loss of the original DNA sequence (Rocha et al., 2005). On the other hand, homologous recombination relies on an intact copy of the broken region that serves as a template for repair.

1.2.4.1.1 RecBCD activity

The RecBCD complex recognises blunt double-strand ends and travels in 5' to 3' direction degrading DNA by a combination of two helicase domains and a single-strand endonuclease activity (Smith, 2012). RecBCD is one of the fastest and most processive-known endonucleases. The RecB subunit contains a 3'-5' helicase and nuclease domain and RecC contains a 5'-3' helicase domain. The remaining subunit, RecD is responsible for the recognition of an octameric sequence called χ-site (5'-GCTGGTGG-3') in an orientation-dependent manner. Upon χ recognition, RecBCD complex changes its activity: it stops degrading DNA, and the activity of RecD helicase motor is reduced. The 3'-5' helicase activity from RecB is responsible for accumulat-

-ing a 3' single-stranded loop which serves as a substrate for the binding of RecA (Amundsen et al., 2000). Reports indicating that RecB interacts with RecA monomers *in vitro* suggest that RecBCD may actively promote the loading of RecA into DNA (Lucarelli et al., 2009).

It is worth mentioning that χ-sites are the most represented octameric sequences in the *E. coli* genome and the orientation is most abundant facing reverse from the direction of DNA replication (Halpern et al., 2007). This bias in orientation is consistent with the expectation that most naturally-occurring double-strand ends result from the reversal or broken replication forks.

1.2.4.1.2 RecBCD activity *in vivo*

Most of the understanding of RecBCD activity comes from *in vitro* studies (reviewed in (Smith, 2012)). Recently, the activity of RecBCD has been studied *in vivo* by analysing the pattern of RecA loading across the chromosome upon induced site-

specific double strand breaks (Cockram et al., 2015). It was found that RecA loading by RecBCD is consistent with χ recognition, as RecA could not be detected bound to regions preceding χ sites. Consistently, RecA can be detected immediately from the break site in a Δ*recD* mutant(White et al., 2018). Additionally, RecA enrichment could be found near χ at various distances from the break site. A mathematical model where the probability of recognising χ-site is less than one was shown to reproduce the pattern of RecA enrichment on DNA (Cockram et al., 2015)).

1.2.4.2 RecFOR complex initiate single-strand gap repair

Single-strand gaps can also be repaired by homologous recombination, but require other enzymes to load RecA into the lesion, as single strand regions are normally coated by SSB (single-strand binding protein). Two alternative pathways exist to remove SSB and promote the binding of RecA into ssDNA: one relying on proteins RecF, RecO and RecR; and another only needing RecO and RecR. Both differ in their efficiency and molecular mechanism, suggesting either of them may be more useful depending on the context (Sakai and Cox, 2009). In principle, not all single-strand gaps require homologous recombination for repair, as alternative mechanisms can restart DNA synthesis and repair the gap, for example, those generated on the lagging strand during DNA replication (Kurth and O'Donnell, 2009).

1.2.4.3 RecA nucleofilament catalyses homologous strand exchange

Homologous recombination depends on the activity of the RecA protein for homology search and strand exchange. RecA is a small protein able to polymerise on single-stranded DNA and less efficiently on double-stranded DNA. Once sufficient identical bases are recognised (approx. 8 nucleotides minimum), base pairing can stabilise the interaction between ssDNA and dsDNA (Hsieh et al., 1992). Strand exchange is then facilitated by a preferential affinity of the strong DNA-binding site of RecA for dsDNA, propagating the strand invasion across the filament (Mazin and Kowalczykowski, 1996; Chen et al., 2008)). RecA protein has two DNA binding sites: one with high affinity, which is occupied by ssDNA during polymerisation; and a weaker second site, able to bind transiently to dsDNA important for sampling during homology search process (Mazin and Kowalczykowski, 1996; Bell and Kowalczykowski, 2016).

1.2.4.3.1 Dependence of RecA activity on ATP

RecA is also an ATP hydrolase, which is important for some of RecA functionality. Initial RecA oligomerization is ATP dependent, a process known as nucleation. Once an oligomer is formed, the filament can extend in both directions, although polymerisation is 50% faster in the 5' end (Bell and Kowalczykowski, 2016). Segments within the RecA filaments can be found in two distinct conformations depending on ATP binding: one is extended when bound to ATP, and the second is approximately 30% shorter when bound to ADP. Only the ATP-bound form of RecA has the correct dimensions for base pairing sampling (Bell and Kowalczykowski, 2016). However, ATP hydrolysis is not strictly required for strand exchange (Renzette and Sandler, 2008). Instead, ATP hydrolysis appears to be important for depolymerisation of RecA, as RecA-ADP has less affinity for DNA (Menetski et al., 1990), and may be relevant for rejecting short homology regions as ATP hydrolysis can destabilise strand exchange intermediates (Danilowicz et al., 2017).

1.2.4.3.2 Modulation of RecA filament stability by other proteins

The stability of the RecA-ssDNA filament is affected by other proteins. Two specific examples are *dinI* and *recX* genes. DinI has a dual role depending on its concentration: at lower levels, it serves to stabilise RecA-ssDNA, whereas at higher levels has the opposite effect (Lusetti et al., 2004; Yoshimasu et al., 2003). On the other hand, *recX* is co-transcribed with the *recA* gene, and has been shown to destabilise and prevent extension of the RecA-ssDNA filament (Lusetti et al., 2004; Drees et al., 2004; Ragone et al., 2008). The UvrD helicase (Helicase II) is able to disassemble RecA-ssDNA filaments, together with RecA filaments after strand exchange (Florés et al., 2005; Veaute et al., 2005). In addition, the RuvAB complex is able to disassemble RecA from strand exchange products during the resolution of the joint molecules (see subsection 1.2.4.4 below).

1.2.4.3.3 RecA activity *in vivo*

The duration of RecA filaments after induction of site-specific double-strand breaks have been studied *in vivo* using fluorescent fusions to RecA (Renzette et al., 2005, 2007; Centore and Sandler, 2007; Amarh et al., 2018). RecA filaments appear as fluorescent foci due to RecA polymerisation. Cleaving DNA using a restriction endonu-

clease leads to the observation of long filaments, lasting for $\sim$ 50 minutes (Lesterlin et al., 2014). It was reported that the filaments migrate from one cell pole to the other, presumably searching for the sister copy of the chromosome. In contrast, a study using replication-dependent double-strand breaks (see 1.2.3) reported foci lasting 1-8 minutes (1.5 mins average) (Amarh et al., 2018). Recently a new fluorescence probe based on a truncated form of the λ-repressor has been described, which has the advantage that binds preferably to active RecA filaments (Ghodke et al., 2019).

1.2.4.3.4 RecA as a coprotease

In addition to the aforementioned activities of RecA filaments, RecA-ssDNA serves as a coprotease (promotes the cleavage of other proteins). In particular, it promotes self-cleavage of the LexA transcriptional repressor, phage transcriptional repressors and one of polymerase V subunit (UmuD) (Butala et al., 2011). Coupling protein cleavage with RecA-ssDNA activity serves a strategy to detect the occurrence of DNA repair, which will be presented in detail in subsection 1.3.1.

1.2.4.4 DNA synthesis and the resolution of joint molecules

To complete DNA repair, it is necessary to synthesise the lost DNA sequence, separate the joint molecules and ligate the DNA ends. In contrast to the initiation of replication at *oriC* by DnaA, the restart of DNA replication during homologous recombination is dependent upon the protein PriA. PriA is a helicase with affinity for branched DNA junctions, and is able to initiate a cascade of protein interactions leading to the assembly of the replication machinery (Kreuzer, 2005; Michel et al., 2018).

After strand invasion, joint molecules are converted into a more stable conformation called the Holliday junction. The pathway responsible for resolution of the junction depends on the RuvABC complex (West, 1997). The RuvAB complex recognises Holliday junctions and is able to actively migrate the branch connecting both DNA molecules. RuvAB is responsible for recruiting RuvC, an endonuclease able to cleave the junction (West, 1997). After cleavage, a DNA ligase can restore the continuity in the DNA sequence. Until recently it was believed that an additional pathway dependent on *recG* was able to solve Holliday junctions, based on analysis of mutants phenotypes and *in vitro* activity (Lloyd and Buckman, 1991; Azeroglu and Leach, 2017). RecG is a helicase with preferred binding to DNA junctions following strand invasion, whose

role is to load DNA synthesis machinery in the correct orientation to restore the lost DNA sequence (Azeroglu and Leach, 2017).

1.3 Adaptation to variable levels of DNA damage

In natural environments, bacteria may be exposed to various levels of DNA damage. Therefore, it is not surprising to find regulatory mechanisms that are able to sense DNA damage and help cells to respond accordingly. The main response in *E. coli* is the activation of the SOS regulon, controlled by the repressor LexA and activated by RecA bound to single-stranded DNA (Radman, 1975; Kreuzer, 2013; d'Ari, 1985). The SOS pathway is conserved in many bacteria, albeit with variations (Erill et al., 2007). Since its initial discovery, it has served as a canonical example of stress response and transcriptional regulation. Nowadays, there is renewed interest because of its role in mutagenesis and antibiotic resistance.

1.3.1 The SOS response

The two major players in the regulation of the SOS pathway are RecA and LexA. LexA is a transcriptional repressor that binds to a $\sim$20 bp DNA region (SOS-box) as a dimmer (Wade et al., 2005; Butala et al., 2009). A site with endonuclease activity is hidden inside the LexA native conformation. RecA bound to single-stranded DNA (RecA-ssDNA) interacts with LexA, changes its conformation, and results in LexA cleaving itself (Butala et al., 2011). The induced self-cleavage of LexA marks the beginning of the SOS pathway, as it decreases native LexA concentration freeing SOS promoters from repression.

Although hundreds of genes can be found to be induced under DNA damage (Khil and Camerini-Otero, 2002), the core LexA-regulated genes (SOS regulon) is composed of about 30 genes in *E. coli* (see table 1.1).

1.3.1.1 Gradual SOS activation by DNA damage

DNA repair by homologous recombination leads to the formation of RecA-ssDNA filament, and activates the SOS pathway. The concentration of active LexA during SOS induction will depend on the lifetime and concentration of RecA-ssDNA filament

during DNA repair. This results in a certain gradation of SOS induction for different promoters, depending upon the number of LexA binding sites and the relative binding affinity (Janion, 2008; Culyba et al., 2018). Promoters with strong binding for LexA will require lower LexA levels to be induced, whereas genes with weaker binding will be induced more easily.

The expression of *lexA* gene is also under control of LexA, presumably to allow fast resumption of normal LexA levels once DNA repair has completed (Rosenfeld et al., 2002). The cleaved products of LexA have a small affinity for DNA promoters, however, self-cleavage exposes recognition sites for ClpXP and Lon proteases, meaning once LexA is cleaved those products can be removed and do not interfere with SOS induction (Butala et al., 2011).

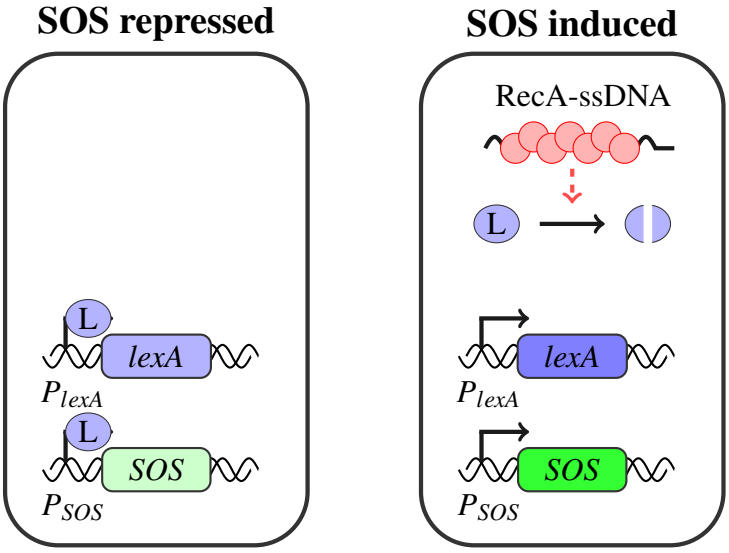

Figure 1.6: **The SOS regulon is induced by DNA damage**. Schematic illustration of the main components in the SOS response. In the absence of DNA damage, LexA repressor binds to SOS promoters preventing their transcription. Upon DNA damage by double-strand breaks or single-strand gaps, RecA nucleoprotein filament is formed (RecA-ssDNA), which induces the self-cleavage of LexA. Reduction in full LexA concentrations permits expression from SOS promoters, inducing the SOS response.

Table 1.1: **Genes induced during the SOS response in *E.coli***. Genes repressed by LexA that have been shown to be induced during the SOS response. The number of LexA binding sites were taken based on annotation in the Regulon database (Gama-Castro et al., 2016). Some of these genes have been described to have additional transcriptional regulation, taken from Regulon database, or their proteins levels controlled by proteases, taken from EcoCyc database (Keseler et al., 2017). A number of genes for which some LexA binding sites have been described were excluded from the list. The reason was either that the gene product was not functional (*molR*, *hokE*, and *dinS*); or there was no experimental evidence for them to be actually induced (*ftsZ* operon, *recBD* operon, *uvrYC* operon, *ybiB*, and the *rpsU-dnaG-rpoD* operon).

Gene	**Function**	**LexA binding sites**	**Additional regulation**	**Degraded by**
lexA	SOS repressor	3		RecA-ssDNA (self-cleavage)
recA	DNA recombination	1		
recX	RecA inhibitor	1		
dinI	RecA activity modulator	1		
ssb	ssDNA-binding protein	1	Arc-P	
phr	deoxyribodipyrimidine photolyase	1	RpoS	
uvrA	excision nuclease subunit	1	Arc-P	
uvrB	excision nuclease subunit	1	DnaA	
uvrD	DNA helicase II	1		
cho	UvrAB dependent endonuclease	1		
ruvA	branch migration complex subunit	4		
ruvB	branch migration complex subunit	4		
recQ	DNA helicase	?		
dinG	DNA helicase	1		
sbmC	DNA gyrase inhibitor	1	CRP-cAMP	
recN		2	DnaA	
rmuC	DNA recombination	1		
sulA	cell division inhibitor	1	RcdA	Lon, ClpYQ

Gene	Function	LexA binding sites	Additional regulation	Degraded by
ftsK	cell division DNA translocase	1		
polB	DNA polymerase II	1	RpoS	
dinB	DNA polymerase IV	1	RpoS	
umuD	DNA polymerase V subunit	2		RecA-ssDNA (self-cleavage), Lon, ClpXP
umuC	DNA polymerase V subunit	2		Lon
tisB	membrane toxin	1	small RNA istR1	
dinQ	membrane toxin	2	small RNA AgrB	
symE	toxic protein	1	small RNA SymR	Lon
yafN	antitoxin for YafO	1		
yafO	mRNA interferase	1	YafN	
dinJ	antitoxin for yafQ	1	DinJ-YafQ, DnaA	Lon, ClpXP
yafQ	mRNA interferase	1	DinJ-YafQ, DnaA	
dinF	Putative transport protein	3		
ybiB	unkown	1		
dinD	unkown	1		
ybfE	unknown	1		
ydjM	unknown	2		
yebG	unkown	1		

1.3.1.2 Mechanism for LexA induced cleavage

Decades of studying the induced cleavage of LexA *in vitro* have formed a picture of how this process may operate in living cells (Little et al., 1980; Little, 1991; Kovačič et al., 2013). Under no DNA damaging conditions, most of LexA is expected to be as a dimmer and bound non-specifically to DNA (about 20% of LexA is expected to be freely diffusing) (Butala et al., 2011). LexA dimers interacting with SOS promoters are not able to interact with RecA filaments due to steric constraints, meaning DNA acts as an allosteric regulator of LexA-induced cleavage (Butala et al., 2011). RecA-ssDNA interaction with LexA dimmer has been mapped to a deep groove within RecA-ssDNA

filament, with seven RecA monomers interacting with one subunit of LexA dimmer (Yu and Egelman, 1993; Kovačič et al., 2013).

Studies *in vitro* have also helped determine the relevance of RecA-ssDNA conformation and activity for LexA cleavage. RecA-ssDNA ATP binding is required for inducing LexA cleavage, presumably due to RecA-ssDNA extended conformation when bound to ATP (Rehrauer et al., 1996). RecA-ssDNA recombination (binding to dsDNA) and coprotease activities appear to be mutually exclusive (Harmon et al., 1996).

The rate of LexA cleavage in live cells may be modulated by proteins interacting with RecA-ssDNA. In isolation, LexA degradation rates follow classic Michaelis-Menten dependency with RecA concentration. The addition of single-strand binding protein (SSB) changes dependency of cleavage rate to a sigmoidal curve, probably due to competition between SSB and RecA for ssDNA (Little, 1991; Rehrauer et al., 1996). In addition to their role in modulating RecA filament stability, DinI and RecX proteins can also inhibit RecA coprotease activity: RecX inhibits both LexA and UmuD cleavage, whereas DinI inhibits only UmuD (Stohl et al., 2003; Yasuda et al., 1998, 2001).

1.3.2 SOS induction contributes to DNA repair

Mutants of LexA unable to be self-cleaved have higher sensitivity to DNA-damaging agents, highlighting the relevance of SOS induction to tolerate DNA damage (Mount et al., 1972; Lin and Little, 1988). Several genes involved in DNA repair and tolerance are part of the SOS response. In general, binding of LexA to these promoters is weak, allowing some basal expression of these genes even when SOS is repressed.

The list of genes with various roles in DNA repair processes are: homologus recombination (*recA*); branch migration during homologous recombination (*ruvA*, and *ruvB*); chromosome cohesion for homologous recombination (*recN*); repair of damage by UV-radiation (*phr*); and nucleotide excition repair (*uvrA*, *uvrB*, *uvrD*, and *cho*). A few other genes have multiple roles in DNA repair, such as single-strand binding protein SSB (Shereda et al., 2008), helicase RecQ (Hishida et al., 2004) and helicase DinQ (Voloshin et al., 2003; Boubakri et al., 2010)).

Another DNA repair gene induced by SOS is *recN*, a cohesin-like protein helping to keep sister chromatids together (Odsbu and Skarstad, 2014; Vickridge et al., 2017). RecN has been shown to be recruited by RecA (Keyamura et al., 2013) and this inter-

action is important for RecA recombination activity (Uranga et al., 2017)).

Finally, two genes have been implicated in the protection against DNA damaging agents. The gene *sbmC* codes for a protein that inhibits gyrase at an early step, therefore protecting the cell against drugs poisoning this enzyme (Chatterji and Nagaraja, 2002; Chatterji et al., 2003). The protective effect of *sbmC* against quinolone antibiotics has been reported to be only partial (Chatterji et al., 2003). The gene *dinF* forms an operon with *lexA*, and has homology to known membrane transporters (Saier et al., 2016). It has been suggested its role may be to export toxic agents, such as reactive-oxygen species (Rodríguez-Beltrán et al., 2012).

1.3.3 Both SOS and DNA damage delay cell division

A phenotype commonly associated with DNA damage is cell filamentation. This results from delaying cell division via two complementary mechanisms: one dependent on SOS induction; and second from a delay in chromosome segregation (Huisman et al., 1982; Cambridge et al., 2014). The benefit of delaying inhibition is most likely to allow enough time for cells to repair, and ensure proper chromosomal segregation into daughter cells.

SOS has another role in coordinating chromosome segregation and cell division by inducing the expression of *ftsK* (Wang and Lutkenhaus, 1998). This gene is essential and has two important roles in cell division: coordinate chromosome segregation in the terminus region (Stouf et al., 2013); and recruit other members of the septum aparatus (Chen and Beckwith, 2001; Grenga et al., 2008).

1.3.3.1 Inhibition by SulA

SOS induces the expression of SulA (also known as SfiA), which prevents FtsZ ring formation by sequestering FtsZ monomers (Dajkovic et al., 2008; Chen et al., 2012). To facilitate the resumption of cell division, SulA protein is degraded by two proteases, Lon and ClpYQ (Huisman et al., 1984; Wu et al., 1999). It has been observed that once cell division is resumed, cells go through several faster division events, sometimes asymmetric, probably dependent on MinCD for septum positioning (Bi and Lutkenhaus, 1993; Wehrens et al., 2018). The expression of *ftsZ* is dependent on several factors such as growth conditions, meaning that susceptibility of cells to SulA expression may be variable (Nazir and Harinarayanan, 2015).

1.3.3.2 Nucleoid occlusion

Although not strictly part of the SOS response, a related mechanism is called nucleoid occlusion, which prevents the formation of the septum before chromosomes are segregated, resulting in delayed cell division. Prevention of cell division is dependent on the DNA-binding protein *slmA* (Bernhardt and de Boer, 2005). SlmA oligomers bound to DNA interact with FtsZ inhibiting its assembly, by binding to a 12 bp palindromic sequence enriched near the origin region of the chromosome (Tonthat et al., 2011; Cho et al., 2011). There is evidence for an additional mechanism for cell division delay independent of *slmA* and *sulA* in response to DNA damage (Cambridge et al., 2014).

1.3.4 SOS induction and genetic instability

In principle SOS induction and DNA repair serve to maintain the integrity of the bacterial genome, but they also have a role in promoting genomic instability (Darmon and Leach, 2014). This is because of an increase in site-specific mutagenesis and horizontal gene transfer.

1.3.4.1 Induction of translesion DNA polymerases

Under normal conditions, *E. coli* relies mostly on DNA polymerase III for DNA synthesis. As Pol III can be blocked by DNA adducts, bacteria have alternative DNA polymerases able to bypass some of these adducts. In *E. coli* those are Pol II, Pol IV and Pol V, which are induced as part of the SOS response. Although not being a DNA repair mechanism in itself, translesion DNA synthesis (TSL) can be seen as a mechanism to tolerate certain kinds of DNA damage (Andersson et al., 2010; Vaisman et al., 2012). In addition to the control by SOS, expression of Pol II and Pol IV is also controlled by the general stress response (Storvik and Foster, 2010; Dapa et al., 2017). Pol V is subject to more complex regulation, as it requires cleavage of one its subunits and transfer of one RecA-ATP monomer to generate an active and stable complex (Jiang et al., 2009; Robinson et al., 2015; Goodman et al., 2016). A side effect from utilising translesion DNA polymerases, is an increase in site-specific mutagenesis. The consequences of most single nucleotide mutations appear to be neutral, suggesting that the cost of increased mutagenesis may be less than the potential benefit of acquiring an adaptive mutation, which has raised the interesting possibility that increasing mutage-

nesis in response to stress may be beneficial for bacteria (Matic, 2017; Robert et al., 2018; Schroeder et al., 2018).

1.3.4.2 SOS induction stimulates horizontal gene transfer

There are also known links between horizontal gene transfer by conjugative plasmids and SOS induction, which could influence the spread of antibiotic resistance genes. Conjugative plasmids are transferred as ssDNA, which can potentially lead to SOS induction if they are coated by RecA. Indeed, plasmid transfer has been correlated with SOS induction (Baharoglu et al., 2010). Other conjugative plasmids carrying genes whose products inhibit SOS induction sequester freely-diffusing RecA (Petrova et al., 2009). Another connection between SOS and horizontal gene transfer is that in some conjugative plasmids, the genes responsible for inducing transfer are under LexA repression, which is consistent with the increased conjugation transfer induced by DNA damage conditions (Beaber et al., 2004; Baharoglu and Mazel, 2014; Shun-Mei et al., 2017).

1.3.4.3 SOS induction stimulate DNA mobile elements

In addition to single nucleotide changes in DNA sequence, large rearrangements in DNA sequences (such as translocations, insertions and deletions) are important contributors to genetic diversity. One example linked to SOS induction is the finding that the regulation of many naturally occurring DNA mobile elements, for example, bacteriophages and pathogenicity islands, are coupled to SOS induction by having LexA repress some of their genes are also (Fornelos et al., 2016; Liu et al., 2017). From the perspective of mobile genetic elements, there may be a selective advantage for increasing mobility in situations when the host cells are under stress (Fornelos et al., 2016).

1.3.5 SOS toxin-antitoxin modules

Several genes from Toxin-antitoxin modules whose expression can be toxic for cell growth are controlled by SOS. Toxin-antitoxins were first described as a mechanism for plasmid stability. Plasmids encoding a long-lived toxin coupled with a short-lived antitoxin are more stable in a population (Harms et al., 2018). This is because cells losing the plasmid due to missegregation would be killed by the more stable toxins (post-segregational killing).

The actual physiological role for these genes in the SOS response is not clear. It has been proposed that they may act as a checkpoint to reduce metabolism, similar to the eucaryotic DNA-damage response (Finn et al., 2012). However, the evidence is not conclusive, given that many of these experiments have been carried in mutants over-expressing these toxins. Alternatively, these toxins could serve to counter-select incorrect chromosome segregation, similarly to plasmids (Sinha et al., 2017). The role of stochastic induction of SOS toxins in antibiotic tolerance will be discussed later in this section.

1.3.5.1 SOS toxins targeting the membrane

Two toxins induced by SOS (TisB and DinQ) have been described as small membrane peptides leading to cell depolarisation (Weel-Sneve et al., 2013; Berghoff et al., 2017). Translation of *tisB* mRNA is regulated in two ways. Firstly, for the *tisB* transcript to be translated it must be cleaved, given that the full transcript adopts a conformation unable to bind ribosomes efficiently. Secondly, the small RNA IstR1 can bind to the cleaved *tisB* transcript, preventing ribosome binding and leading to cleavage by RNase III (Darfeuille et al., 2007; Berghoff et al., 2017). Regulation of DinQ is very similar to TisB, but instead ArgA and ArgB act as small inteference RNAs (Weel-Sneve et al., 2013).

1.3.5.2 SOS toxins promoting RNA degradation

Three toxins induced by SOS (SymE, YafO, and YafQ) inhibit growth by promoting mRNA degradation. SymE over-expression leads to inhibition of protein synthesis and mRNA degradation, probably by interacting with ribosomes. The expression of this toxin is negatively regulated by the small RNA SymR (Kawano et al., 2007). The YafQ toxin has been shown to interact with ribosomes and cleave mRNA near the translation start site (Zhang et al., 2009). The gene *yafQ* is co-transcribed with *yafN* from a promoter repressed by YafN protein (Christensen-Dalsgaard et al., 2010). The toxin YafO has also been shown to cleave mRNA bound to ribosomes, but at a specific codon sequence (Prysak et al., 2009). Overexpression of YafQ appears to affect growth only in solid media, and not in liquid conditions, perhaps due to its codon-specific degradation activity (Kolodkin-Gal et al., 2009). YafQ is inhibited in two ways by co-transcribed gene *dinJ*: DinJ binds to YafQ blocking its RNase activity, and the complex also acts as a transcriptional repressor for the promoter of this operon (Ruangprasert

et al., 2014).

Given the function of SymE, YafO, and YafQ toxins in mRNA degradation, it has been proposed that the role of these toxins could be to accelerate RNA turnover (Rooney et al., 2009). These toxins could also serve to accelerate global rearrangements in gene expression during DNA-damage conditions. It is worth mentioning that similar toxins controlled by SOS have been found in other bacteria (Kirkpatrick et al., 2016).

1.3.6 SOS induction and antibiotic tolerance

An alternative way to tolerate antibiotic treatment is to reduce cell growth, as most antibiotics target growth-related processes. In contrast to antibiotic resistance which commonly results from acquisition or modifications of specific genes, persistence to antibiotics can result from phenotypic heterogeneity within a population (Brauner et al., 2016; Radzikowski et al., 2017; Erickson et al., 2017b).

1.3.6.1 Link bewteen toxin-antitoxins and antibiotic tolerance

Heterogeneous expression of toxin-antitoxin modules has been linked to antibiotic persistence, including some SOS-induced toxins. However, recent findings have brought into question the significance of toxin-antitoxin modules in antibiotic tolerance. A commonly used strain with ten toxins deleted was found to be contaminated with bacteriophage ϕ80, meaning that reduction of persistence previously associated with deleting toxins were, in fact, due to bacteriophage-induced cell lysis (Harms et al., 2018; Goormaghtigh et al., 2018). Interestingly, expression of ϕ80 genes happen to be induced by the SOS response (Rotman et al., 2010).

1.3.6.2 Evidence for SOS-induced toxins affecting antibiotic tolerance

Despite the controversy on the role of toxin-antitoxin modules, it appears that at least two toxins induced by SOS can affect antibiotic tolerance under certain conditions (see subsection 1.3.5 for the descriptions of mechanism and regulation). The first is toxin TisB, which has been shown to be partially responsible for the frequency of persister cells after high doses of ciprofloxacin, a fluoroquinolone (Dorr 2009, Dorr 2010). Secondly, deletion of *yafQ* was shown to reduce the frequency of cells tolerant to several antibiotics during bacterial biofilm formation (Harrison et al., 2009; Wu et al., 2015). The mechanism for the effect of *yafQ* was found to be dependent on

quorum sensing signalling. DinQ toxin cleaves mRNA at one specific codon, and the mRNA of one gene relevant for quorum sensing (tryptophanase) happens to be enriched in this codon (Hu et al., 2015).

1.3.7 SOS induction in single cells

Fluorescent proteins expressed from SOS promoters have been used to study SOS expression in single cells. Consistent with spontaneous DNA damage being relatively rare, about 1% of the population in normal condition shows SOS induction compared to a genetic background where LexA is mutated and cannot be cleaved (Pennington and Rosenberg, 2007). This frequency is less than what could have been expected from mutants unable to repair by homologous recombination (Kuzminov, 1999), and it has been speculated that only a fraction of RecA activity events lead to SOS induction (Massoni et al., 2012). Substantial cell-to-cell variability has been observed in conditions when DNA damage is induced by exogenous agents, which can be partially attributed to variability in the level of damage experienced by single cells (Uphoff, 2018). Interestingly, experiments studying at SOS induction in single cells following UV damage revealed oscillations in the levels of transcriptional induction, and they were shown to oscillate with a period equivalent to the division time (Friedman et al., 2005).

1.3.8 Mathematical modelling of SOS induction

Several studies have attempted to provide mathematical modelling of SOS induction, several of them motivated by the observation of oscillation in SOS expression under UV damage (Friedman et al., 2005). Due to limitation in controlling DNA damage, most available experiments follow a transient pulse of DNA damage, for example UV exposure. Typically, control of transcription and LexA cleavage are represented by phenomenological functions (Hill functions) (Markham et al., 1985; Aksenov, 1999; Culyba et al., 2018). The observations of single cell variability in SOS expression have motivated several stochastic models with various degrees of detail (Krishna et al., 2007; Ni et al., 2008; Baralla, 2008; Belov et al., 2009; Belov, 2011; Shimoni et al., 2009; Hilbert et al., 2011).

1.3.9 Induction of other stress responses by DNA damage

There is evidence indicating that under certain DNA damage conditions, the general stress response (RpoS) is activated independent of SOS induction (Merrikh et al., 2009a; Dapa et al., 2017). RpoS is a key sigma factor accumulated during the transition to stationary phase and other stressful conditions, which controls about 10% *E. coli* genome (Weber et al., 2005).

1.3.9.1 Induction of RpoS via IraD

One mechanism explaining increasing RpoS levels is via *iraD*, as it has been shown to be induced by various DNA-damaging agents, including direct DNA breaking agents such as Phleomycin (Merrikh et al., 2009a). IraD functions by inhibiting the proteolysis of sigma factor RpoS from ClpXP, prolonging its lifetime (Bougdour et al., 2008; Merrikh et al., 2009b; Micevski et al., 2015). The mechanism leading to the induction of *iraD* by DNA damage is not well established, as the regulation of *iraD* expression is quite complex. The *iraD* gene has two promoters which are controlled by at least four regulators related to growth and nutrient availability. Transcription of *iraD* is induced by ppGpp and Fnr, and repressed by DksA and H-NS (Merrikh et al., 2009b; Battesti et al., 2012).

1.3.9.2 Induction of RpoS via oxidative radicals

Alternatively, it has been proposed that the response to oxidative damage may be responsible for increased levels of RpoS activity during DNA damage, as many DNA-damaging agents can lead to the formation of reactive oxygen species (Duval and Lister, 2013). Recently, an increase in RpoS following mitomycin C treatment was shown to be dependent on oxidative damage and not *iraD* (Dapa et al., 2017), in particular via BarA-UvrY a two-component signalling pathway which has been implicated in sensing oxidative stress (Suzuki et al., 2002; Sahu et al., 2003).

1.3.9.3 Evidence for increase in ATP levels following DNA damage

Early observations indicated that following exposure to Norfloxacin (quinolone) and UV, cells displayed a transient increase in ATP levels (Barbé et al., 1986; Dahan-Grobgeld et al., 1998). The increase in ATP was shown to be specific to DNA damage, although recovery to normal ATP levels required DNA repair. The mechanism respon-

sible for changing ATP levels in response to DNA damage is unknown at present. It is possible that a transient increase in ATP is reflecting an overall reduction in ATP-consuming processes and interestingly similar effects have been observed by inhibiting translation (Schneider and Gourse, 2004).

1.3.9.4 DNA damage tolerance is enhanced when inhibiting ribosome production

A current strategy aimed at improving antibiotic treatment is the combination of different classes of antibiotics (Chevereau and Bollenbach, 2015). Some combinations have been shown to be synergistic, whereas others have been shown to be suppressive (antagonistic). Beyond their potential medical application, the effect from combined antibiotics can be helpful in revealing overall relations between different physiological processes (Nichols et al., 2011). One interesting example is the combined effect of antibiotics damaging DNA and those inhibiting translation. The reduction in growth rate by sublethal doses of DNA-damaging antibiotics (quinolones and trimetroprim) have been shown be antagonised by sub-lethal levels of chloramphenicol, which inhibits translation (Deitz et al., 1966). This effect has been proven to be dependent on ribosome expression, as deleting some ribosomal operons leads to similar antagonistic effects (Bollenbach et al., 2014).

1.4 Global consequences from changes in growth rate

It has been observed that sensitivity to DNA-damaging agents, characterised by the fraction of surviving cells, is influenced by growing conditions, for example, the quality of nutrients (Sufya et al., 2003; Sutera and Lovett, 2006). Many potentially related processes are affected by changes in growth, for example, DNA replication (a main source for DNA damage) and gene expression (which could influence SOS induction). In this section, we will review some of the physiological adaptations in bacteria to changes in growth. To some extent, these considerations could be relevant in the context of infectious diseases. For example, *E. coli* has been estimated to divide every 3 hours inside the intestine, whereas estimates for division time in the urine (bladder) is about 20-30 minutes (Myhrvold et al., 2015; Forsyth et al., 2018).

1.4.1 Balanced and steady state growth

Bacteria respond to levels of nutrient availability by activating cellular growth and cell division. This results in distinct physiological states which are important when evaluating the role of specific cellular processes (Schaechter, 2006). In addition to the classic distinctions of growth phases, those are lag-phase, exponential-phase, and stationary phase (Monod, 1949), a few additional definitions are useful when comparing such physiological states. Exponential growth does not necessarily imply that all variables within the cell increase at the same rate. Thus the concept of "balanced growth", which is defined as the state where all components of the cell increase at the same rate, and it is assumed that if nutrient conditions are not limiting, eventually growing populations would converge to a balanced growth state Campbell (1957); Jun et al. (2018). A similar concept, but including the possibility of cellular heterogeneity, is the one of "steady state growth", which is characterised by the following property: the distributions for any random variable is invariant in time (Painter and Marr, 1968; Jun et al., 2018). For the following, we will talk exclusively of "balanced growth" conditions, or "steady state growth" when considering random variables.

1.4.2 Proteome reallocation in response to growth limitations

The response of bacteria to changes in nutrient composition can be substantial, including macro-molecular changes in cell composition, cell size and the concentration of individual molecular species (Bremer and Dennis, 2008b). One could have anticipated that the response of bacteria would be specific to each nutrient limitation. However, some changes in the physiological state of bacteria correlate more strongly to the resulting growth rate than to the specific media composition. As a general principle, bacteria appear to regulate their metabolism depending on which factors are most critical for limiting growth. We will limit our description to the main mechanisms involved in global regulation of protein synthesis and its consequences during balanced exponential growth. Later, we will overview the effect changing growth rate has on DNA replication.

Translation of proteins from mRNA is a limiting step for growth, as noticed by the fact that the mass fraction allocated to ribosomes correlates with growth rate, when changing in nutrient quality of the media (Maaløe, 1979; Marr, 1991; Scott et al., 2010). The increase in ribosome concentration is due to a relative increase in transcription

from ribosomal operons with growth rate, mediated by the alarmone ppGpp (Schneider and Gourse, 2003). As we will discuss, this has global consequences on the capacity of bacteria to express genes in different conditions.

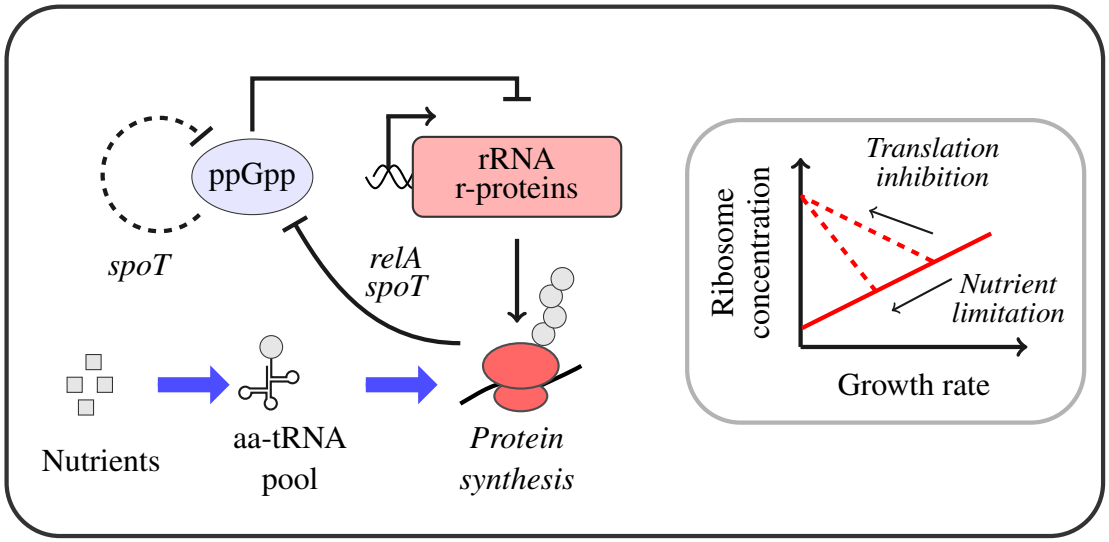

Figure 1.7: **Control protein synthesis via ppGpp**. Diagram illustrating the main modes of regulation in the expression of ribosomes. Direct regulatory relations are represented as solid lines and indirect relation by dashed lines. Thick blue arrows represent metabolic flows. Inlet plots represents approximately how concentrations correlate with changes in growth rate by different limiting conditions. Adapted from (Scott et al., 2010)

1.4.2.1 Coupling protein synthesis and metabolism via ppGpp

The small molecule ppGpp is a key element involved in the regulation of many growth-related processes (Paul et al., 2004). In conditions where the quality of nutrients is modified, the content of ppGpp correlates negatively with growth rate (e.g. carbon source, the presence of animino-acids) (Bremer and Dennis, 2008b; Marr, 1991). In general, ppGpp regulation serves as a way to sense the chemical potential for protein synthesis, helping cells decide whether they would gain from increasing ribosome production or catabolism. Cells unable to regulate ppGpp lack changes in macromolecular composition associated with changes in growth rate (Potrykus et al., 2011). Historically, the effects of accumulating ppGpp upon starvation conditions are referred to as the “stringent response” (Bouveret and Battesti, 2011).

1.4.2.1.1 Control of transcription by ppGpp

The most direct effect from ppGpp is to modify the activity of RNA polymerase on promoters, either by binding directly or via the cofactor DskA. The effect of ppGpp and DskA-ppGpp depends on the particular promoter kinetics. After RNA polymerase binding to the promoter, the rate of transcription initiation depends upon how fast RNA polymerase can switch to an open complex configuration, and how stable this is (Browning and Busby, 2016). ppGpp and DskA-ppGpp have a global effect in destabilising RNA polymerase open complexes, and increasing the rate of complex formation of some promoters (Paul et al., 2004). Promoters of ribosomal operons have very fast open complex formation rates, but the complex is very unstable. Then, increasing levels of ppGpp results in further destabilising of these complexes, and prevent transcription initiation (Barker et al., 2001). On the other hand, the open complex formed from metabolic promoters is already stable, making them less sensitive to ppGpp. In addition, ppGpp-DskA increases the rate of complex formation in some metabolic genes, leading to an increase in transcription (Paul et al., 2005).

1.4.2.1.2 Regulation of ppGpp levels

The levels of ppGpp accumulate as a result of the activity of two synthetases: RelA and SpoT. RelA activity appears to be very low in growing cells and is induced by stalled ribosomes generated from starvation (Murray and Bremer, 1996). In contrast, SpoT possesses both a weak domain with synthase activity and a strong second domain with ppGpp hydrolase activity. SpoT ppGpp synthetase activity increases upon a number of nutrient stress conditions, however, the mechanism by which it is regulated remains unclear (Murray and Bremer, 1996; Bremer and Dennis, 2008a; Hauryliuk et al., 2015). The hydrolase activity is essential to maintain low ppGpp levels in growing conditions (Xiao et al., 1991). The expression from *spoT* is repressed by factor DskA-ppGpp, meaning reduced levels of ppGpp to higher expression of *spoT* (Lemke et al., 2011), which in normal growth conditions serves mostly as a hydrolase.

The balance between synthase and hydrolase activities is responsible for maintaining ppGpp levels. Synthases activity depends on the rate of translation and expression of SpoT hydrolase increases with lower ppGpp levels forming a positive feedback (double negative regulation). Then, faster ribosome elongation due to higher levels of protein synthesis reactants (tRNAs carrying aminoacids) results in ppGpp decreasing with the

quality of nutrient conditions (Schneider and Gourse, 2003; Potrykus et al., 2011).

1.4.2.2 Resource allocation principle

Several studies using proteomics and ribosome profiling have revealed how *E. coli* allocates its proteome towards different functions, depending on the growth condition (Li et al., 2014; Hui et al., 2015). The overall view is that bacteria reallocate their proteome to the functional areas most limiting growth, weighted by global constraints from cellular organisation. In the context of gene expression, it means there is a trade-off between the cost of maintaining the expression of a given gene, and the gain by its function, whether a metabolic gene or ribosomal gene. This perspective has been useful in understanding a variety of physiological processes, for example, the relation between respiration and fermentation (Basan et al., 2015a), the control of biosynthesis pathways (Li et al., 2014), the transition between different nutrient sources (Erickson et al., 2017a; Korem Kohanim et al., 2018) and the response to osmotic stress (Dai et al., 2018).

1.4.2.3 Response to translational limitation by antibiotics

Growth can be reduced by a number of perturbations, not just changes in nutrient quality, meaning that the correlations described between ribosome expression and growth rate are not necessarily conserved. For example, to antibiotics inhibiting translation by targeting ribosomes. Cells respond to this inhibition by increasing ribosome expression as a compensating mechanism, probably by reducing further ppGpp levels after translational inhibition (Scott et al., 2010; Greulich et al., 2015).

1.4.2.4 Response to protein overexpression

Sufficient levels of ectopic gene induction reduce growth rate as a result of diverting cellular resources into proteins that do not contribute to metabolism, which is commonly referred to as “metabolic burden” (Bentley et al., 1990; Ceroni et al., 2018). Similar to the observations made for chloramphenicol, fast-growing bacteria are more sensitive to the burden of protein overexpression (Scott et al., 2010).

Interestingly, the burden of protein overexpression was shown to increase cell size and DNA content, whereas the size of cells treated with chloramphenicol was unaffected (Basan et al., 2015b). Both cell size and DNA content could be explained by the

hypothesis that DNA replication partially controls cell size (Bremer and Churchward, 1991; Si et al., 2017) meaning protein overexpression could affect DNA replication initiation or DNA synthesis speed. Recently, the transcription profile of cells under overexpression burden has been studied, revealing induction of genes controlled by sigma factor σ32, which is associated with a number of stressful conditions, such as abundant protein miss-folding, heat shock, and carbon starvation (Zhang et al., 2014). Interestingly, chaperones induced by σ32 have been observed to interact with DnaA (initiator of DNA replication)(Grudniak et al., 2015), and DnaA-ATP represses transcription of the σ32 core subunit (Wang and Kaguni, 1989), which could be the mechanistic link between metabolic burden, cell size, and DNA content.

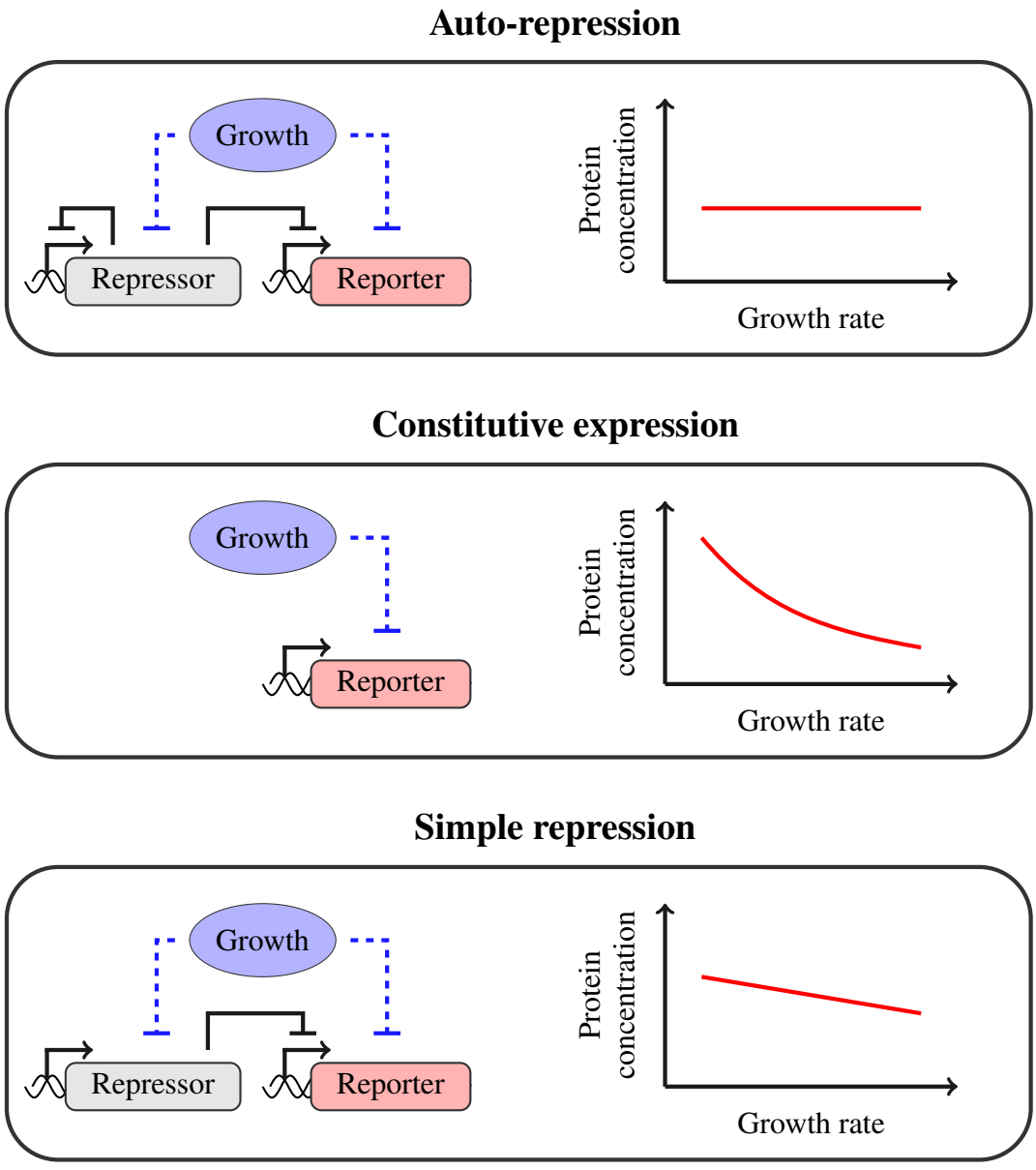

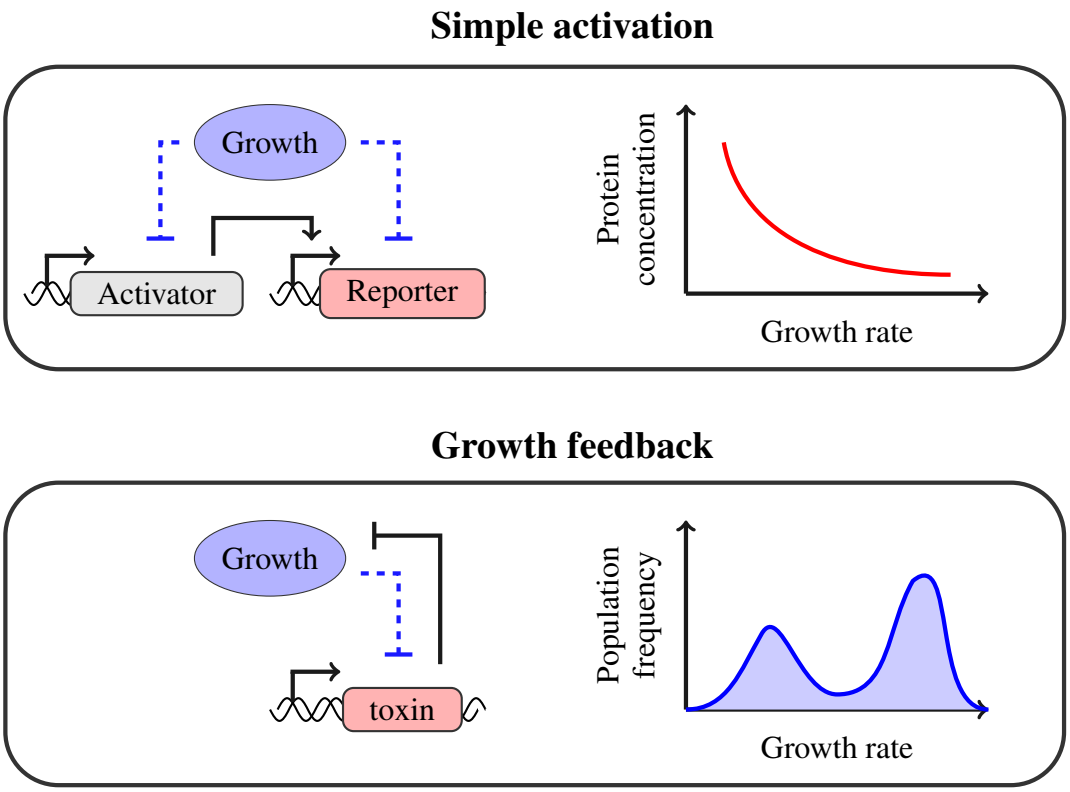

Figure 1.8: **Influence of growth on gene-expression by resource allocation**. Diagram illustrating the expected profile of protein concentration expressed from genes with different kinds of transcriptional regulations. Diagrams were adapted from (Klumpp and Hwa, 2014).

1.4.2.5 Global concequences of resource allocation in gene expression

As resources for gene expression are limited, the allocation towards protein synthesis genes has an overall negative impact on gene expression, simply as from mass balance considerations (Scott et al., 2010; Keren et al., 2013). The negative impact is most dramatic for genes whose expression is not regulated (constitutive). The outcome from resource allocation constraints on regulated genes would depend on the dominant regulatory mechanism. Examples of the expected influence of growth condition on gene-expression are illustrated in figure 1.8. In general, genes negatively regulated can increase their expression with growth rate, whereas genes positively regulated would follow the opposite trend. The dependency on growth can be largely alleviated by negative feedbacks, such as those from auto-repressors which are a common motif in bacteria (e.g. SOS repressor LexA). Positive feedbacks are common motifs for switch-like behaviour, and in certain conditions can generate bi-stability (Ferrell,

2002). Genes whose product are toxic for growth can lead to positive feedbacks, given that more expression reduces growth and increase in growth can decrease its expression. This has been observed for synthetic regulatory circuits (Tan et al., 2009), and has been proposed to occur in natural toxic genes (Klumpp et al., 2009).

1.4.3 Coupling DNA replication, growth, and division

Duplicating the chromosome and segregating each copy into daughter cells is a necessary step for growth and division. This implies that DNA replication and growth are to be coordinated. *E. coli* has evolved sophisticated mechanisms to ensure its only chromosome is correctly replicated and segregated so that one copy is passed to each daughter cells (Reyes-Lamothe et al., 2012).

Early studies of DNA synthesis during transitions in media composition hinted at the existence of some element that needed to be accumulated in order to initiate DNA replication (Cooper, 1969), that is DnaA-ATP and perhaps other factors such as Fis (Rao et al., 2018). The control of DNA replication involves several overlapping layers of regulation, integrating diverse cellular functions, and new mechanisms continue to be discovered (reviewed in Skarstad and Katayama (2013); Hansen and Atlung (2018). Over the years, several mathematical models attempting to explain the cycle of DNA replication initiation have been proposed, however, it remains unclear exactly how the frequency of DnaA-ATP oscillations are set (Bremer and Churchward, 1991; Hansen et al., 1991; Donachie and Blakely, 2003; Grant et al., 2011).

1.4.3.1 Cooper and Helmstetter model

Fast-growing *E. coli* can replicate its chromosome in 40 minutes. However, *E. coli* can divide in 20 minutes in rich nutrient conditions. Fast-growing bacteria manage to solve this problem by overlapping rounds of replication (figure 1.9). This was first proposed in Cooper and Helmstetter (1968) from measurements on the rate of DNA synthesis in synchronised cell populations (Helmstetter, 1967; Helmstetter et al., 1992). The proposed model became known as the “Cooper and Helmstetter” (C&H) model.

The C&H model relates the timing of chromosomal replication with growth rate, by assuming a constant DNA synthesis rate ($1/C$) and constant period (D) between the completion of chromosome replication and cell division. For different formulations

of this model see Jun et al. (2018). The C&H model predicts that within a population of growing cells chromosomal regions closer to the origin are more abundant than those in the terminus, which has been verified by several methods of DNA quantification (Chandler and Pritchard, 1975; Rudolph et al., 2013; White et al., 2018). The difference in DNA copies per cell across the genome (gene dosage) appears to offer an evolutionary bias, for genes related to growth processes appear to be most commonly found near the origin of replication in many fast-growing bacteria (Rocha, 2008).

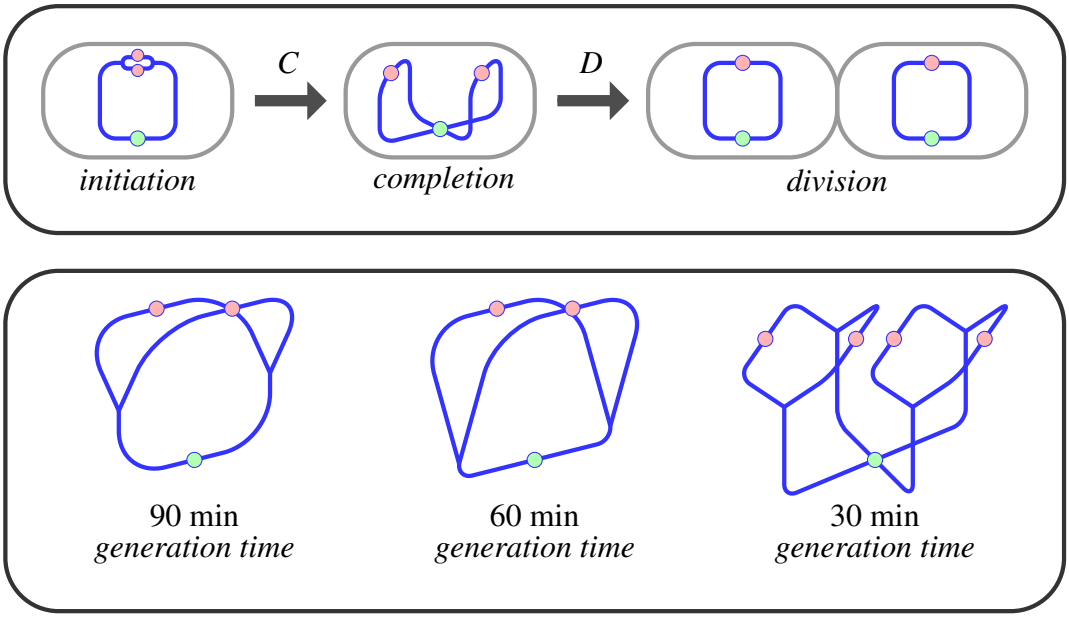

Figure 1.9: **Cooper and Helmstetter model of DNA replication**. Schematics illustrating Cooper and Helmstetter model of DNA replication. The time it takes to replicate the chromosome is assumed to be constant (C) and also a fixed delay between replication reaching terminus and cell division is assumed (D). At the bottom, the expected state of the chromosome at the middle of the cell cycle is illustrated for different generation time ($C = 40$ minutes, and $C = 20$ minutes)

It is important to mention that values for C and D periods may depend on the specific growth conditions. These are approximately constant only at relatively fast growth regimes ($\geq 1/hr$ doubling rate), and have been observed to increase in slower growth conditions (Helmstetter, 1996; Michelsen et al., 2003; Stokke et al., 2012)). Adding this correction, the C&H model appears to be consistent with currently available measurements.

1.5 Motivation and scope of this thesis

The stability of a cell lineage depends on their capacity to grow and proliferate in different conditions. This depends on their capacity to respond accurately to stressful conditions, such as when confronted with antibiotics. Previous reports indicate that susceptibility to DNA-damaging agents is dependent on growth conditions. The reasons for this effect could be multiple, as changes related to growth can affect the likelihood of DNA damage by affecting DNA replication, and the ability of cells to activate the expression of the SOS regulon, which is important for tolerating damage. Previous studies using fluorescent reporters for SOS expression have revealed considerable single cell variability, and the impact of growth condition on SOS expression in single cells has not been evaluated. Understanding quantitatively the ways cell physiology and the SOS response are coupled is relevant in the context of bacterial infection treatment; as many antibiotics target DNA and the activation of the SOS response can lead to genetic instability and antibiotic persistence.

Chapter 2

Materials and methods

2.1 Growth conditions

For strain and plasmid construction cells were grown in LB, or LB agar supplemented with the corresponding selection markers. Unless stated otherwise, concentrations employed for antibiotics were: ampicillin 100 μg/ml, kanamycin 50 μg/ml, chloramphenicol 30 μg/ml, and gentemycin 10 μg/ml. All actual measurements where done using M9 media: (49 mM Na_2HPO_4, 22 mM KH_2PO_4, 8.6 mM NaCL, 19 mM NH_4CL, 2 mM $MgSO_4$, and 0.1 mM $CaCL_2$). M9 media was supplemented with either 0.5% w/v glycerol, or 0.5% w/v glucose, or 0.5% w/v glucose and a mix of amino-acids (1X MEM Non-Essential Amino Acids and 1X MEM Amino Acids, both manufactured by Gibco®). Otherwise LB media was used (per litter: 10 gr Bacto® tryptone, 5 gr Oxo® Yeast extract, 10 gr NaCl, and pH corrected to 7.2 with NaOH).

For experiments in balanced growth conditions, cells were taken from frozen stocks at -80 C, and grown 10-16 hours in LB media. Then they were grown overnight in their respective M9-based media, plus any antibiotic in case of a selection marker. Overnight cultures were diluted 1:200 in fresh media (without antibiotic), and grown until OD_{600} 0.1 (approximately three division times). From there, they were diluted in fresh media and experiments performed the next day, after at least 12 division times. Any additional agent such as ciprofloxacin or chloramphenicol was added at this step. Dilution factors were approximately 10^4, 10^5, and 10^6-10^7 for media supplemented with glycerol, glucose, and glucose+amino-acids respectively. Samples were not allowed to reach OD_{600} higher than 0.1-0.15, and were re-diluted when necessary. All experiments were carried out in 50 ml falcon tubes agitated at 37°C, with no more than 5 ml volume, with exception of samples collected for RecA ChIP-seq experiments, where 1L glass flasks where used to grow 100 ml of culture.

2.2 Plasmid construction

Plasmids were constructed following a similar strategy based on Gibson assembly (Gibson et al., 2009). Backbone vectors were digested with two restriction enzymes and gel-purified. Single insert for construction of clone-integration plasmid were amplified by PCR, with 20-40 basepair homology overhangs for Gibson assembly. Similarly deletion vectors by PMGR were amplified by colony PCR, with products having 300-500 bp homology to regions flanking the gene of interest. Exceptions are plas-

mids for integration of *recA* fusions using PMGR (pSJR096 and pSJR097), where the whole vector was amplified by PCR instead of using enzyme digestion. Details of construction for each plasmid can be found in table A.2.

2.3 Strain construction

E. coli MG1655 was used as wild type strain, unless when testing *sbcDC* induction with arabinose. For strain construction, gene expression reporters were inserted into the genome by clone-integration (CLI) (St-Pierre et al., 2013). Insertion of interrupted palindromes *ascB::pal246* and *lacZ::pal246* was done via P1 transduction. All other genetic modifications were performed by plasmid mediated gene replacement (PMGR) Merlin et al. (2002).

2.4 Microscopy and microfluidics

2.4.1 Microscopy

All images were captured using a Nikon Ti-E inverted microscope equipped with EMCCD Camera (iXion Ultra 897, Andor), a SpectraX Line engine (Lumencor) and a 100X Nikon TIRF objective (NA 1.49, oil immersion). Nikon Perfect-Focus system was used for continuous maintenance of focus. The filter set for imaging GFP consisted of ET480/40x (excitation), T510LPXR (dichroic), and ET535/50m (emission); whereas for mKate2 the set ET572/35x (excitation), T590LPXR (dichroic), and ET632/60m (emission) was used. Filters used were purchased from Chroma. GFP fluorescence was measured using 80 milliseconds exposure, whereas mKate2 fluorescence was imaged for 100 milliseconds, both at minimal gain and maximum lamp intensity. Microscope was controlled from MATLAB via MicroManager (Edelstein et al., 2010) using a custom made user interface. Code accessible at `https://gitlab.com/MEKlab/MicroscopeControl`.

Unless specified, samples were mounted on agar-pads for imagining. In particular, 5-10 μl from cultures near OD_{600} 0.05 were placed in 1% agarose pads (Gene-frame 65 μl) made with the corresponding media. About 150-200 stage positions were imaged per sample, comprising a total of 3000-6000 cells.

2.4.2 MACS: Microfluidics-Assisted Cell Screening

Implementation of MACS was done similarly to what was described in (Okumus et al., 2016, 2018). The basic principle is to trap cells into the field of view using a pneumatic valve. This achieved by having a microfluidic device composed of two layers, one open ended where the sample flows, and a second on top closed on one end which collapses into the lower layer when pressured (see figure 2.1 for schematics). Minor modifications from published method were made regarding the loading of samples, as we manually added them into tube connected to the flow channel. Another difference was washing in between samples, as we manually remove the needle connected to the flow channel was manually removed and connected to waste collector. With exception of manual steps, valves for air pressure control (solenoid valve, SMC S070B-58C), valves for liquid flow control (solenoid valve, LEE LFAA1201418H), and a fixed displacement pump (50 μl pump, LEE LPA2420050L), were controlled from MATLAB with the help of a Data acquisition processor (Measuring Computing USB-140FS), and an electronic circuit modulating the devices source voltage (see diagram in figure 2.2). Full electronic circuits, plus 3D printed accessories, such an stage adapter and holders, can be found at `https://gitlab.com/MEKlab/Microfluidics/tree/master/Accessories`.

This is a full overview of the protocol used for image acquisition. Before using a flow channel, 0.5 ml of phosphate saline buffer (PBS) plus 20 mg/ml bovine serum albumin (BSA) was flushed thought, which acted as a surfactant agent preventing cells from getting attached to the PDMS during compression. Then the path connected to the flow channel was washed 6 times with 1ml of water, and 6 times with 1 ml of media. For each sample, 1 mg/ml of BSA was added before loading the sample into the sample tube. The flow and pneumatic valve pressures (P_f and P_v) were manually calibrated for each experiment (typically 10-15 psi). The pneumatic valve pressure was set for the first sample of the experiment, and used for the rest of the experiment. Typically cells were collected for about 1-3 seconds, and 1 second was allowed before image acquisition to relax cells into their final position, and then cells were released by flowing media for 0.5 seconds. This cycle was repeated about 150 times. For each sample leading to acquiring 5000-20000 cells per sample. In between samples, the path was rinsed consecutively 6 times with 1 ml of PBS + 10% ethanol, 6 times with 1 ml of water, and 6 times with 1 ml of media.

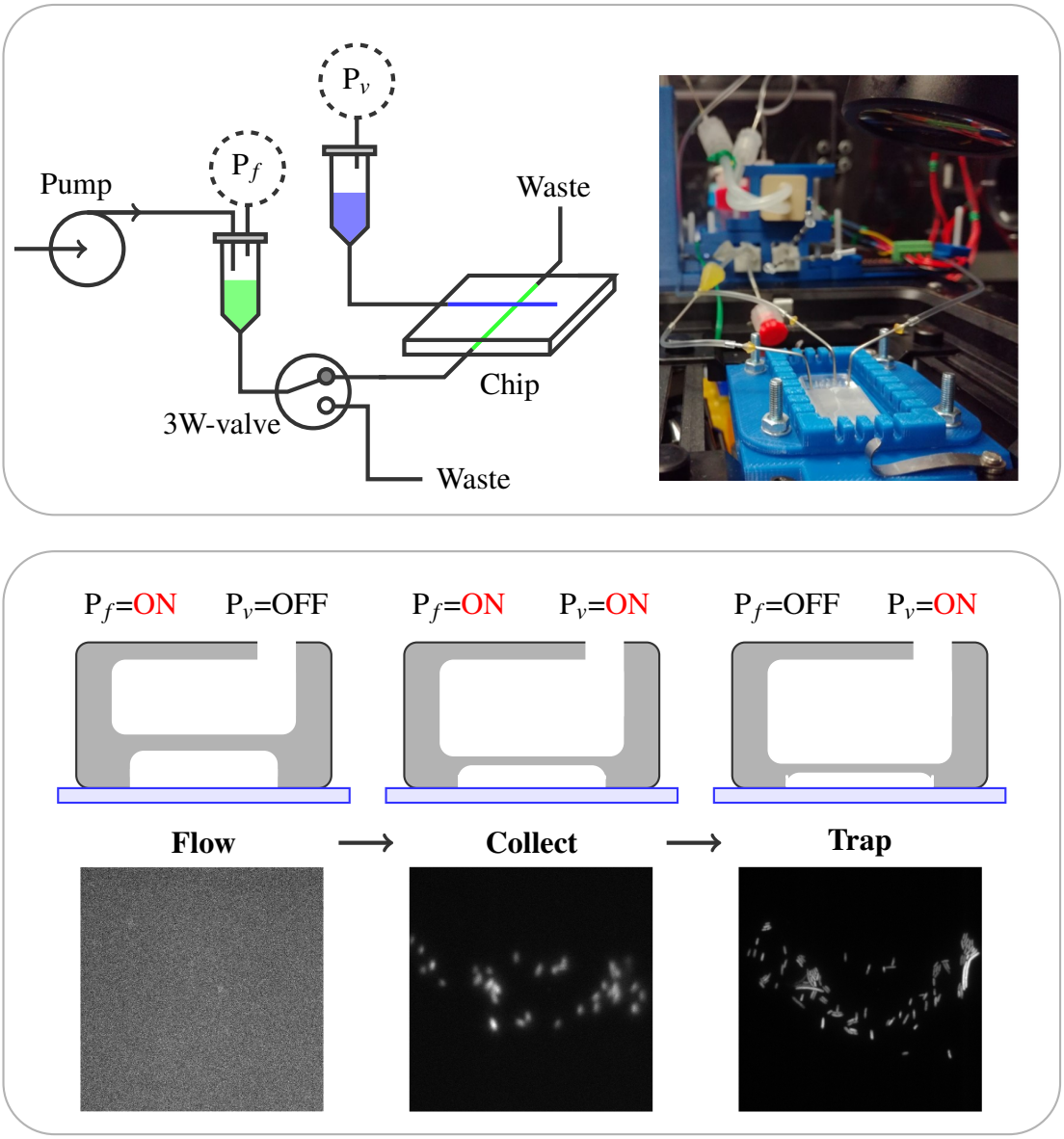

Figure 2.1: **High throughput sampling with MACS**. Microfludic setup for high throughput image acquisition. (**Top**) Microfluidic chip with two layers: one open ended (flow channel, in green), and a second closed in one end (valve layer, in blue). Air pressure on each channel is controlled using ON/OFF valves. On the right is a picture of such chip mounted in the microcope for reference. (**Bottom**) Schematic of acquisition cycle. In a first stage, the sample is flushed through to remove any cells attached. Then the top layer is pressured, such that it compresses the bottom layer flowing perpendicularly, leading to cell accumulating within the field of view. Finally the pressure on the flow channel is set OFF, which fully collapses the channel trapping cells, at which images are acquired.

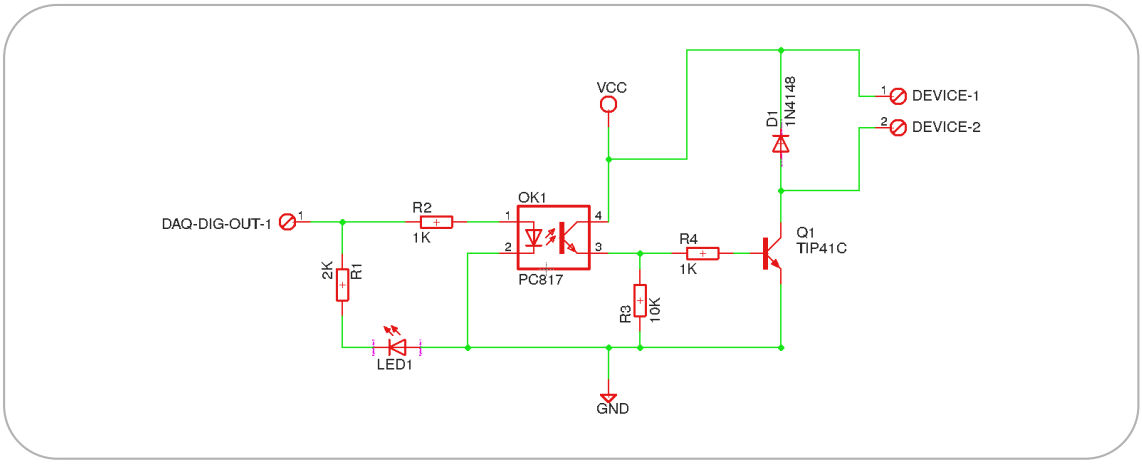

Figure 2.2: **Commutator for controlling electronic devices**. Diagram of the electronic circuit for controlling power source of one device (*e.g.* pump or valve) using the digital output of a Data acquisition processor (DAQ). An opto-isolator and a transistor serve to connect the device to ground only when DAQ output is ON (3-5 Volts). Intended VCC source is 24 Volts. Design by Jhony Oswaldo Turizo Tenjo from Universidad de los Andes, provided by Juan Carlos Arias Castro.

2.4.3 Mother machine

For mother machine experiments, silicon wafer was provided by Alex McVey (T. Pilizota lab, University of Edinburgh). Growth chambers were 1.05 μm in height, approximately 0.9 μm in width and 25 μm in depth, which were suitable for cells growing in M9+glucose media. 5 ml of culture were grown to balanced growth and left until $OD_{600} \approx 0.2$-0.3. Before loading cells into the device, a 0.1% of Tween was added to culture as surfactant agent. Then cells were centrifuged and re-suspended in 0.5 μl. Concentrated culture was injected into the device, and centrifuged at 3220$\times$g for 10 minutes, in order to load them into the chamber. Then the device was connected to a peristaltic pump on one end (Ismatec IPC ISM932D), and to fresh media + 0.1% Tween on the other end, in order to flow fresh media through the device. Peristaltic pump rotation speed was set to 5% of its maximum rate, and internal diameter of the peristaltic tube was 0.44 mm. Cells were left for 5-6 hours before imaging.

2.4.4 Image analysis

In order to automate the detection of cells from fluorescent images (cell segmentation), we developed a custom algorithm based on edge-detection using low-pass filters

(detailed in algorithm 1) and a graphical user interface to facilitate manual curation of the segmentation (see figure 2.3).

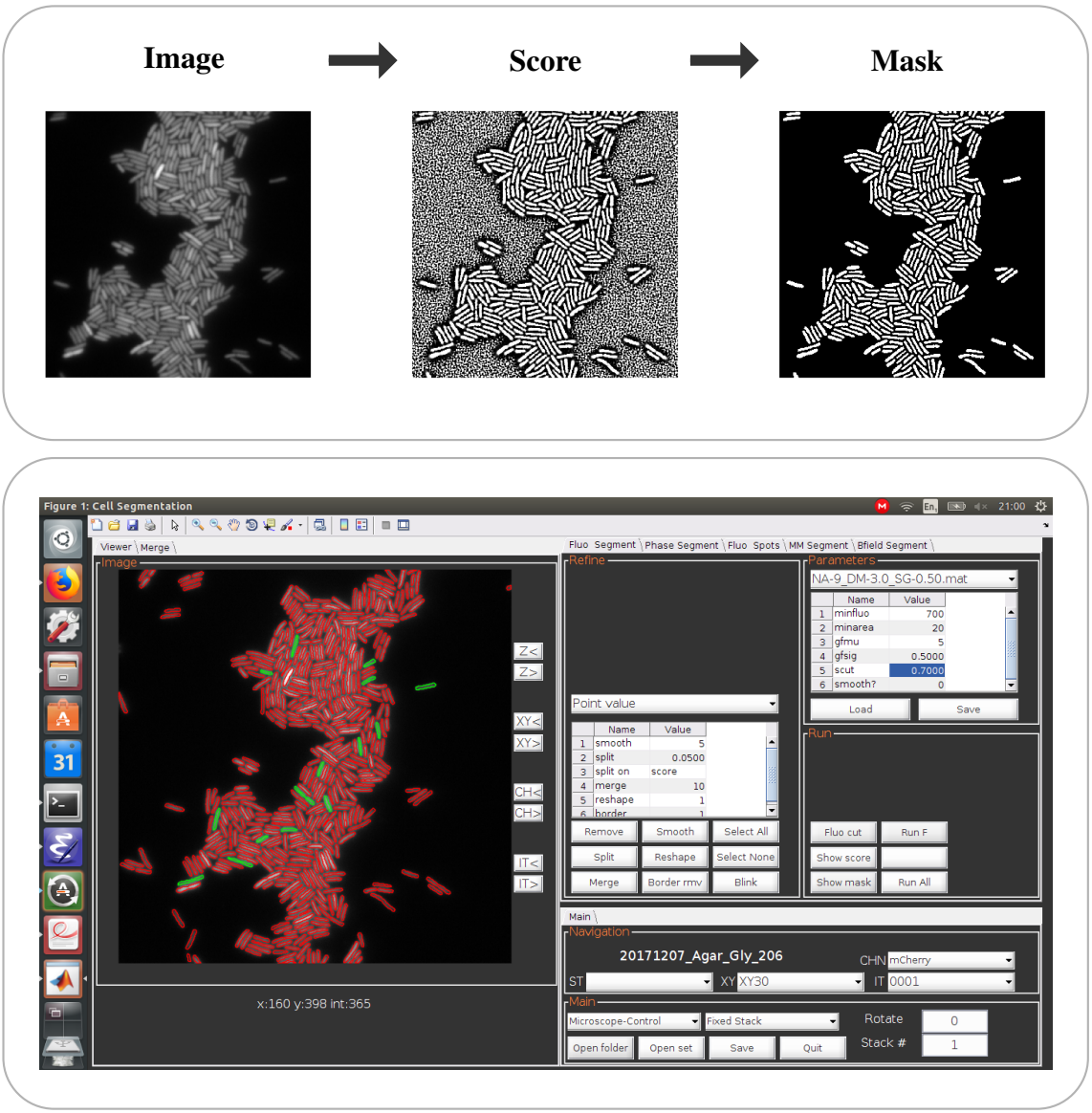

Figure 2.3: **Semi-automated cell detection**. **Top)** Example of computed score and mask for a given image. **Bottom)** Snapshot of the graphical user interface in MATLAB. In addition to facilitate finding correct parameters, it is possible to perform operations in individually selected cells, such as “remove”, “smooth”, and “merge”. Selected cells appear in green, whereas not selected are in red.

The algorithm was designed to detect cell edges using a custom convolution filter, that compares each pixel value relative to its neighbours. This strategy was inspired on Gabor filters (Lee, 1996), but instead of using trigonometric functions, the filter is

constructed by summing many 2D Gaussian distributions, with mean position moving from the center of the filter with an angle (see pseudocode 2). From the filtered image at each orientation, a score is computed that is able to distinguish local edges (see example in top panel figure 2.3). Then, a threshold is applied to the score to generate a mask from which cells are identified as individual connected components. Finally, the resulting segmentation is manually curated to remove any potential misidentified cell (GUI snapshot in figure 2.3).

For single-cell fluorescence quantification the mean intensity per pixel was used as a measure of fluorescent protein concentration. For images taken using MACS, this value was subtracted by its mean local background, which was necessary for getting reproducible measures. Local background was estimated by dilating each connected component by a factor of 1.3, and computing by the mean intensity along the border. About 3-15% of cells resulted in negative values, due to the presence of a neighbouring brighter cell. These were discarded from the analysis. Despite of this caveat, we found that correcting for background locally yielded more reproducible single-cell quantification using MACS.

Algorithm 1: Cell segmentation from fluorescence image.

Algorithm for segmenting a fluorescent image using an array of spacial low-pass filters. It takes any image as input, plus seven parameters, and returns a mask containing where regions that appears as "valleys" in the intensity landscape have been removed

Require: Input image: img. Parameters: minimum intensity value i_0; μ and σ (gaussian filter); pixel length d, width w, and set of angles $A = \{A_1, A_1 + \pi\}$ (for low pass filter); and a score threshold s_0. Some predefined functions: IMFILTER that applies a convolution filter to an image; GAUSSFILTER that return a gaussian filter; THRESHOLD that thresholds an image returning a boolean matrix; LOWPASSFILTERS that computes custom low-pass filters (see algorithm 2); IMCOMPLEMENT that computes the complement of an image; POSBOOL that returns one if the value is positive; PAIRWMULT that computes the pairwise multiplication of matrices; and PAIRWDIV that computes the pairwise division of matrices.

1: **function** SEGMENTATION_MASK(img,i_0,μ,σ,d,w,A,s_0) ▷ Returns $mask$

2: $img \leftarrow$ IMFILTER(GAUSSFILTER(μ, σ), img) ▷ Filter image noise

3: $mask0 \leftarrow$ THRESHOLD(img, i_0) ▷ Threshold image

4: $Filts \leftarrow$ LOWPASSFILTERS(d, w, A) ▷ Set low pass filters

5: $na \leftarrow \text{LENGTH}(A)$ ▷ Number of filters
6: **for** $j \leftarrow 1$ to na **do**
7: $Fimg_j \leftarrow \text{IMFILTER}(Filts_j, img)$ ▷ Set of filtered images
8: **for** $j \leftarrow 1$ to $na/2$ **do**
9: $Himg_j \leftarrow Fimg_j + Fimg_{j+na/2}$ ▷ Sum opposite angles
10: $S_+ \leftarrow \sum_1^{na/2} \text{PAIRWMULT}(Himg_j, \text{POSBOOL}(Himg_j))$ ▷ positives sum
11: $S_- \leftarrow \sum_1^{na/2} \text{PAIRWMULT}(Himg_j, 1 - \text{POSBOOL}(Himg_j))$ ▷ negatives sum
12: $S_r \leftarrow \text{PAIRWDIV}(S_+, (S_- + 1))$ ▷ Ratio between scores
13: $S_l \leftarrow \text{LOG}(1 - S_r)$ ▷ Compute log ratio
14: $score \leftarrow \text{EXP}(\text{IMCOMPLEMENT}(S_l))$ ▷ Compute score
15: $mask \leftarrow \text{PAIRWMULT}(mask0, \text{THRESHOLD}(score, s_0))$ ▷ Final mask
16: **return** $mask$

Algorithm 2: lowpassfilters function.

Pseudocode for constructing an array of low pass filters. Each filter will compare each value relative to its neighbours, but only in an angle. Constructing the filter using a 2D Gaussian density function makes the filter less sensitive to image noise.

Require: Parameters: pixel length d, width w, and set of angles $A = \{A_1, A_1 + \pi\}$. Some predefined functions: GAUSSPROJ returning the integral of a 2D gaussian density function over a space grid centred with mean x, y and standard deviation w; and SUM2 that sums all elements of a matrix.

1: **function** LOWPASSFILTERS(d,w,A) ▷ Returns cell array $Filts$
2: $na \leftarrow \text{LENGTH}(A)$ ▷ Number of filters
3: $ngrid \leftarrow 2d + 1$ ▷ Size of filter
4: **for** $j \leftarrow 1$ to na **do** ▷ Compute filter for each angle
5: $Filts_j \leftarrow \text{ZEROS}(ngrid, ngrid)$ ▷ Initialise to zeros
6: $a \leftarrow A(j)$ ▷ angle
7: **for** $q \leftarrow 1$ to d **do** ▷ move from center to d
8: $x \leftarrow q * \text{COS}(a)$ ▷ X projection
9: $x \leftarrow q * \text{SIN}(a)$ ▷ Y projection
10: $Filts_j \leftarrow Filts_j + \text{GAUSSPROJ}(x, y, w)$ ▷ Accumulate 2D distributions
11: $\theta \leftarrow \text{SUM2}(Filts_j)$ ▷ Sum all values so far
12: $Filts_j \leftarrow \theta * \text{GAUSSPROJ}(0, 0, w) - Filts_j$ ▷ Final local difference filter
13: **return** $Filts$

2.5 Numerical simulation of reaction-based models

We have created a pipeline for numerical simulation of reaction based models in MATLAB. These models are fully defined by reaction rate functions, stoichiometric relations, and initial conditions. These are defined in a text file following a simple syntax. From there a set of functions import the model into MATLAB, compile and solve the corresponding ODE using the ODEMEX package (`http://bmi.bmt.tue.nl/sysbio/software/CVode.html`), and facilitate extracting values of interest after numerical ODE integration. The implementation, together with few examples, can be found at `https://gitlab.com/MEKlab/rxnm`. Part of this pipeline was implemented while doing an internship with Yaakov Benenson at ETH Zurich in 2013.

2.6 RecA ChIP-seq

For quantification of RecA binding across the genome, RecA Chromatin Immuno-Precipitation followed by deep sequencing (ChIP-seq) was performed. This work is part of a collaboration with Benura Azeroglu (D. Leach lab, University of Edinburgh).

2.6.1 Chromatin ImmunoPrecipitation

Cells were fixed by the addition of formaldehyde (final concentration 1%) for 10 min at 22.5°C to crosslink proteins to DNA. Crosslinking was quenched by the addition of 0.5 M glycine. Cells were then collected by centrifugation at 1500×g for 7 min before washing three times in ice-cold 1x PBS and re-suspending in 250 μl of ChIP buffer (10 ml ChIP buffer consists of 200 mM Tris-HCl (pH 8.0), 600 mM NaCl 4% Triton X and 1 cOmpleteTM protease inhibitor cocktail EDTA-free tablet). Samples were then sonicated using a Diagenode Bioruptor® at 30 seconds intervals for 10 minutes at high amplitude. After sonication, 350 μl of ChIP buffer was added to each sample and the samples gently mixed by pipetting. Immunoprecipitation was performed overnight at 4°C using 1/100 anti-RecA antibody (Abcam, ab63797). Immunoprecipitated samples were then incubated with Protein G Dynabeads® for 2 hours with rotation at room temperature. All samples were washed three times with 1 X PBS + 0.02% Tween-20 before re-suspending the Protein G Dynabeads® in 200 μl of TE buffer + 1% SDS. 100 μl of TE buffer + 1% SDS were added to the input samples and all samples were then incubated at 65°C for 10 hours to reverse the formaldehyde cross-links.

DNA was isolated using the Qiagen PCR purification kit according to manufacturer's instructions. DNA was eluted in 100 μl of TE buffer using a 2-step elution. Samples were stored at -20°C. Two biological repeats of each strain were acquired.

2.6.2 Illumina ChIP-seq Library Preparation

Libraries of the immunoprecipitated DNA were made using NEBNext® ChIP-Seq library preparation kit. Briefly, the samples were first subjected to end repair to fill in ssDNA overhangs, remove 3' phosphates and phosphorylate the 5' ends of DNA. Klenow exo- was used to adenylate the 3' ends of the DNA and NEBNext DNA adaptors (provided in the NEBNext Multiplex Oligos for Illumina kit) were ligated using T4 DNA ligase. After each step, the DNA was purified using the Qiagen MinElute PCR purification kit according to the manufacturer's instructions. After adaptor ligation, the adaptor-modified DNA fragments were enriched by PCR using primers (provided in the NEBNext Multiplex Oligos for Illumina kit) corresponding to the beginning of each adaptor. Finally, agarose gel electrophoresis was used to size select adaptor-ligated DNA with an average size of approximately 350 bp. All samples were quantified on a Bioanalyzer (Agilent) before being sequenced on Illumina® NovaSeq6000 by Edinburgh Genomics.

2.6.3 Mapping read and estimating RecA enrichment

50 bp pair-end reads were mapped to the *E. coli K12 MG1655* (NC000913.3) genome using Novoalign version 2.07 (`www.novocraft.com`). Novoalign uses the Needleman-Wunsch algorithm to determine the optimal alignment of reads. Sequences were mapped with default parameters, allowing for a maximum of one mismatch per read. In order to report reads that have multiple alignment loci we specified the r parameter as "Random" thereby equally disturbing these hits to all locations (Webb et al., 2014). PyReadCounters was used to calculate the overlap between aligned reads and *E. coli* genomic features.

After mapping reads to the genome, these were binned over a 100 base pairs intervals across the genome. To smooth the curves, these were averaged by a 100 invervals moving window, equivalent to 10^4 base pairs. RecA enrichment was defined as the relative frequency of smoothed reads, relative to the corresponding value for wild-type

in the same condition.

2.7 Antibiotic tolerance assay

To measure antibiotic tolerance to Ampicilin, cultures in balanced exponential growth were exposed to the antibiotic and the fraction of surviving cells was quantified by serial dilution and counting colony forming units on LB plates. For each time-point two parallel serial dilutions were done, and 100 μl was taken from two dilution factors (1:10 steps) to ensure good spreading of colonies on plate. Liquid was spread using 5 to 10 sterile beads. Plates were incubated at 37°C, and colonies were counted after 24 hrs, and a second time after another 24 hrs in case new colonies appeared. The average from all countable plates (less than 200 colonies per plate) was used to calculate the concentration of viable cells. For each experiment ampicillin was dissolved from powder in distilled water on the same day and stored at 4°C to prevent decay.

Chapter 3

The SOS response to quinolones is influenced by growth

3.1 Introduction

Bacteria are able to respond and adapt to stressful situations, such as antibiotic toxicity. Most antibiotics target growth-related processes, meaning growth conditions could influence the susceptibility to antibiotic stress. In general, fast-growing bacteria have been shown to be more sensitive to DNA damaging agents (Sufya et al., 2003; Sutera and Lovett, 2006). This increase in sensitivity is consistent with observations that the processes involved in DNA replication are the main mechanisms leading to lethal DNA lesions, e.g. double-strand breaks (DSBs) (Kuzminov, 2001; Michel et al., 2004, 2018). The frequency of DNA replication correlates with growth rate, which could increase the likelihood of DSBs by increasing growth rate. However, changes in growth conditions could also influence the capacity of cells to induce the SOS response, which is important for cells to survive DNA damage. The reason SOS induction may be limited is because of global constraints on gene expression imposed by re-allocation of resources towards translation in fast-growing cells (Scott et al., 2010; Klumpp and Hwa, 2014). Understanding how factors influence induction of the SOS response may provide useful insights into how survival after DNA damage may vary in different conditions.

Experiments monitoring SOS expression using fluorescent reporters in single cells have revealed considerable single-cell variability in SOS induction, both under spontaneous DNA-damage (Pennington and Rosenberg, 2007), and when DNA-damage is induced by an exogenous agent (Friedman et al., 2005; Kamenšek et al., 2010; Culyba et al., 2018). This may be a result of single-cell variability in DNA damage, DNA-repair, or intrinsic to the SOS pathway. The role that growth conditions may play in the variability of SOS has not been explored, and could be of relevance in understanding how growth conditions may influence downstream effects of SOS, such as survival to DNA-damage, mutagenesis, and antibiotic persistence.

3.2 Influence of growth in spontaneous SOS induction

In order to quantify the expression of SOS genes, we decided to use transcriptional fusions of SOS promoters to mGFP (P_{recA}, P_{recN}, P_{sulA}). From fluorescence intensity per unit of area, we get an approximation of mGFP concentration inside the cell. In order to evaluate the influence of growth conditions in SOS expression, we measured

the levels of fluorescence in steady-state populations grown with different nutrients: glycerol (doubling time approximately 100 minutes), and glucose plus amino-acids (doubling time approximately 35 minutes). As changes in growth have global effects on gene expression, we also quantified the levels of a fluorescent protein transcribed from a constitutive promoter (P_{tet01}-*mKate2*).

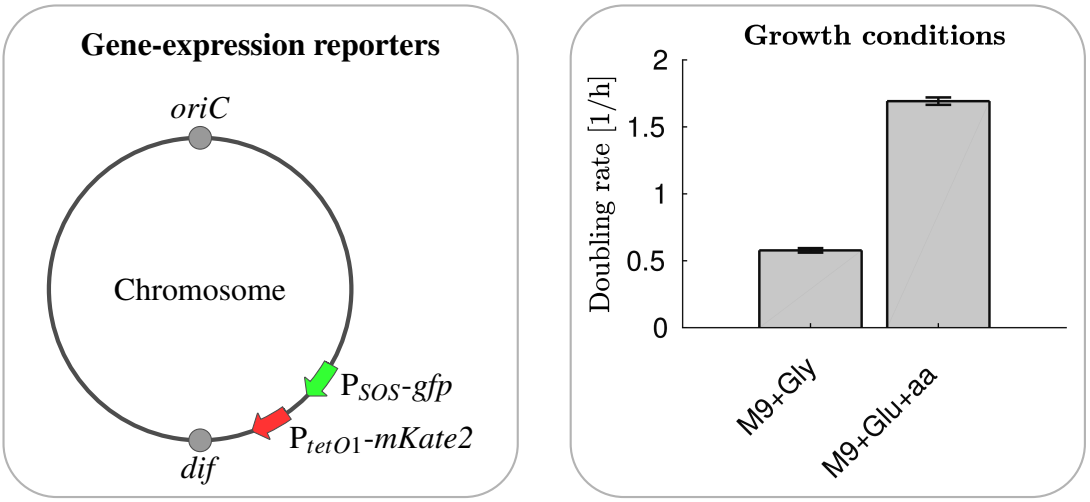

Figure 3.1: **Monitoring the influence of growth conditions on SOS and constitutive gene expression**. Transcriptional fusions to SOS and constitutive promoters were inserted in *E. coli* chromosome. Two growth conditions differing in nutrient quality were used to study the effect of growth: glycerol (slow), and glucose with amino-acids (fast).

3.2.1 Median SOS induction without damage is independent of growth rate

Consistent with the principle of resource allocation Scott et al. (2010), we have found that expression from our constitutive reporter P_{tet01}-*mKate2* negatively correlates with growth rate (right panel, figure 3.2).

Negative feedback such as the ones controlling the transcription of SOS genes (via LexA) are expected to compensate for resource allocation constraints (Klumpp and Hwa, 2014). Indeed, we find the concentration of mGFP reporters transcribed from three SOS promoters to be largely independent of growth conditions (left panel, figure 3.2). Consistent with previous reports, we find that basal expression of the *recA* promoter is relatively higher when compared to *sulA* and *recN* (Huisman et al., 1982; Fernández De Henestrosa et al., 2000; Culyba et al., 2018). The difference between

P_{recA} and P_{sulA}, is most likely the result of the difference in binding affinity of LexA. Low basal expression from P_{recN} promoter can be explained by the fact it contains two binding sites for LexA. In fact, the level of fluorescence measured from the P_{sulA} and P_{recN} promoters was almost identical to auto-fluorescence in this channel (data not shown), evidencing the strong repression of LexA in this promoters.

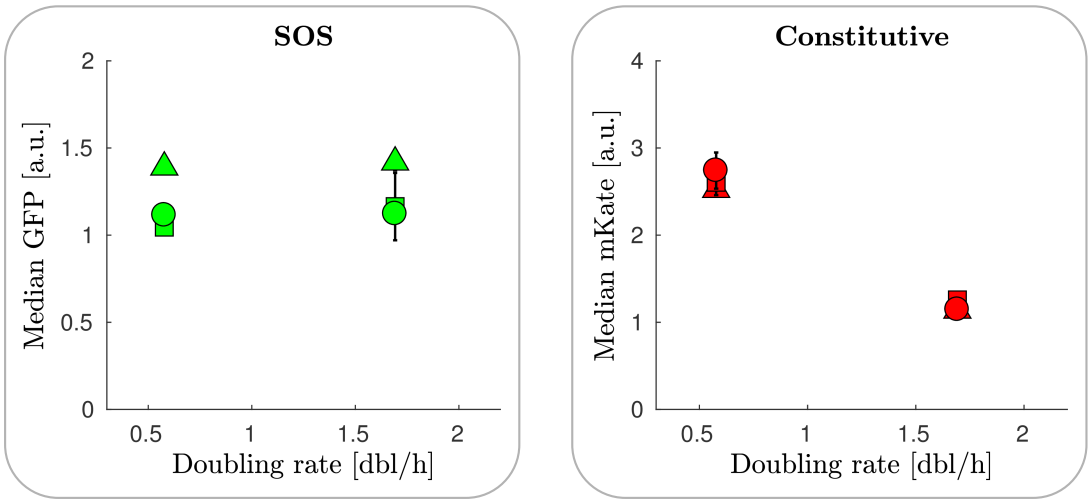

Figure 3.2: **Basal levels of SOS expression are invariant to changes in growth conditions**. Expression of constitutive and SOS reporters in slow-growing and fast-growing conditions. Data points are the average ± standard error of three biological repeats. **(Left)** Expression from three SOS promoters are approximately constant (P_{recA}, P_{recN}, and P_{sulA}). The dotted line was obtained using slow-growth values as reference. **(Right)** Constitutive expression is inversely proportional to the doubling rate (dotted line). The dotted line was obtained using slow-growth average value as reference.

3.2.2 Cells with spontaneous SOS-induction are more frequent in slow-growing conditions

Spontaneous SOS induction has been reported to be very rare, within the order of 1% of the population (Pennington and Rosenberg, 2007). Thus, we decided to evaluate in more detail the distributions of SOS-induction in single cells. Consistent with the observations for the population median describe above, we observed that the distributions of SOS for the majority of the population are comparable across growth conditions (top panel, figure 3.3). The only exception appears to be P_{sulA} expression, where the distribution shows a longer tail in slow-growing conditions.

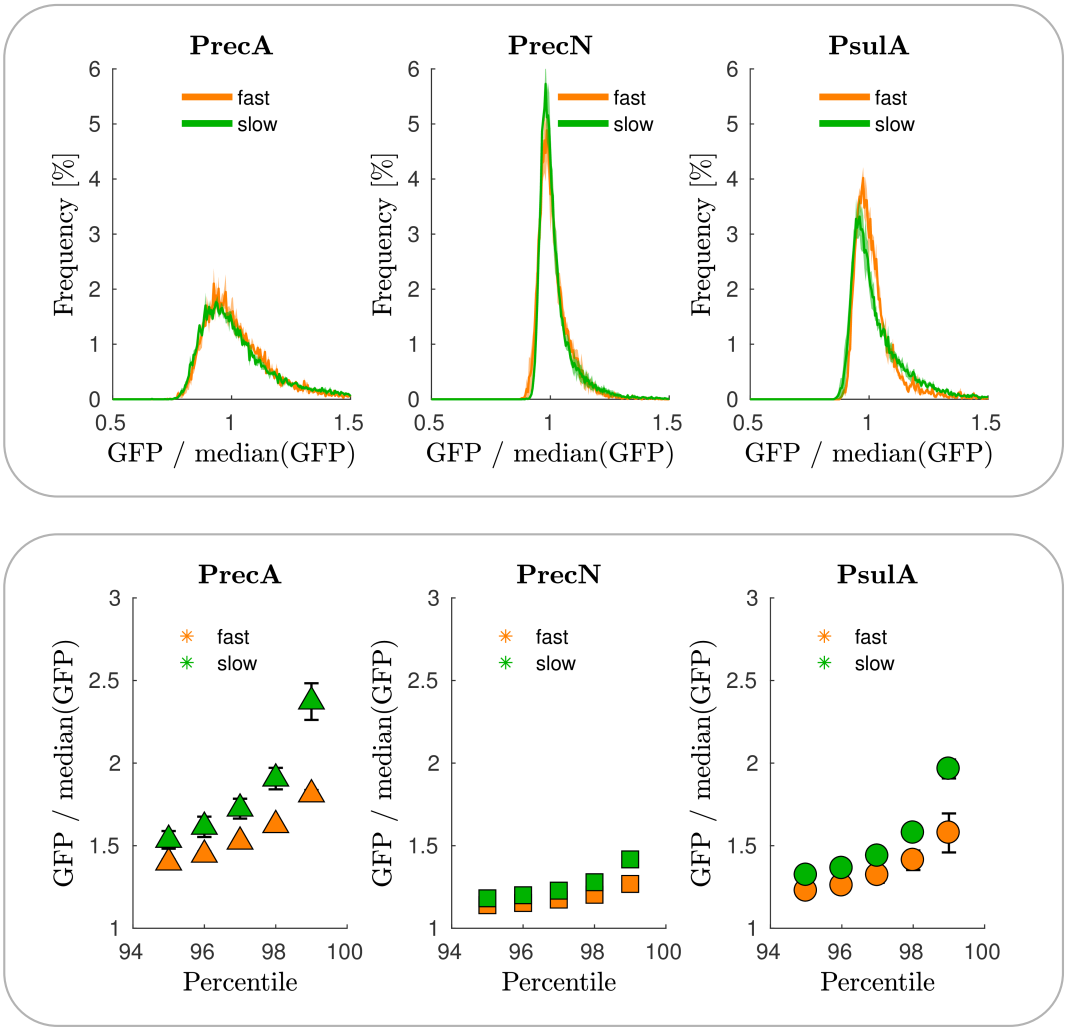

Figure 3.3: **Cells with spontaneous SOS-induction are more frequent in slow-growing conditions**. **(Top)** The distributions of SOS expression in single-cells relative the population median are comparable across growth conditions. The relative frequency of three biological repeats were averaged while making this plot. **(Bottom)** However, the SOS expression levels for the high-end of the distribution is affected by growth conditions. At the same percentile, higher SOS expression is more frequent in slow growing conditions. Data points are the average $\pm$ standard error of three biological repeats.

Despite the apparent similarity for the majority of populations, we found that the cells with very high SOS expression are more frequent in slow-growing conditions (top 1-2% of the population, bottom panel in figure 3.3). This difference is most pronounced for P_{sulA} reporter, then for P_{recA}, and less noticeable for P_{recN}. This order is consistent with expectations of LexA binding affinities for these promoters: P_{recN} has two binding sites; and the basal expression from P_{recA} is higher than P_{recN}. We ob-

served that this trend was not presented in a background unable to induce SOS (*lexA3*), indicating that these differences indeed reflect spontaneous SOS induction (data not shown).

Because of the frequency in DNA-replication, one may have expected that spontaneous SOS induction would be more frequent in fast-growing conditions. However the mechanism for spontaneous DSBs are not understood in detail, so DNA-replication may not be the limiting factor. It is possible that not all events of RecA activity lead equally to SOS induction. Supporting this view, we found that deleting *recA* reduces population growth rate by 30%$\pm$10, whereas we could not detect a significant difference in slow-growth conditions (data not shown). This speaks of a higher requirement for homologous recombination in fast-growing cells, yet we find high SOS cells more frequent in slow-growing conditions. We believe this indicates that SOS induction may intrinsically be more variable in slow-growing conditions, either as a result of variability in the duration of the SOS signal (RecA-ssDNA) or some other mechanism.

3.2.3 SOS expression in the absence of LexA appears to be independent of growth rate

One open question is whether SOS promoters are limited by resource allocation in the same way constitutive promoters are. In that case, it could help explain why high SOS-induction is more abundant in slow-growing conditions.

In order to confirm that expression of SOS genes is equally limited as constitutive genes by changes in growth conditions, we decided to quantify the maximum SOS expression in the absence of LexA. Our expectation was that deleting *lexA*[1] should remove the negative feedback regulating SOS genes, resulting in equal susceptibility to changes in resource allocation as constitutive genes. Unexpectedly, the levels of SOS expression where unaffected when comparing slow-growing and fast-growing conditions (right panel, figure 3.4). In order to maintain protein concentrations constant, gene-expression must balance the effect of dilution, meaning that the expression from our SOS reporters should increase with growth. No additional regulation of these promoters has been described in the literature, so would be very surprising for the transcription of these promoters to increase with growth. Direct quantification of mRNA transcript levels would be necessary to confirm this is indeed reflecting transcription.

[1] Deleting *sulA* is required to remove *lexA*, otherwise, cells would not be able to divide.

Even if that is the case, further studies would need to evaluate whether this is an indirect effect of full SOS induction or other mechanisms that may operate in normal conditions.

We observed a moderate decrease of population growth rate by deleting both *lexA* and *sulA* (figure 3.4). This was somewhat expected, as over-expression of SOS genes could lead to metabolic burden (Scott et al., 2010; Ceroni et al., 2018). However, the observed behaviour of constitutive gene expression in the Δ*lexA* Δ*sulA* background argues against a simple burden by SOS expression. The reason is that we would have expected constitutive expression to decrease as a result of less resource availability (see numerical simulations in appendix B.4), but instead we see a moderate increase (figure 3.4). This suggests that the decrease in growth rate is not related to burden by SOS over-expression.

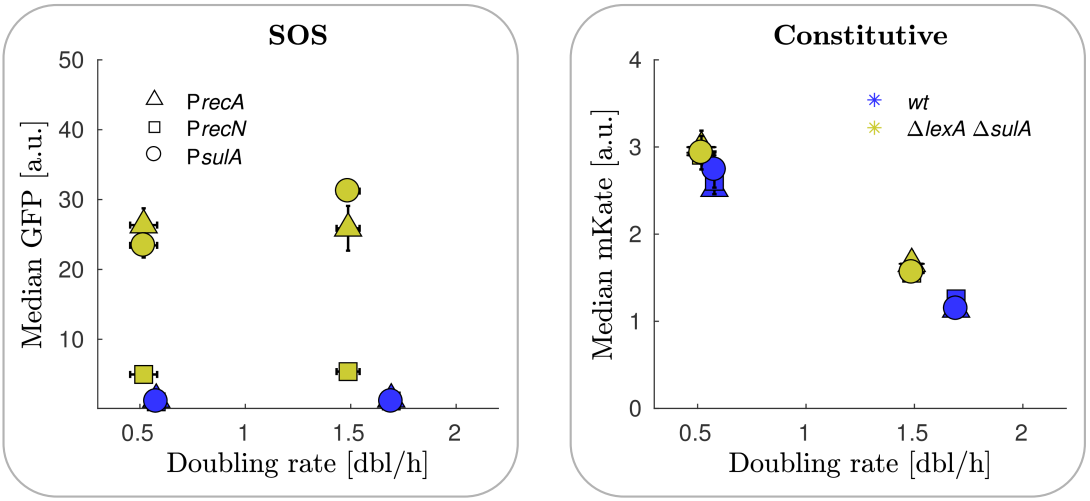

Figure 3.4: **Levels of SOS expression without LexA are invariant to changes in growth conditions**. Effect from deleting repressor LexA (Δ*lexA* Δ*sulA*) in constitutive and SOS expression. Data points are the average ± standard error of three biological repeats. **(Left)** Contrary to expectations, expression from three SOS promoters are approximately constant in the presence and absence of LexA (P_{recA}, P_{recN}, and P_{sulA}). The dotted line was obtained using slow-growth values as reference. Please note that the Y-axis is in log-scale. **(Right)** Constitutive expression appears to moderately increase without LexA. The dotted line was obtained using wild-type slow-growth average value as reference.

3.3 Influence of growth in the SOS induction by ciprofloxacin

Next, we decided to evaluate how growth conditions would impact SOS-induction under sub-lethal doses of the quinolone ciprofloxacin (1-3 ng/ml). The reason for using sub-inhibitory concentrations is such to compare the steady-state in different growth conditions. In this concentration range, we observed a moderate decrease in population growth as monitored by OD (approximately between 0 and 10%).

The reduction in population growth could indicate an overall reduction in cellular growth or a small reduction in cell viability. By time-lapse microscopy we could observe occasionally cells dying, marked by a very rapid loss of fluorescence signal (data not shown), similar to cell death by a high dose of the β-lactam ampicillin (100 μg/ml), suggesting a possible compromise of the cell wall integrity. One possible explanation could be the accumulation of oxidative damage induced by ciprofloxacin (Pribis et al., 2018). Further experiments would be required to quantify the events of cellular death and establish their cause. We wish to point out that given changes in cell size can have complex effects in optical density readings (Stevenson et al., 2016), which could influence as well our estimations of population growth rate.

We found that expression from a constitutive reporter, P_{tet01}-*mKate2*, was not affected by ciprofloxacin, characterised by the population median presented in figure 3.5. This would indicate that the decrease in population growth under ciprofloxacin is not equivalent to changing nutrient quality (Klumpp and Hwa, 2014). This could reinforce the possibility that the decrease in growth may be due to a deficiency in viability, but could very well be by other means, such as a sub-population of cells reducing growth in response to ciprofloxacin.

3.3.1 Median SOS induction under ciprofloxacin is reduced by growth rate

We decided to characterise the SOS-induction for the majority of the population using the median expression from the P_{sulA} reporter. As expected, increasing doses of ciprofloxacin resulted in higher levels of SOS-expression. We could observe that the median SOS-induction between both growth conditions was comparable, only with a small reduction in median SOS-expression for fast-growing conditions.

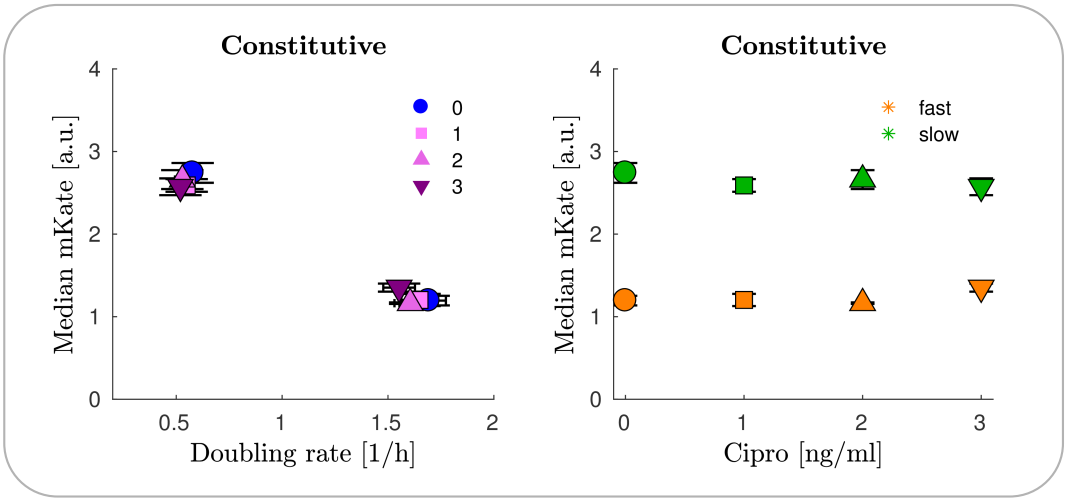

Figure 3.5: **Small doses of ciprofloxacin do not affect constitutive gene expression**. Expression of constitutive reporter (P_{tetO1}-*mKate2*) is not affected by ciprofloxacin treatment. Constitutive expression as function of population doubling rate (left) and as a function of ciprofloxacin (right). Data points are the average $\pm$ standard error of three biological repeats.

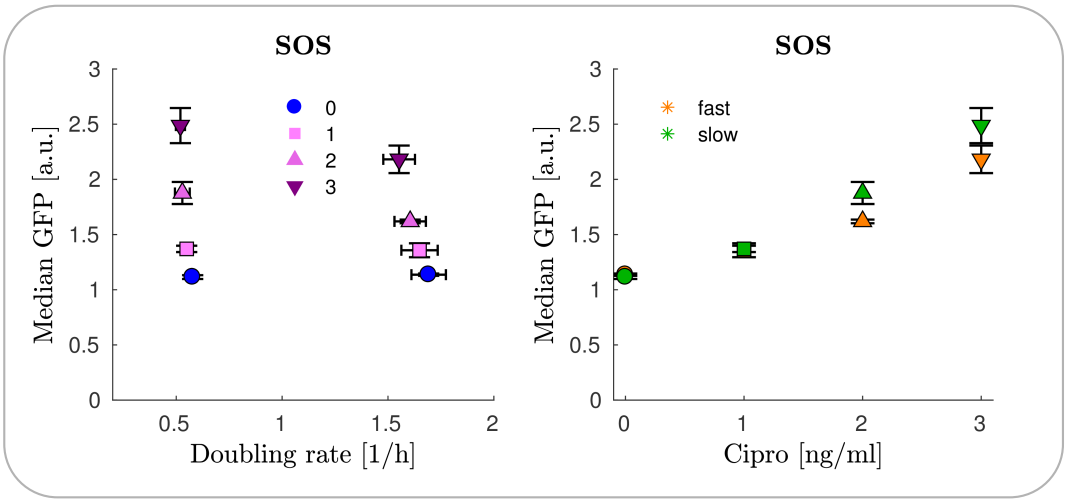

Figure 3.6: **Median SOS induction by ciprofloxacin is affected by growth conditions**. Expression of SOS resporter (P_{sulA}-*mGFP*) in slow-growing and fast-growing conditions under different levels of ciprofloxacin. SOS expression as function of population doubling rate (left) and as a function of ciprofloxacin (right). Data points are the average $\pm$ standard error of three biological repeats.

The observation that SOS-induction by ciprofloxacin may be reduced in fast-growing conditions it is interesting, and it could be due to many reasons. Permeability to drugs has been shown to be influenced by growth conditions (Greulich et al., 2015), particularly the type of carbon source (glycerol v/s glucose), presumably because of changes in the composition of cellular transporters (Chapman and Georgopapadakou, 1988; Piddock et al., 1999). Also, the mechanism inducing DSBs by ciprofloxacin remains unclear, with the debate concerning the contribution of replication-dependent and independent breaks (Drlica et al., 2008), and is possible that oxidative damage way contribute to some degree to the induction of SOS (Pribis et al., 2018).

3.3.2 SOS induction by ciprofloxacin is more variable in slow-growing conditions

As we observed that cells with very high-SOS induction were more abundant without an external source of DNA damage, we wished to evaluate if this would hold when DSBs are induced by ciprofloxacin. We observed a high degree of single-cell variability in SOS-induction under ciprofloxacin. When comparing across growth conditions we found that cells with very high SOS induction are again more abundant for slow-growing cells (figure 3.7). This can be appreciated by comparing the interquartil distance (IRQ) as a measure of distribution variability (top right panel, figure 3.7), or the value of the percentile 95 (bottom right panel, figure 3.7).

We believe these differences may reflect single-cell variability in DNA damage or repair, consistent with DSBs being relatively rare events. For example, it could be that the duration of the SOS signal (RecA-ssDNA) has a higher degree of variability in slow-growing conditions, which could be expected, given that slow-growing cells are smaller with fewer molecule copies per cell (Raser and O'Shea, 2005). However, we cannot discount other possibilities, for example, that our reporter may average more DNA replication cycles (and then more DSBs events) in fast-growing conditions. That is because of the GFP protein half-life, which is approximately 1-2 hours (Andersen et al., 1998), and thus, our measurements could average the variability between individual SOS induction events. In any case, we should expect the many SOS induced genes that are not degraded by proteases should follow the same trends as for our GFP reporter.

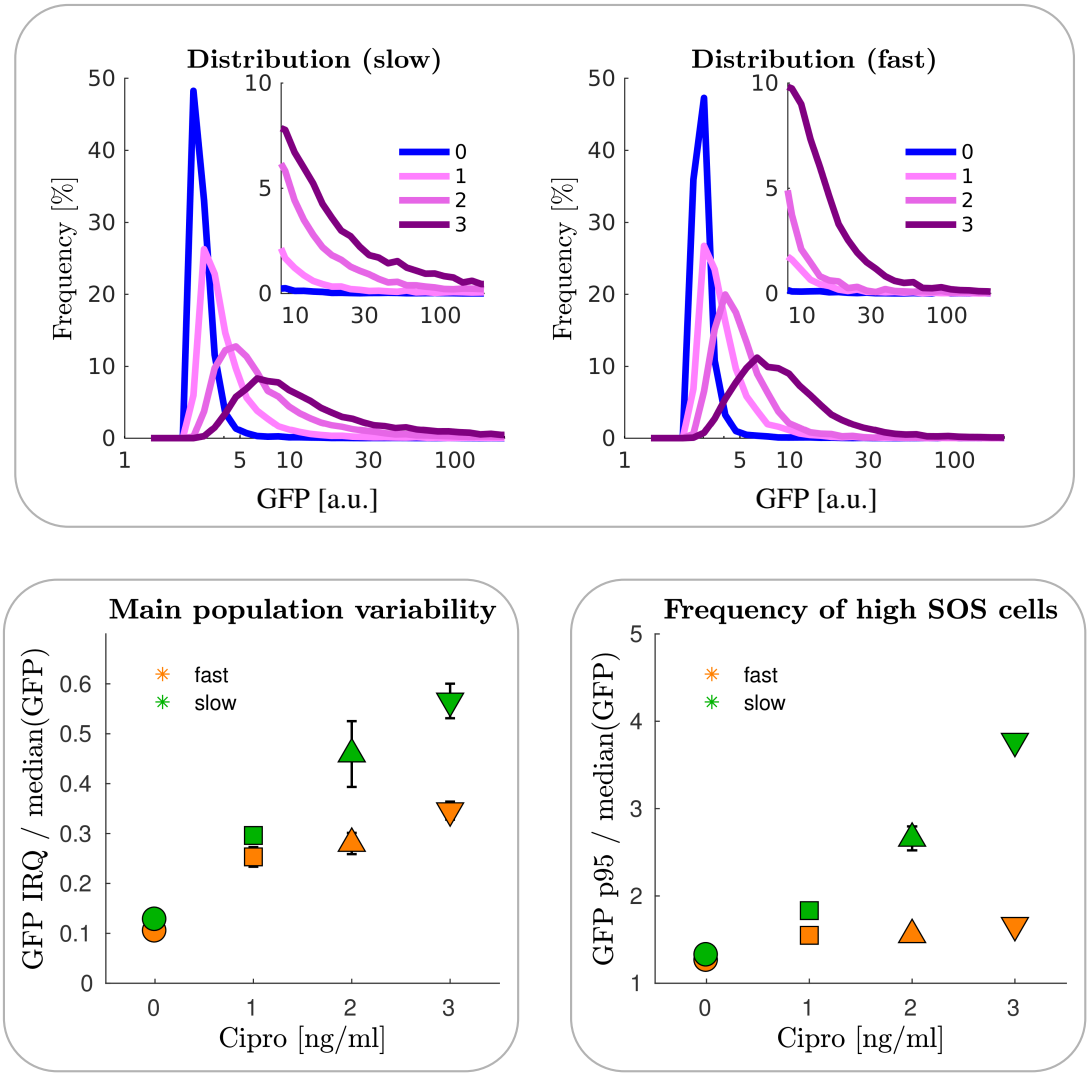

Figure 3.7: **Single-cell variability in SOS induction by ciprofloxacin is affected by growth conditions**. Expression levels of SOS reporter (P_{sulA}-*mGFP*) in single-cells are more variable in slow-growing conditions. (**Top**) Distribution of SOS expression in each growth condition under different ciprofloxacin concentrations. The relative frequency of three biological repeats were averaged while making this plot. (**Bottom left**) We used the interquartile distance (IRQ) over the distribution median to quantify, variability within the main population. For moderate concentration of ciprofloxacin variability is higher in slow-growing conditions. (**Bottom right**) We quantify how SOS expression in the top 5% of the population (GFP percentile 95) increases with ciprofloxacin concentration. We find that the percentile 95 scales with the population median in fast-growing conditions, whereas it increases more than the median in slow-growing conditions, indicating a different behaviour of SOS induction in single-cells. Data points are the average $\pm$ standard error of three biological repeats.

3.4 Influence of growth on cell filamentation by DNA damage and SOS

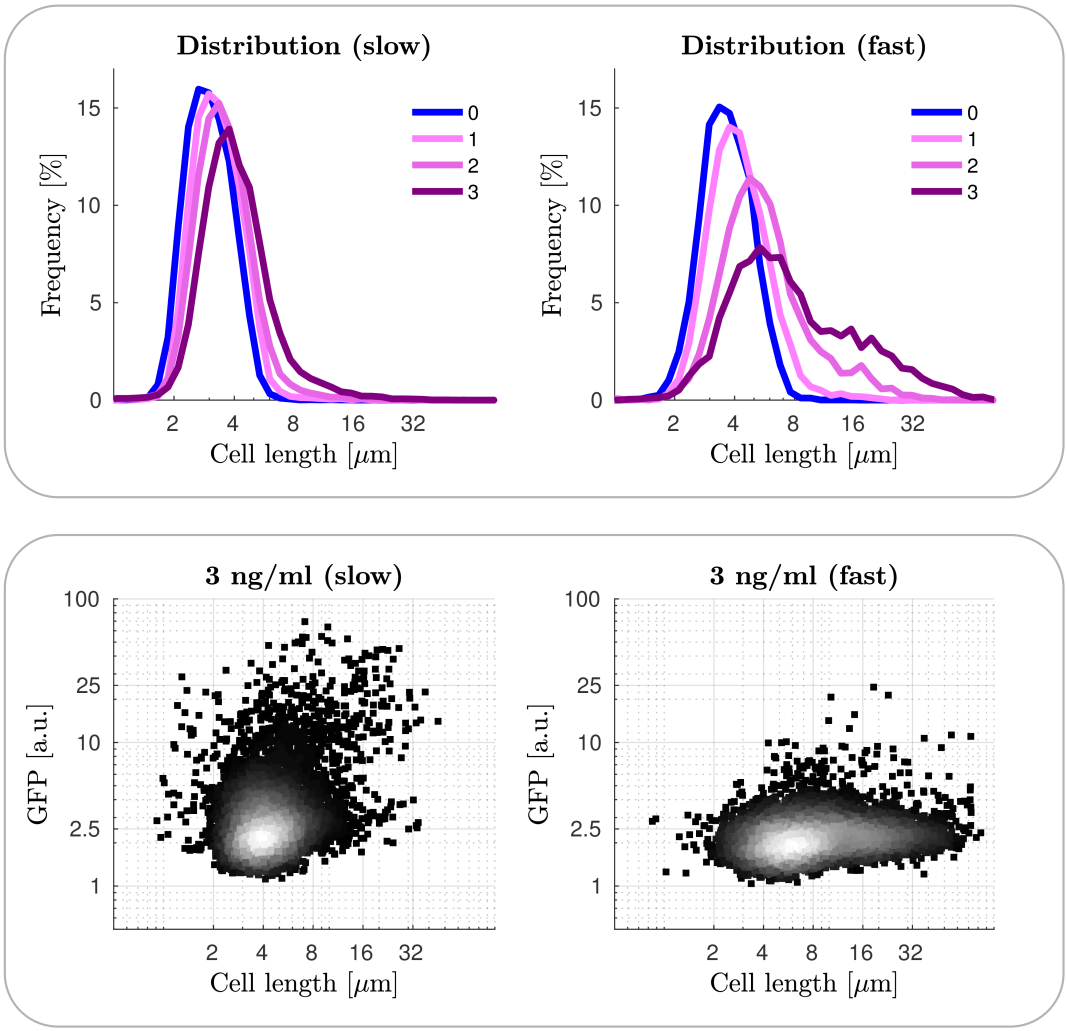

Figure 3.8: **Fast growing cells filament more under ciprofloxacin treatment**. **(Top)** Cell length distributions in single cells at different concentrations of ciprofloxacin treatment, in fast-growing and slow-growing conditions. The relative frequency of three biological repeats were averaged while making this plot. **(Bottom left)** Median of the populations as a function of ciprofloxacin concentration. Data points are the average $\pm$ standard error of three biological repeats. **(Bottom)** Scatter plot showing the correlation bewteen SOS and cell length in single-cells. Each point represents one cell out of 20000 randomly selected, and the grey color indicate the density of values sounding that point.

An increase in cell length (filamentation) is commonly associated with DNA damage. This is the result of delaying cell division, either by increasing *sulA* expression (SOS) and/or delaying chromosome segregation (nucleoid occlusion). Cell size is commonly used as phenotypical evidence of DNA damage. Therefore, understanding how different growth conditions affect filamentation could help the utilisation of cell length as a marker.

3.4.1 Fast-growing cells are more sensitive to filamentation by ciprofloxacin

We observed that augmenting doses of ciprofloxacin resulted in a moderate increase in cell length for slow-growing cells, and a significant increase in cell length for fast-growing cells (top and bottom left panels in figure 3.8). This may be expected from the fact that similar time-delays in cell division would translate in different cell sizes because of cell elongation that is exponential in time. Meaning that we could expect fast-growing cells to elongate more because cell elongation is exponential in time (Taheri-Araghi et al., 2015; Wehrens et al., 2018). Mathematical modelling would be needed to evaluate whether differences cell elongation rates are enough to explain our observations.

We observed that the increase in cell size did not necessarily correlate with an increase in SOS expression, as measured by our fluorescent reporter (bottom panel in figure 3.8). This is to be expected, given that a delay in cell division can occur from SulA (SOS dependent) and nucleoid occlusion (SOS independent). In addition, SulA protein is degraded by Lon protease, meaning our fluorescent reporter does no reflect the actual concentration of SulA in single cells. It would be interesting to evaluate the increase in cell length in a *sulA* mutant background in order to distinguish the potential contribution from each mechanism.

3.4.2 Full SOS induction can increases cell size in the absence of SulA

Interestingly, we found that cells without *lexA* and *sulA* (full SOS induction without DNA damage) were longer compared to wild type. Similar to observations for changes in cell length by ciprofloxacin, cells in fast-growing conditions had an increase in

length compared to cells grown in slower conditions (see figure 3.9).

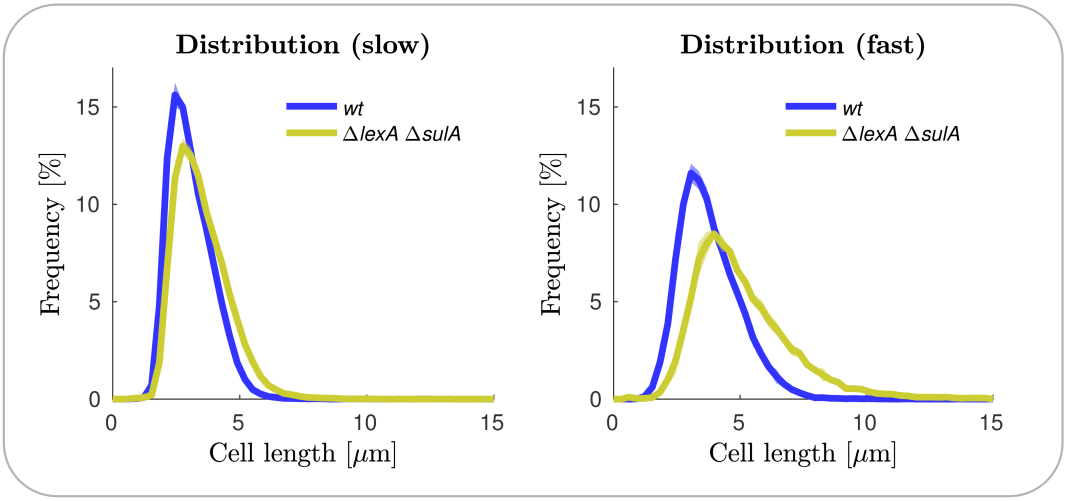

Figure 3.9: **Deleting *lexA* increases cell length independent of SulA**. Effect of deleting *lexA* and *sulA* in cell length in two growing conditions. The relative frequency of three biological repeats, were averaged for making this plot.

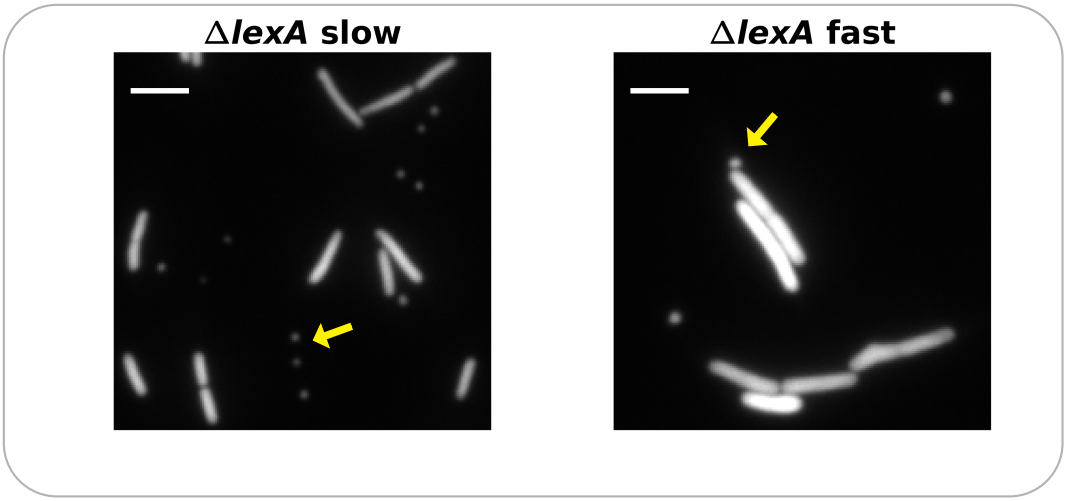

Figure 3.10: **Full SOS induction may cause problems in cell division control**. Δ*lexA*Δ*sulA* mutants may have problems in cell division control. These images are of Δ*lexA*Δ*sulA PsulA-mGFP*, imaged on GFP channel, and were selected because they contain more "mini-cells" (yellow arrows), so are not representative. "Mini-cells" cells were removed from the analysis of cell size, as it is not easy to automatically distinguish them from dirt or small errors in segmentation. For reference, white bar represents 3μm.

It is possible that full SOS induction may delay cell division independently of *sulA*, which could relate to previous reports indicating that deleting *sulA* and *slmA* (nucleoid occlusion) did not completely abolish an increase in cell size by DNA damage (Cambridge et al., 2014). One possible candidate among SOS induced genes is *ftsK*, which participates in cell division and is induced by SOS (Grenga et al., 2008; Stouf et al., 2013). Ectopic *ftsK* over-expression has been shown to inhibit cell division (Draper et al., 1998). An interesting observation is that we observed occasional very small round cells (figure 3.10) reminiscent of "mini-cells" typical of some mutations in the cell division genes (Rang et al., 2018), reinforcing further the idea that this background may have troubles in coordinating cell division.

3.5 Discussion

Contrary to expectations from increasing the frequency of DNA-replication, we observed that cells with very high levels of SOS induction are more abundant in slow-growing conditions, but for spontaneous SOS-induction from promoters P_{recA}, P_{recN}, and P_{sulA}; and for P_{sulA} under sub-inhibitory doses of the quinolone ciprofloxacin (1-3 ng/ml).

In principle, this observation could have been explained by the principle of resource allocation (Scott et al., 2010; Klumpp and Hwa, 2014), meaning that slow-growing cells could have a higher potential for expressing SOS genes. Surprisingly we found that expression from our SOS reporters did not behaved like constitutive promoters after deleting the repressor LexA, suggesting the presence of additional regulators acting in this conditions. Further experiments directly measuring mRNA levels would be need to confirm this finding, and will be discussed futher in section 5.2.

The exact mechanism for spontaneous SOS-induction is not clear (Pennington and Rosenberg, 2007), so many factors could be influenced when changing growth conditions. For example, it is possible that conflicts arising DNA-replication such as blockage could lead to the formation of single-strand gaps, which could then promote RecA loading (Ghodke et al., 2019). In this light, would be interesting to evaluate how much the single-strand gap repair pathway contributes to the differences observed by growth conditions. Alternatively, these observations could evidence fluctuations in the dynamics of DNA-repair, which would then translate into SOS expression. These

considerations will be discussed further at the end of this thesis (see section 5.3).

Another factor to keep in consideration is the potential link between stress responses and spontaneous sources of conflicts in DNA-replication (Gibson et al., 2010; Wimberly et al., 2013). It is possible that some cells experience these problems with a low probability, and this chance is increased in slow-growing conditions. Studying how these stress response relate to growth-conditions and spontaneous SOS may be difficult, especially because mutations in stress pathways often can lead to altered cell physiology. However, it should be possible to monitor the induction of stress responses using transcriptional fusions, and evaluate whether they correlate with SOS-induction in single cells. This may provide a better understanding of spontaneous sources of DNA-damage in the future.

Chapter 4

The SOS response to DSBs is influenced by growth

4.1 Introduction

The ability of bacteria to repair DNA damage, particularly double-strand breaks, has important consequences in the context of antibiotics, as failures in DNA repair can lead to cell death (Kohanski et al., 2010; Kreuzer, 2013; Michel et al., 2018). An important feature of DNA repair is the induction of the SOS response, that is, the transcriptional activation of several genes involved in DNA repair and DNA damage tolerance induced during DSB repair. In our previous chapter, we evaluated the influence of growth conditions in SOS induction by the antibiotic ciprofloxaxin, which causes indirect double-strand breaks. In this chapter, we will focus on a more controllable method for inducing double-strand breaks, based on the replication of palindromes introduced in the chromosome of *E. coli*.

Hairpins formed by palindromic sequences can be cleaved by the SbcCD complex, which makes it a useful tool to study double-strand break repair (see section 1.2.3).During DNA replication, palindromes form a hairpin in one of the strands (presumably the lagging strand), which is recognised by the structure-dependent endonuclease SbcCD, leading to a double-strand break, and moderate induction of the SOS response is required for survival in this chronic DSBs condition (Darmon et al., 2014). One palindrome located at *lacZ* has a marginal effect on population growth in rich growing conditions (e.g. LB media), but it reduces growth more in poor growing condition (e.g. M9 glycerol media) (Darmon et al., 2014; Amarh et al., 2018). This is somewhat unexpected as the generation of double-strand breaks is replication dependent, so it would be expected that breaks would be more frequent in fast-growing conditions. This suggest that growth conditions may influence the response to chronic DSBs in other ways.

Translation happens to be one of the limiting factors for cellular growth in bacteria (Lynch and Marinov, 2015). This explains the positive correlation between growth rate and ribosome gene expression, when changes in nutrient quality are used to modify growth rate (Scott et al., 2010). Given that resources for gene expression are limited within the cell (e.g. ribosomes), large changes in gene-expression have global consequences as a result of mass balance constraints (resource allocation). In other words, increasing ribosomal gene expression reduces globally expression of other genes. Expression from constitutive genes (unregulated) would be most directly affected, however, the effect may be non-trivial for regulated genes (Klumpp and Hwa, 2014). Genes

whose expression is negatively regulated (e.g. SOS LexA repressor) would be less sensitive to changes in resource allocation. Unexpected effects such as bi-modal populations can emerge from genes whose expression is toxic for growth, because this leads to a positive feedback between expression and growth (Klumpp and Hwa, 2014).

4.1.1 Scope of this chapter

In this section, we will be working with *E. coli* under chronic DSBs caused by palindromes (Eykelenboom et al., 2008) and monitor how they respond in different growth conditions. Given DSBs by palindromes are dependent on DNA replication, we expect more breaks in faster growing conditions, which bares the question: would this translate to higher SOS induction? To address this question we will be utilising fluorescence microscopy to quantify SOS expression in single cells. Later in this section, we will be looking in more detail at the influence of growth condition in DSB repair, by quantifying the loading of RecA across the genome under chronic DSBs. Finally, we will evaluate the influence of growth in antibiotic tolerance induced by chronic DSBs, in particular to β-lactam antibiotic.

4.2 Chronic DSBs reduce population growth

We have constructed strains carrying palindromes at two specific loci: *lacZ* (right-palindrome) and *ascB* (right-palindrome). These loci are at approximately the same distance from the origin of replication, meaning that this should lead to a similar frequency of chronic DSBs. Changes in the frequency of DNA replication may influence the number of DSBs induced per round of replication. We expect cells to replicate one copy of each palindrome in slow conditions, and four copies of each palindrome in fast-growing conditions[1].

We found that population growth was moderately reduced in strains carrying palindromes, both in fast (glucose plus amino-acids) and slow (glycerol) growth conditions (see figure 4.1). The population growth-rate is slightly more sensitive to chronic DSBs in slow-growing conditions. This is somewhat unexpected given we expect fast-growing cells to suffer more DSBs per cell given multifork replication, and we wondered whether this could be a result of differences in SOS induction that is required for

[1] Gene dosage was estimated using Cooper and Helmstetter model. See section B.2

surival.

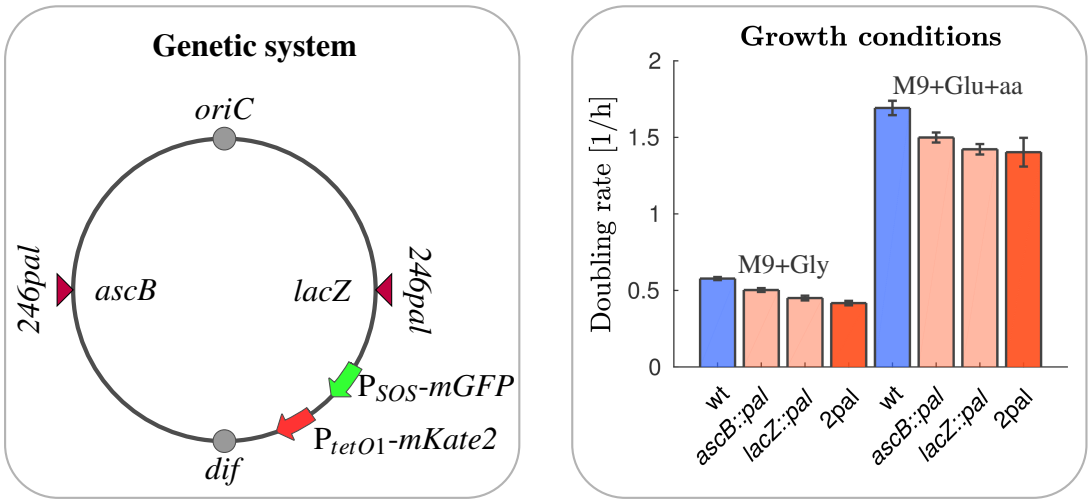

Figure 4.1: **Genetic system for monitoring SOS induction under chronic double-strand breaks**. Interrupted palindromes (246 bp) were inserted at *lacZ* and *ascB* loci, in order to generate chronic replication dependent double-strand breaks (Eykelenboom et al., 2008; Cockram, 2013). Through the text we will refer locations as left-palindrome (*ascB*) and right-palindrome (*lacZ*). In addition, two fluorescent reporters were inserted in the chromosome: mGFP under the control of the promoter P_{sulA} (to monitor SOS expression), and mKate2 under the control of P_{tet01} (to serve as an internal control for constitutive gene expression).

4.3 Growth influences the abundance of cells with very high SOS-induction

In order to study the influence of growth on SOS induction, we decided to use a transcriptional fusion P_{sulA}-*mGFP* as a reporter for SOS expression. Also, we used P_{tetO1}-*mKate2* as a control for global changes in gene expression, in addition to serving as an image segmentation marker. Initially, we will present observations made for strains carrying two palindromes, and subsequently present observations for strains carrying single palindromes. Most single-cell fluorescence measurements presented

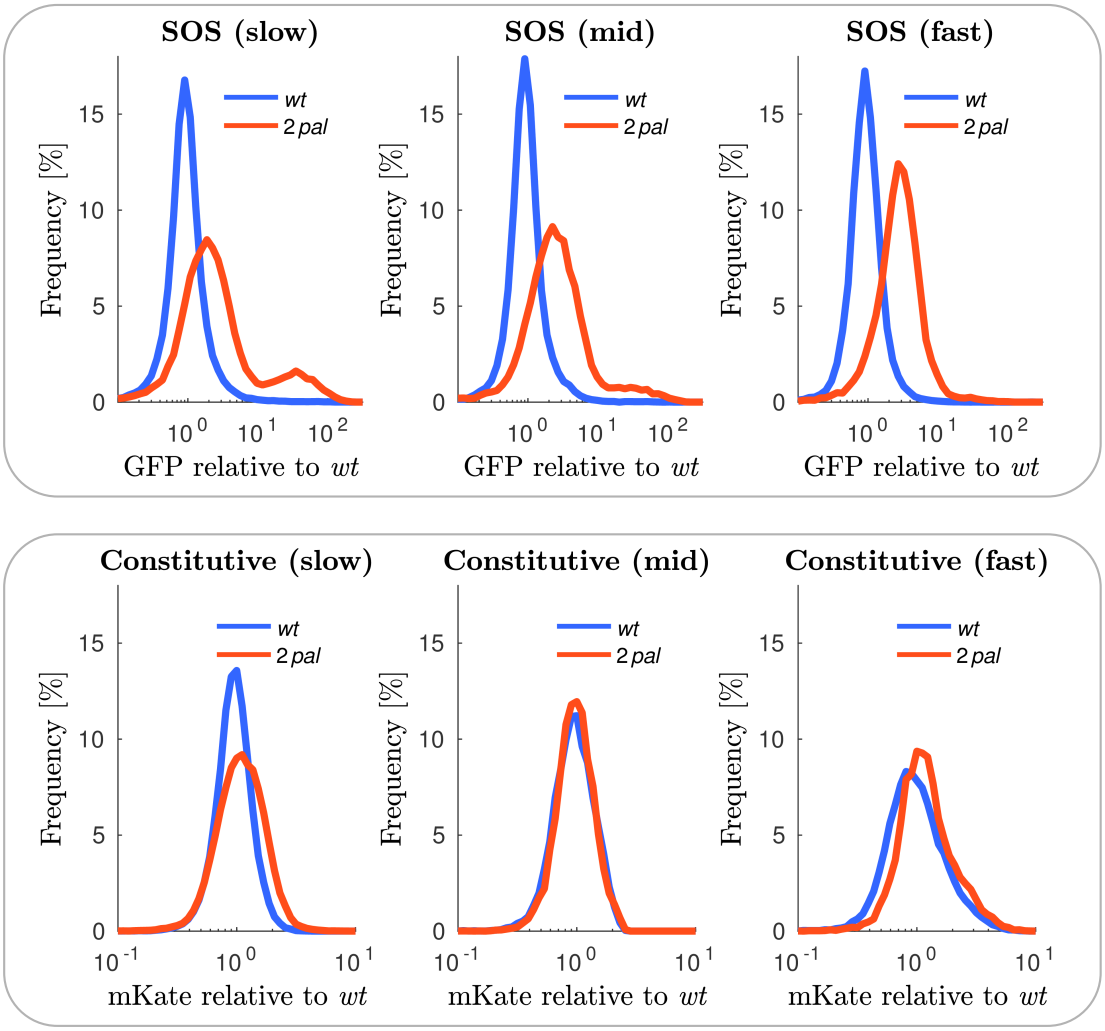

Figure 4.2: **Single-cell variability in SOS induction by chronic double-strand breaks is affected by growth conditions**. Expression levels of SOS reporter (P_{sulA}-*mGFP*) in single-cells are more variable in slow-growing conditions. In slow (glycerol) and mid (glucose) growth conditions, we observe two populations with different levels of SOS induction (top panels). Curves represent the average for each binning interval from at least three biological repeats, with the exception of intermediate growth conditions wich are a single repeat. On the other hand, we observe a moderate increase in constitutive gene expression by chronic double-strand breaks, except at mid-growth conditions (glucose). More repeats in that condition are needed. Standard errors very small and not included in the graph. Data was acquired using MACS and each dataset represents at least 5000 cells.

in this chapter were obtained using a microfluidic device for high-throughput sampling (Okumus et al., 2016, 2018). This device depends upon compressing cells at the microscope field of view. We found that fast-growing cells were more sensitive to compression, affecting the amount of fluorescence per pixel recorded, which is our proxy for fluorescent protein concentration. In order to compare arbitrary units across growth conditions, we present values normalised by the median of wild type.

Quantifying induction of SOS expression by chronic DSBs in single-cells revealed that the main influence of growth condition is the shape of the distribution (top panel, figure 4.2). We observed a bi-modal distribution of SOS induction in slow-growing conditions: one population with moderate levels of SOS induction; and a second subpopulation with very high levels. The frequency of the high-SOS subpopulation decreased at intermediate growth conditions (glucose only), and was almost absent in fast-growing conditions (glucose plus amino-acids). No significant difference was observed in the location of the main peak of SOS induction between growth conditions. A very small increase in constitutive expresion could be detected (lower panel, figure 4.2), which is consistent with the observation that the population growth of this cells is lower.

Overall, the observation of SOS induction in single-cells indicate that the reduction in population growth is not a lack of SOS induction. In fact, it could be that cells with very high-SOS induction are responsible for the reduction in population growth. The finding that SOS expression distribution is influenced by growth to such an extent was unexpected. We interpret this as evidence for single-cell variability in the damage and repair processes, leading to some cells experiencing very high SOS induction, or perhaps it is an intrinsic property of SOS induction under different growing conditions.

4.3.1 SOS induction by chronic DSBs depends on the genomic locus

Before proceeding, we decided to evaluate how much individual palindrome contribute to the induction of SOS expression. In fast-growing conditions, palindromes at a single locus induce intermediate levels of SOS, demonstrating that the effect is additive in this condition. Whereas in slow-growing condition, the left-palindrome (*ascB*) induced higher levels of SOS than the right-palindrome (*lacZ*) (see figure 4.3). It is interesting to notice that this relation is opposite to the observed reduction in population

growth, where chronic DSBs at the left-palindrome locus show a higher reduction.

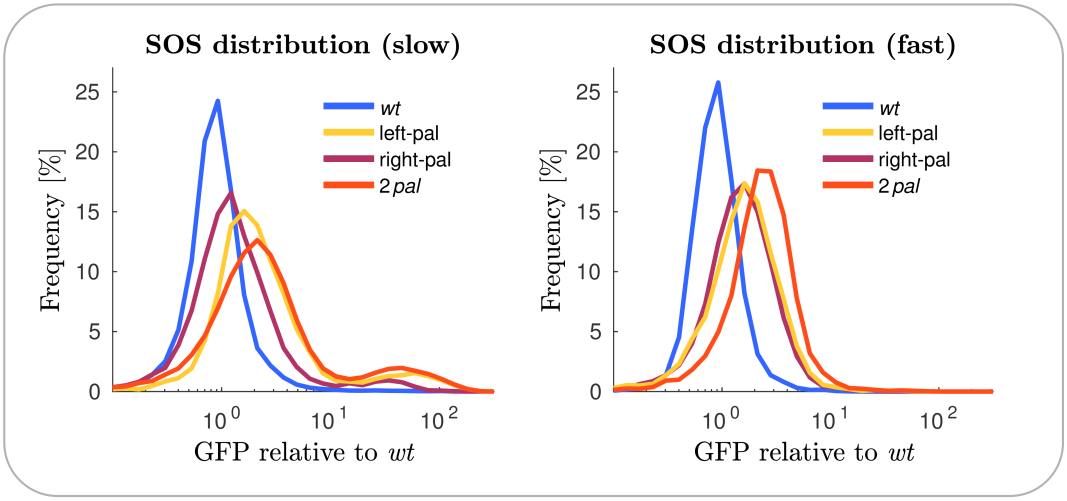

Figure 4.3: **Contribution from each palindrome in SOS induction is influenced by growth conditions**. Strains carrying single-palindomes induce similar expression of SOS reporter (P_{sulA}-*mGFP*) in fast-growing conditions (right plot). In slow-growing conditions, strains with single palindromes differ in SOS induction levels, and the left palindrome predominantly contributes to SOS induction (left plot). Each curve was obtained using at least 5000 cells. Populations were sampled using MACS.

In principle, the frequency of DSB formation could depend on genomic locus, for example, by affecting the likelihood of forming a hairpin to be cleaved by SbcCD. An alternative explanation is that DSB repair differs to some extent between loci, with downstream concequences in SOS induction given the signal for SOS induction is RecA-ssDNA formed as intermediate during repair. We will show later evidence suggesting that the difference in SOS induction bewteen individual palindrome may be due to the χ-site distribution surrounding the break sites (section 4.5).

4.3.2 Toxin-antitoxin modules are not relevant for SOS induction in slow-growing conditions

Theoretically, a positive feedback in SOS could lead to bi-stable populations with different levels of expression (Klumpp and Hwa, 2014). For example, double negative feedback formed by a toxic element induced by SOS and growth. The reason for this is that expression reduces growth, and growth reduces gene expression, forming a positive feedback loop (Klumpp and Hwa, 2014).

At least five different toxins from toxin-antitoxin modules are induced by SOS, meaning induction of SOS toxins could be responsible for the second population observed at slow-growing conditions (see section 1.3.5). We have constructed a strain without three of these toxins (Δ*tisAB*, Δ*symE*, and Δ*yafNOP*)[2], and found that they do not affect SOS induction by chronic double-strand breaks in slow-growth conditions (figure 4.4). Furthermore, we constructed a strain with an additional *dinQ* deletion. Preliminary inspection of a few hundred cells of this strain (with four toxins deleted) indicates that the expression of these toxins is not the cause of the high SOS-inducing subpopulation present in slow-growing conditions, as a similar frequency of high SOS cells were observed (10-15%) (data not shown). The remaining toxic gene *yafO* has been shown to prevent growth only in solid media, so it was not tested (Christensen-Dalsgaard et al., 2010).

In conclusion, our results indicate that our subpopulation (i.e. high SOS-induction by chronic DSBs present in slow-growth conditions), is not a consequence from a positive feedback between growth and expression of SOS toxins.

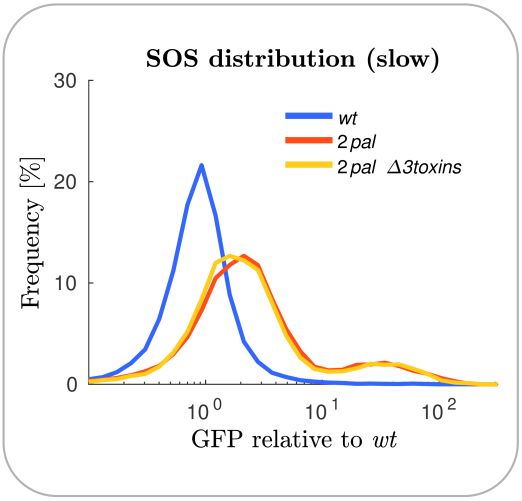

Figure 4.4: **Removing SOS toxins does not affect SOS induction by chronic site-specifc double-strand breaks in slow -rowing conditions**. Induction of SOS reporter expression (P_{sulA}-*mGFP*) is not affected by removing three SOS-induced toxins (Δ*tisAB* Δ*symE* Δ*yafNOP*) in slow-growing conditions. Data was acquired using MACS, and each dataset represents at least 5000 cells.

[2]The reason for deleting the toxin together with the antitoxin in some cases is completely by accident. In retrospect, would have been better to delete toxins only.

4.3.3 Response to translational inhibition under chronic DSBs in slow-growing conditions

In order to rule out the possibility of unknown toxic effects from SOS induction that could lead to a positive feedback loop, we tested how SOS induction is affected by limiting gene expression. In principle, reducing overall gene expression could prevent acquiring critical concentrations required for growth toxicity, thus, disrupting a potential positive feedback. To this end, we decided to use small doses of chloramphenicol antibiotic. Chloramphenicol reduces protein synthesis, which induces ribosome gene expression, resulting in the reduction of global translational resources for other genes, with a concomitant reduction in cellular growth (Scott et al., 2010).

Consistent with inhibition of translation, expression from our constitutive marker was reduced by chloramphenicol in wild type cells. Basal levels of SOS expression were less affected, perhaps because of the auto-repression feedback controlling LexA expression (top panel, figure 4.5). SOS induction by chronic double-strand breaks was not affected by translational inhibition, reducing the possibility that our high-SOS subpopulation originates from a positive feedback bewteen SOS and growth (bottom panel, figure 4.5).

Surprisingly, translational inhibition induced a bi-modal distribution of constitutive expression in cells under chronic double-strand breaks (bottom panel, figure 4.5). The relative frequency between these two modes appeared to be dependent on chloramphenicol concentration, favouring high constitutive expression when increasing transitional inhibition. We also found the induced subpopulation with high constitutive gene expression correlated with a reduction in cell size. This can be observed from cells growing in agar-pads using time-lapse microscopy (figure 4.6). The phenotypes in constitutive expression persisted over successive cell divisions, indicating that these are relatively stable states.

The phenotype observed is reminiscent of cells under starvation. There is evidence that IraD, a positive regulator of sigma factor RpoS which coordinates the general stress response, is upregulated by different DNA damaging agents (Merrikh et al., 2009a). Given *iraD* transcription is also regulated by ppGpp, it is possible that the combination of DSBs plus chloramphenicol activate the RpoS pathway. This hypothesis could explain our observations and be tested in future work by genetic means.

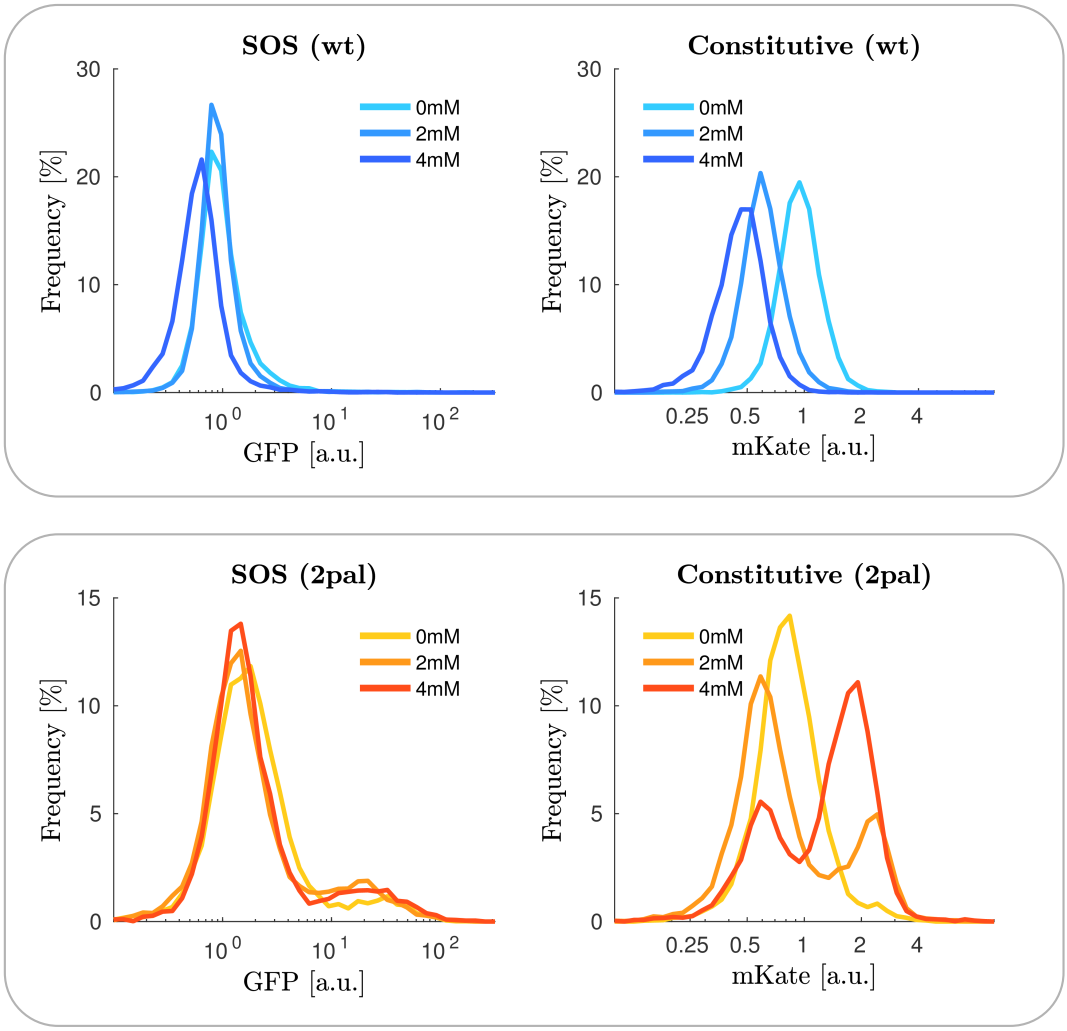

Figure 4.5: **Translational inhibition affects gene expression in cells under chronic double-strand breaks**. Effect of translational inhibition by chloramphenicol on SOS expression (P_{sulA}-*mGFP*) and constitutive expression (P_{tetO1}-*mKate2*) under chronic double-strand breaks, in slow-growing conditions. Respective fluorescence levels were normalised to the median of wild type cells without chloramphenicol. (**Top**) chloramphenicol decreases constitutive expression (right) and moderately decreases SOS expression (left). (**Bottom**) SOS induction distribution by chronic double-strand breaks (2 palindromes) is not significantly affected by chloramphenicol (right). Translational inhibition induced bi-modal distribution in constitutive gene expression. The frequency of the subpopulation with higher expression increased with higher dose of chloramphenicol. Each distribution was obtained from at least 5000 cells. Populations were sampled using MACS.

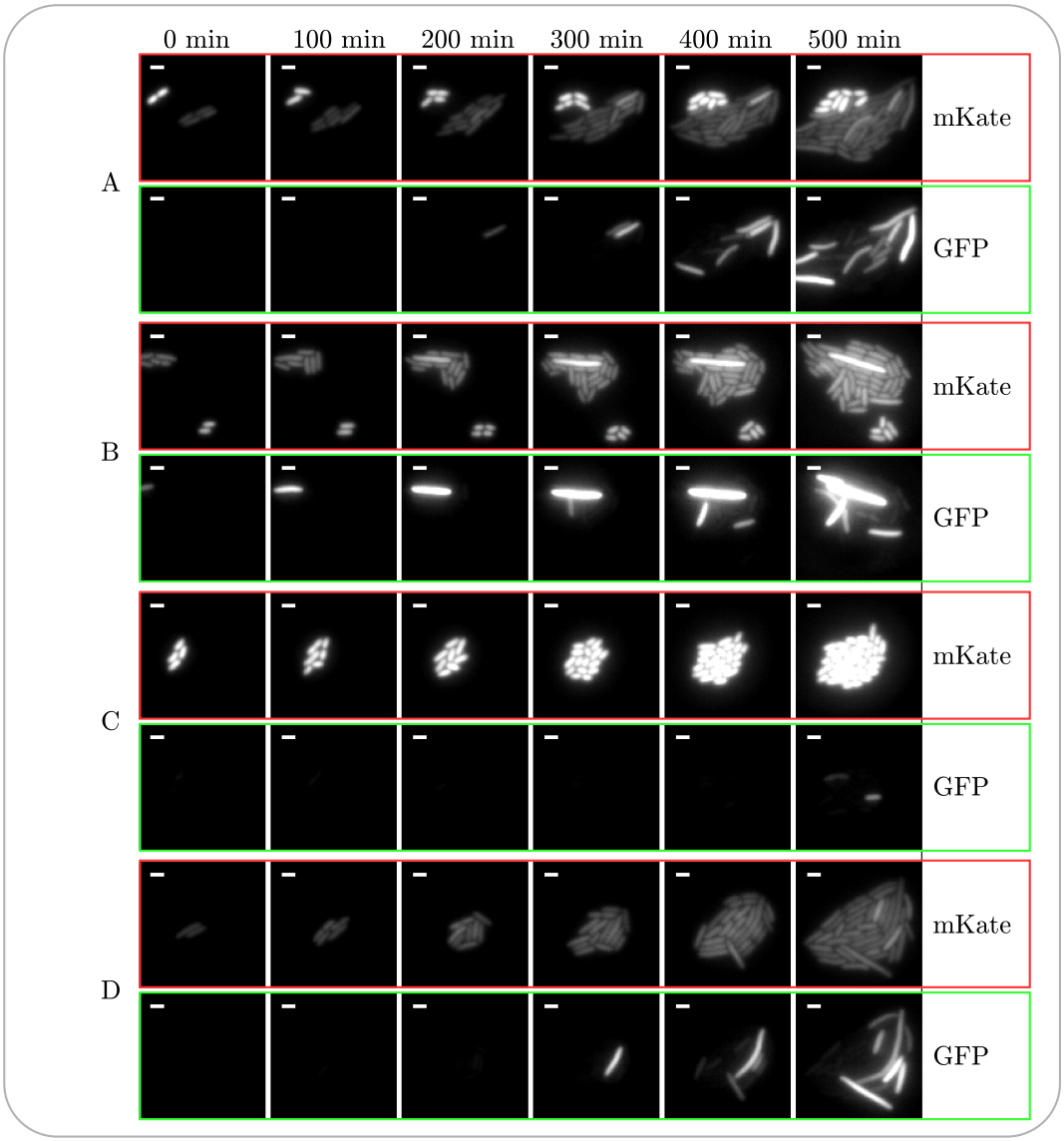

Figure 4.6: **gene expression phenotype induced by translational inhibition are stable**. Cells carrying two palindromes were pre-grown in liquid (M9+glycerol + 4mM chloramphenicol) to steady-state and placed on an 2% agar-pad made with the same media. Cells with high levels of constitutive gene expression (P_{tetO1}-*mKate2*) were found to be smaller and were able to divide. Phenotypes appears to be stable over successive divisions. White bar represents one μm.

4.4 Cells with very high-SOS induction reduce growth under chronic DSBs

In order to better understand how cells respond to chronic DBSs, we decided to study the dynamics of single-cells using time-lapse microscopy. A key question is whether high-SOS cells revert to lower SOS levels, as that would be evidence that these cells are able to repair the induced DNA damage. Preliminary observations using agar-pads indicated that high-SOS cells remained in this state for several hours, and in addition to inhibiting division we observed they could stop elongating (data not shown). It is possible that these cells simply take longer to resume normal growth. However it is not possible to observe single-cell growth for prolonged time on agar-pads, given the space is quickly occupied by faster-dividing cells. It is worth mention that we did not observe evidence for this phenotype in cells grown under fast-growing conditions (data not shown).

To overcome the limitations of time-lapse microscopy with agar-pads, we decided to use a microfluidic device called "mother machine" (Wang et al., 2010). Cells in mother machines are trapped in chambers, with a single-end open to a constant flow of media. The dimensions of the chamber are important for trapping cells. Given this constraint, we found that the device we had available was best suited for cells growing in intermediate growth rates (glucose only media, doubling time 60 mins).

4.4.1 Cells with very high-SOS induction reduce growth

In the following we will present some preliminary results using mother machines. Observations of single-cell lineages confirmed that cells can thought different fates after SOS induction. Cell under chronic DSBs showing moderate levels of SOS induction were able to continue growing and resume division, similar to spontaneous SOS induction events in wild type cells (compare chambers B and E in figure 4.7). The fate of most high SOS cells under chronic DSBs (i.e. approximately 10 times the wild type media) was different. We observed that in most cases high levels of SOS induction were followed by reduced growth (3-6 hours after SOS induction), and subsequent decrease in fluorescence for both mGFP and mKate markers (e.g. chambers F and G). We interpret the decrease in fluorescence as photo-bleaching, suggesting an overall reduction in gene expression. We also observed a few cases of what appears to

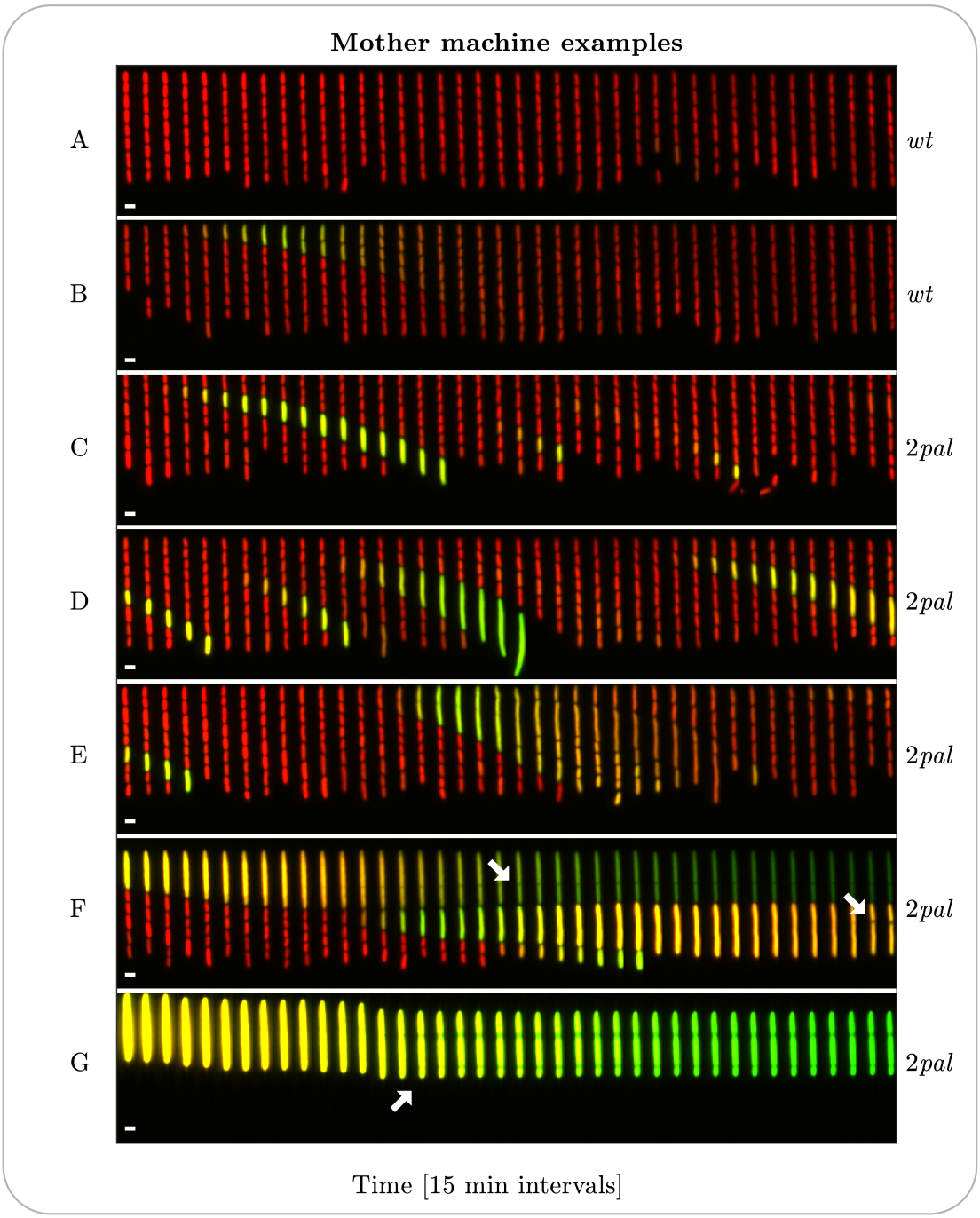

Figure 4.7: **Single-cell dynamics under chronic double-strand breaks**. Selection of time-lapse images for 8 mother machine chambers, two of them with wild type cells (chambers A and B), and 6 of them with cells under chronic double-strand breaks (2 palindromes). Time progression moves from left to right, in 15 min intervals. Image from mGFP (SOS reporter P_{sulA}-*mGFP*) and mKate (constitutive reporter P_{tetO1}-*mKate2*) channels are overlapped in green and red colours respectively. Maximum green is set at approximately ten times the average wild type mGFP intensity value, whereas maximum red is set at approximately two times the average mKate intensity value. White arrows points to what appear to be unsuccessful attempts at cell division. Cells were grown in M9+Glucose media ($\sim$60 mins doubling time)

be an attempt at cell division (e.g. chamber G). From a total of 355 mother lineages, 20% reached mGFP intensity levels 20 times the average, indicating that high SOS-induction events are relatively frequent. For comparison, only 1% of lineages reach 5 times the average for wild type cells. We have also observed growth-arrested cells for longer periods of time (12-24 hours), and we saw no indication that they would resume growth or gene expression. In conclusion, conversion to high-SOS state in most cases appears to be irreversible, and correlates to reduction of gene expression and, subsequently, cell growth.

4.4.2 Cells with very high-SOS induction are not rescued by adding richer media

We speculated that high-SOS cells could resume growth by supplementing with richer media. To this end, we attempted to "rescue" non-growing cells by switching from M9+glucose media to LB, imaging every 20 minutes for a period of 12 hours (data not shown). The majority of high-SOS cells did not recover elongation, and continued to decrease in fluorescence intensity. A few of them even displayed a very quick decrease in fluorescence, reaching the same value as background, reminiscent of cellular lysis. A minority of cells appeared to elongate only for a few hours, after which they stopped elongating. These results argue against the possibility that non-growing cells are metabolically "dormant".

Based on our preliminary observations, we conclude that the majority of high-SOS induced cells are most likely unviable, and their state is characterised by a global reduction in gene expression. To fully confirm these are unviable cells, we would need to sort populations based on their fluorescent levels, and to quantify their viability on a larger scale. We believe a likely explanation is that these cells are the result of failed attempts at repairing DSBs, which could explain their high levels of SOS induction.

4.4.3 Population dynamics partially explains the influence of growth in the abundance of high-SOS cells

The observation that most high-SOS cells do not resume growth and division can explain some of the differences in SOS single-cell distribution between growth conditions (figure 4.3). As cells with very high SOS-induction do not divide, the abundance

of these cells in the population will depend on the rate at which the growing subpopulation divides, which has lower levels of SOS. Increasing the division rate of the dividing subpopulation would naturally bias against a non-dividing fraction. Simple calculations of this bias (details in appendix B.3) predicts that the fraction of non-dividing cells should be inversely proportional to growth rate. This phenomena makes very difficult to interpret steady-state distributions, as variability in SOS induction in single cells is confounded with the correlation of SOS with the division time. Qualitatively, it was very difficult to find cells with very high SOS-induction arresting growth in fast-growing conditions by time-lapse microscopy using agar-pads (1 cells in 30 different stage positions, data not shown). Detailed quantification of the correlation of SOS and the cell cycle in single cells would be needed to disentangle these two effects.

4.5 DSB repair is influenced by growth conditions

The influence of growth condition in SOS induction could be a consequence of differences in DNA repair. The key signal for SOS induction is the active RecA-ssDNA formed as an intermediate during DSB repair, but very little is known about how RecA loading unto DNA may be affected by growth conditions. In collaboration with Benura Azeroglu, we decided to use RecA immunoprecipitation followed by sequencing (ChIP-seq) in order to characterise RecA loading across the genome. The enrichment of DNA reads at particular genome positions is a reflection of how frequent RecA is bound. Ultimately, RecA loading depends on the activity of RecBCD complex.

We have quantified genome-wide RecA enrichment under chronic double-strand breaks in three growth conditions. Given that sequencing reads are not an absolute measure of concentration, we decided to work with frequencies normalized to wild type, which we call RecA fold enrichment. Consistent with expectations, we observe most of RecA enrichment is localised to both sides of the site-specific chronic DSBs (see figure 4.8). In addition, similar to previous reports, we find enrichment near *dif* site, evidencing additional breaks induced at this region (Cockram et al., 2015).

4.5.1 Growth influences RecA-loading near DSB sites

RecA loading near the specific break sites is consistent with RecBCD activity. Loading of RecA in the genome is expected to peak near to properly-oriented χ-sites, fol-

lowed by an exponential decay, dependent on RecBCD processivity (Cockram et al., 2015). We find that almost all peaks in RecA fold enrichment to correlate with χ-site positioning (figure 4.9). The only exception is a peak found near the left-palindrome towards *dif*. It is possible we are missing χ-site in our reference genome, for example from the kanamycin-resistance gene located near to that region, which would need to be evaluated.

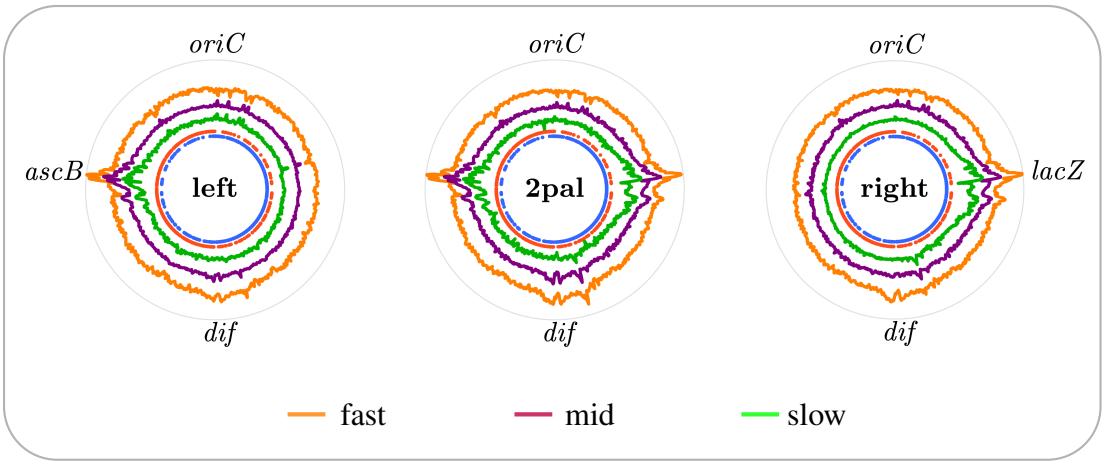

Figure 4.8: **RecA binds to regions near palindromes and *dif* under chronic site-specific double-strand breaks**. Enrichment of sequencing reads by RecA ChIP-sequencing for strains under chronic double-strand breaks, at three growth conditions. The chromosome of *E. coli* is represented in polar coordinates. Frequencies of DNA reads across the genome were normalised to the frequencies of wild type (RecA fold enrichment). Lines in green, purple, and orange represents the logarithm fold enrichment values for slow, mid, and fast growth conditions respectively. Growth condition were shifted to outer radius to facilitate comparison. We can observe that RecA enrichment relative to wild type is specific to areas near site-specific double-strand breaks (palindromes), and near *dif* region (termination of replication). Red and blue dots represent the location of χ-sites in each orientation. For zoom in details see figures 4.9 and 4.10

Similar to our previous observations of SOS induction, we found that RecA loading induced by chronic DSBs is affected by growth conditions. In particular, RecA is loaded further from the break sites (palindromes) in slow-growing populations (figure 4.9). This could be an indication that χ-site recognition by RecBCD is influenced by growth condition, however, we are not aware of any known variables that can affect

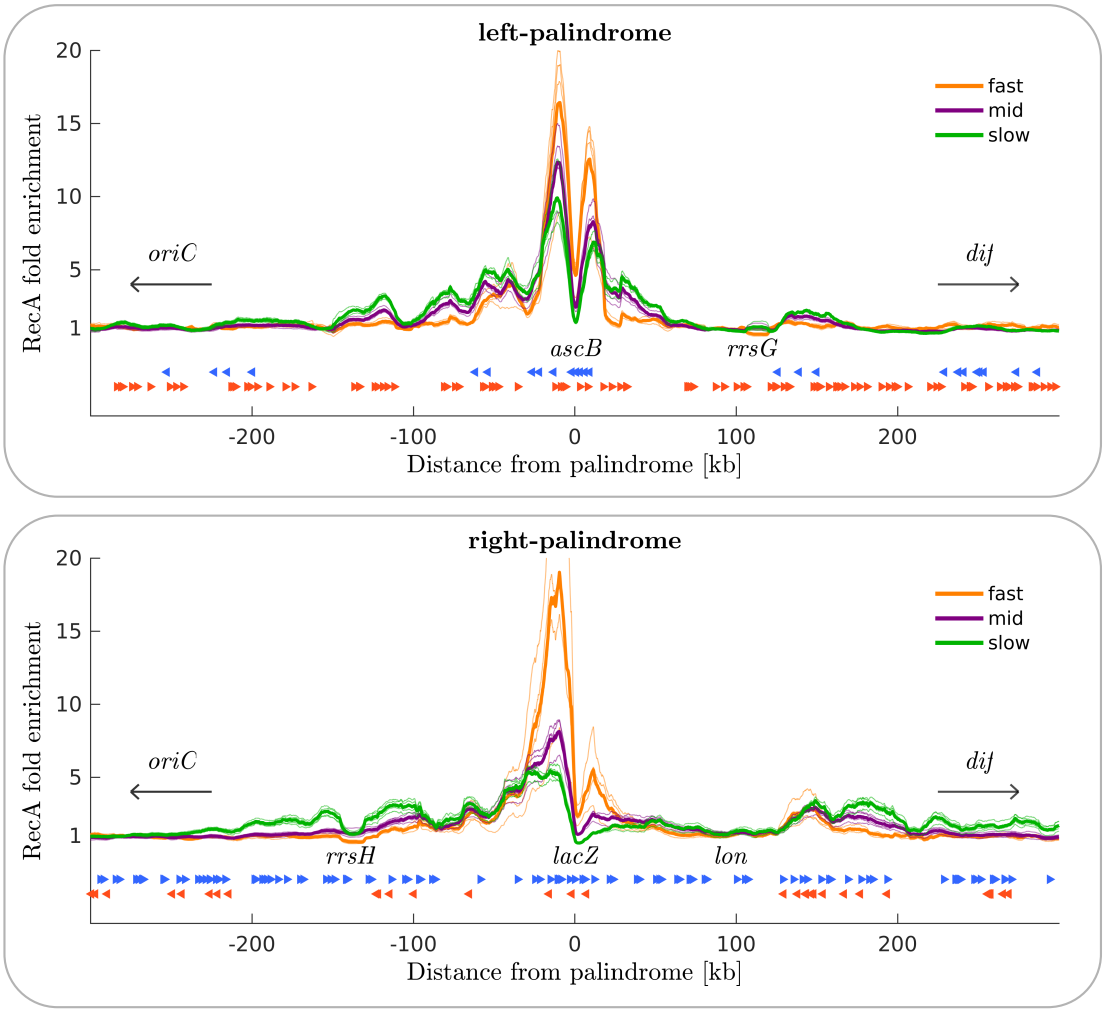

Figure 4.9: **RecA enrichment at regions near chronic double-strand breaks is influenced by growth conditions**. RecA is enriched further from the palindrome locus in slower-growing conditions. Lines in green, purple, and orange represents the fold enrichment values for slow, mid, and fast growth conditions respectively. The RecA enrichment profiles from four conditions were averaged to construct thick lines (single palindrome and double palindrome, plus two biological repeats each). Individual datasets are plotted in thin lines for reference. Red and blue dots represent the location of χ-site in either orientation, which correlate to the peak of RecA enrichment.

Table 4.1: **Genes relevant for cell growth and DNA metabolism within regions with observed RecA enrichment**. Degradation of DNA by RecBCD in those regions could have concequences for cell growth, and even DNA repair. Negative distances are given to regions towards the origin of replication, whereas positive distances to regions towards terminus. This table was based on gene annotation from the EcoCyc database (`https://ecocyc.org/`).

Gene	**Function**	**Essential?**	**Distance to *ascB* [kb]**	**Distance to *lacZ* [kb]**
recBCD	Homologous recombination	no	-114	
relA	ppGpp synthetase	no	-72.9	
pyrG	CTP bio-synthesis	yes	-69	
eno	Glycolysis and gluconeogenesis	yes	-68	
ftsB	Cell division	yes	-33	
rpoS	Stress sigma factor	no	-27	
recA	Homologous recombination	no	16	
clpB	Protein chaperone	no	107	
rrnG	Protein synthesis	no	109	
rpoE	Sigma factor	yes	130	
rnc	RNA processing	yes	136	
era	Ribosome maturation	yes	137	
acpS	Acyl-carrier-protein metabolism	yes	139	
	.....			
lpxABD	Lipid IV_A bio-synthesis	yes		-162
dnaE	DNA polymerase III subunit	yes		-157
accA	Fatty acid bio-synthesis	yes		-155
proS	proline-tRNA ligase	yes		-146
rrnH	Protein synthesis	no		-139
dnaQ	DNA polymerase III subunit	no		-128
proAB	Proline biosynthesis	yes		-103
sbcDC	DNA nuclease	no		52
clpXP	Protease	no		92
lon	Protease	no		96
dnaX	DNA polymerase III subunit	yes		129
adk	ribonucleotide bio-synthesis	yes		133
hemH	Heme bio-synthesis	yes		135

the probability of χ recognition by RecBCD. Alternatively, RecA loaded further from the break could be evidence of multiple instances of RecBCD processing from a single cleavage of the palindrome region (unsuccessful repair events). These two hypothesis may be tested using mathematical modelling of RecBCD activity.

We would like to highlight that many genes relevant for growth and even DNA repair overlap with the regions where we found RecA to be enriched (table 4.1). Degradation of these regions during DSB repair could transiently reduce expression from these genes, with stronger consequences for slow growing cells, as would imply a 50% transient reduction of gene dosage. It is possible that degradation of these genes is the cause of the arrest in growth and gene expression in single cells (as discussed in the previous section). If we were able to sort cells by levels of SOS expression, may be possible to quantify DNA degradation near this region using qPCR.

In conclusion, we observe that loading of RecA by chronic site-specific double-strand breaks is consistent with χ dependent activity of RecBCD. We find that RecA enrichment is relatively more abundant further from the break-sites in slow-growing conditions. This could be explained by growth-dependent χ recognition, or represent multiple events of RecA loading by RecBCD. Some cells may experience variations in DNA degradatio and perhaps DNA repair, which may be the factors causing differences in SOS induction under different growth conditions.

4.5.2 Growth influences RecA loading near terminus induced by chronic double-strand breaks

Consistent with previous observations for chronic DSBs induced by a single palindrome, we observed RecA enrichment near *dif* (Cockram et al., 2015). The enrichment of RecA in this region peaks near χ-sites, indicating double-strand breaks are induced by chronic breaks at the palindrome region (figure 4.10). The precise mechanism inducing additional breaks is unknown. Following the orientation of χ-sites, single-ended breaks appear to originate near *ter* sites (mostly *terA*), and double ended breaks somewhere within the *dif* region.

Induced breaks at terminus appear to be more frequent in fast-growing conditions (figure 4.10). For example, breaks originating at *dif* are undetectable in slow growing conditions. The influence of growth conditions is similar for breaks originating

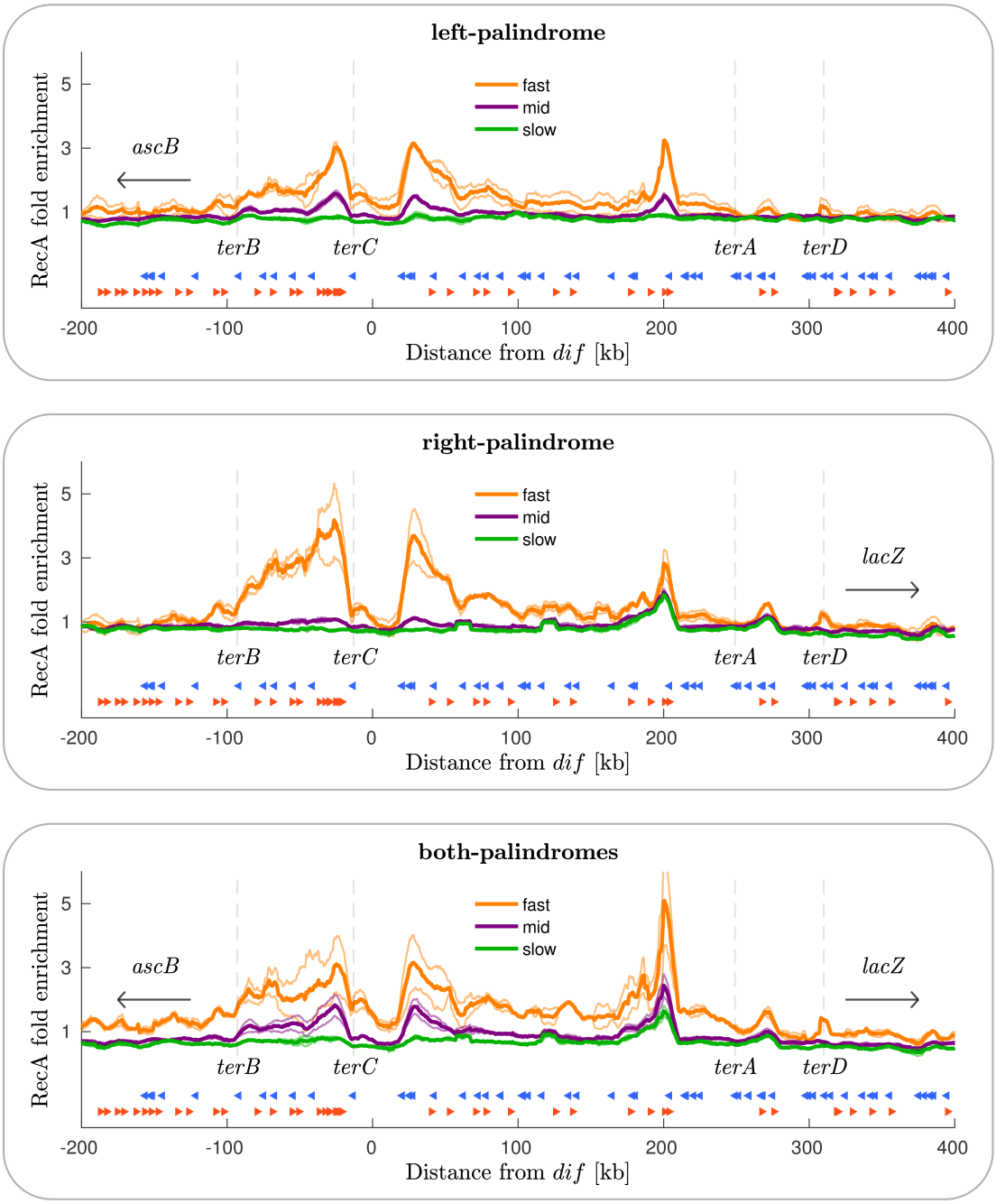

Figure 4.10: **RecA enrichment in the terminus region induced by chronic double-strand breaks is influenced by growth conditions**. RecA enrichment induced at terminus by chronic double-strand breaks is higher in fast-growing conditions. Lines in green, purple, and orange represents the fold enrichment values for slow, mid, and fast growth conditions respectively. The RecA enrichment profiles from two biological repeats (thin lines) were averaged to (thick lines). Red and blue dots represent the location of χ-site in either orientation, which correlate with peaks of RecA enrichment. Following orientations of χ-sites, RecA loading is consistent with double-ended double-strand breaks originating somewhere near *dif*, and single-ended breaks near *ter* sites (mostly *terA*).

at *terA*, although they can still be detected in slow-growing conditions. Interestingly, the combined effect from two palindromes appeared to induce more frequent breaks at *terA*, which coupled with the influence of growth, appears to indicate that breaks at this region correlate to the frequency of double-strand breaks induced by palindromes. Breaks at *ter* sites are related to DNA replication forks stalled by The Tus protein binding to *ter* sites [3], although the exact mechanism for inducing stalled forks is not well established (Michel et al., 2018). Regarding breaks induced at *dif*, no clear difference was observed between strains carrying one and two palindromes. It has been proposed that the cause of these breaks is related to dis-coordination between joint molecules formed during homologous recombination and cell division, perhaps even broken by mechanical constriction (Michel et al., 2018). If this is the case, these events could be more likely in faster-dividing cells.

4.5.3 Difficulties in observing RecA polymerisation in single-cells

We should mention that one explanation compatible with our observations is the possibility of palindromes being cleaved on both strands, leading to breaks unrepairable by homologous recombination. This would be consistent with higher SOS induction, and perhaps also explain RecA being loaded further from the palindrome break site. This appears somewhat contradictory to a study of RecA polymerisation in single cells after transient induction of DSB by a single palindrome, where RecA polymerisation was observed to be transient (Amarh et al., 2018). A major difference between their study and ours that we are working in steady-state conditions.

We have tried using RecA fused to mCherry as in Amarh et al. (2018) but, unfortunately, this system is not well suited for steady-state conditions. The reason is that RecA fusion is under the control of *recA* promoter, meaning that background levels increase with SOS induction, making it harder to detect fluorescent foci in cells with high SOS induction. In addition, given the natural tendency of RecA fusions to aggregate (Amarh et al., 2018), we observed many foci not co-localizing with DNA by DAPI staining (data not shown). In an attempt to avoid the tendency of RecA-mCherry to aggregate, we replaced mCherry by mGFP and Ypet. We found RecA-mGFP aggregates in almost every cell even in the absence of SOS induction, whereas RecA-Ypet

[3] Additional evidence for breaks originating at *ter* sites comes from the fact that RecA enrichment in those regions is abolished in a Δ*tus* mutant, but the enrichment originating from *dif* persists (personal communication from Benura Azeroglu)

behaves similarly to RecA-mCherry (data not shown).

An alternative approach would be to study the transition to chronic DSBs by controlling expression of SbcCD. We tested a system published with *sbcDC* under the control of arabinose promoter P_{BAD}, but unfortunately leaky expression from this promoter is enough to generate a significant increase in the frequency of high-SOS cells in slow growing conditions (glycerol only, data not shown). It is possible that intermediate growth conditions (glucose media) may be more suitable to address this question.

4.6 Antibiotic persistence is induced by chronic DSBs

In the context of antibiotics, a large motivation for studying SOS induction is its correlation to mutagenesis and antibiotic tolerance and persistence. In this final section, we will focus on the latter by evaluating the impact of chronic DSBs in the survival to treatment by the β-lactam ampicillin.

4.6.1 Chronic DSBs induce persistence to ampiclin in slow growing conditions

We have decided to evaluate survival to intermediate concentrations of ampicillin (β-lactam) by measuring the fraction of living cells after adding the antibiotic. After adding 10 μg/ml (2-3 times the minimal inhibitory concentration), we find that less than 1% of the wild type population is alive after 6 hours (see figure 4.11). This is the case in both fast-growing and slow-growing conditions. Cells under chronic DSBs (2 palindromes) are more tolerant to ampicillin in slow growing conditions. Approximately 10% of the population survives after 6hrs in slow growth media, evidence the presence of a persistent sub-population (figure 4.11). Similar results were observed at intermediate growth conditions (glucose only). Within three 3 hours after administering the antibiotic, approximately 90% of the population dies and then the fraction of survival appears to stabilise, indicating the presence of a sub-population with higher tolerance to ampicillin.

Antibiotic persistence is commonly found when cells arrest metabolic activity, conferring survival in presence of antibiotic concentration many times above the minimal inhibitory concentration (MIC) (Aagaard et al., 1991). We found that the increase in

persistence under chronic DSBs is absent at doses typically used in other studies (figure 4.12). This indicates that the mechanism conferring survival is only partial.

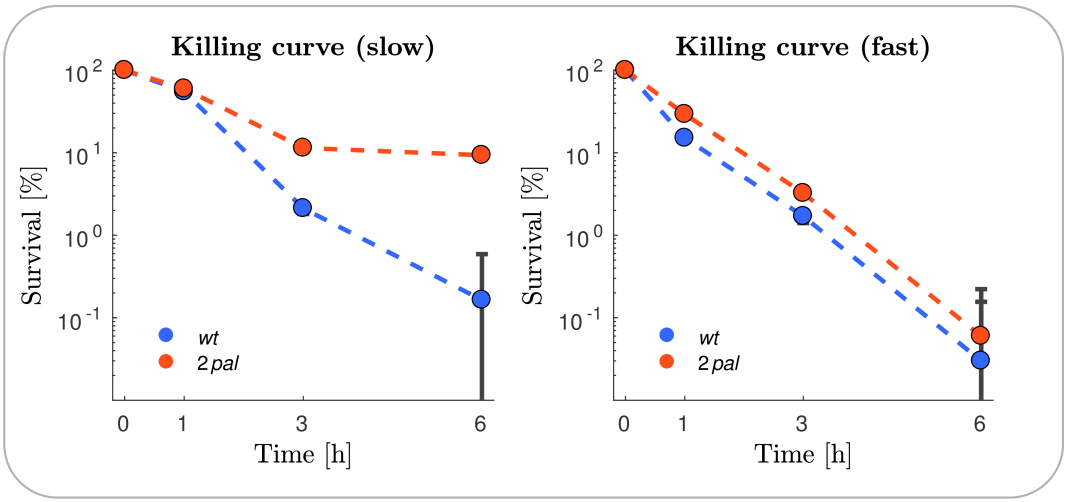

Figure 4.11: **Chronic site-specific double-strand breaks induce a sub-population persistent to ampicillin**. Fraction of the population surviving after adding 10 μg/ml of ampicillin. Surviving cells were estimated by counting colony-forming units. Values represent the mean $\pm$ standard error from three biological repeats.

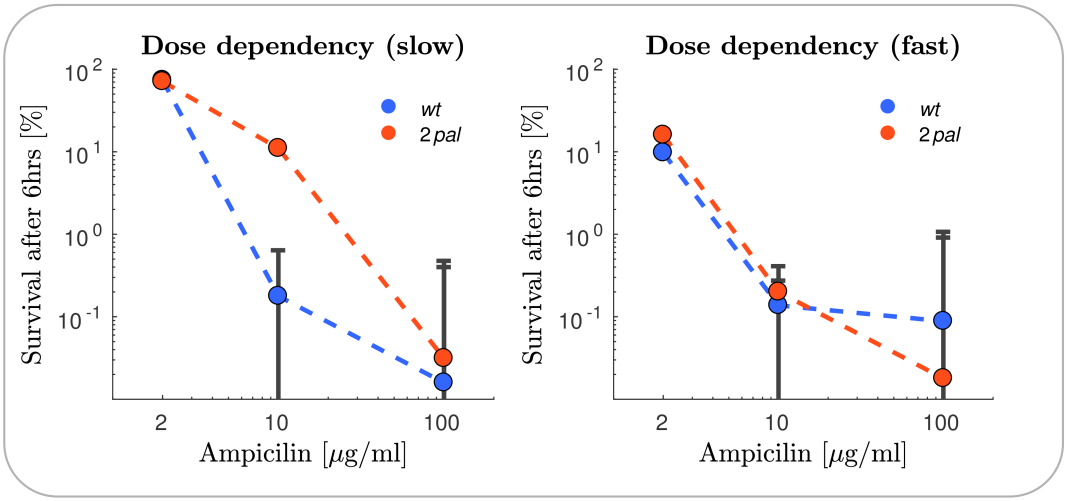

Figure 4.12: **Increase in persistent fraction is dose dependent**. Fraction of the population surviving after six hours from adding ampicillin. Surviving cells were estimated by counting colony forming units. Values represent the mean $\pm$ standard error from three biological repeats.

4.6.2 Increase in persistent fraction is dependent on palindrome locus and *sulA*

Next, we decided to evaluate whether the increase in persistence reduced in cells undergoing chronic DBSs from one palindrome instead of two. We observed that persistence is specific to the palindrome in the right replicore, located at *lacZ* (left panel, figure 4.13). This indicates that the effect is not exclusively due to SOS induction, but is specific to inducing double-strand breaks at that particular locus. Consistent with this observation, we did not detect an increase in persistence by treating cells with ciprofloxacin (up to 3 ng/ml), nor in a Δ*lexA* Δ*sulA* background where SOS is fully induced (data not shown).

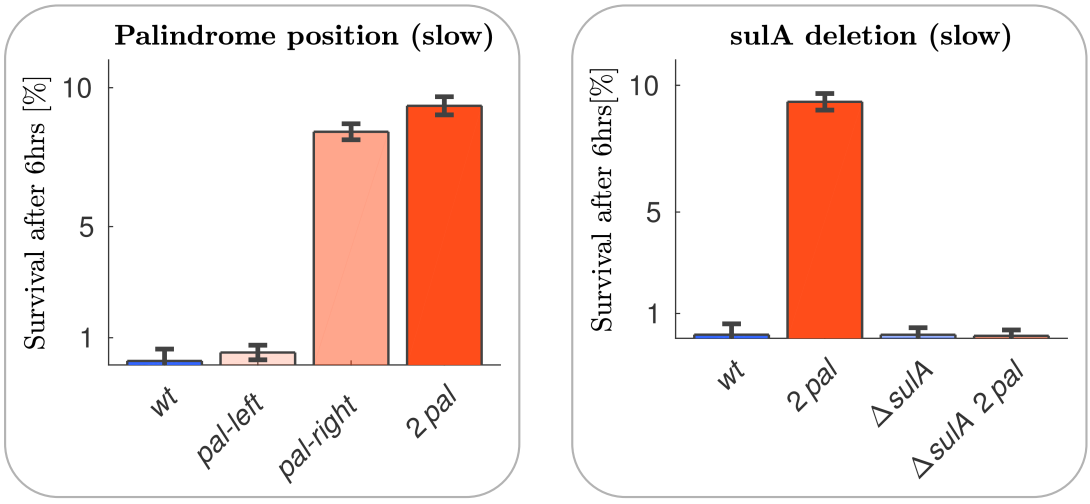

Figure 4.13: **Increase in tolerance is specific to *lacZ* palindrome and dependent on *sulA***. Fraction of the population surviving after six hours from adding ampicillin. Surviving cells were estimated by counting colony-forming units. Values represent the mean ± standard error from three biological repeats.

In summary, we have observed that chronic DSBs induced at *lacZ* (right-palindrome) induce tolerance to ampicillin in slow-growing conditions, and is dependent upon *sulA*. Previous reports indicate that deleting *sulA* (SOS cell division inhibitor) decreases tolerance to ampicillin (Miller et al., 2004). Indeed, we found that removing *sulA* abolished the increase in antibiotic tolerance induced by chronic DSBs (right panel, figure 4.13). However Δ*sulA* did not affect tolerance to ampicillin in cells without chronic DSBs, contrary to the reports in Miller et al. (2004). This discrepancy could arise from

the difference in growth conditions and slightly different antibiotic concentrations (LB media and 4-8 μg/ml of ciprofloxacin were used in that study).

4.6.3 Proximity of the *lon* gene to the DSB site at *lacZ* could explain the effect from *sulA* deletion

A possible explanation correlating *sulA* dependency with specificity to the right-palindrome, comes from the observation that the gene coding for Lon protease (this protein degrades SulA) is located very near *lacZ*, and we have observed RecA loading further from that region by ChIP-seq (figure 4.9). It is possible that degradation of that region by RecBCD reduces expression of *lon*, making cells more sensitive to division inhibition by SulA. The effect of degradation of *lon* could be evaluated by placing this gene at another locus.

In Miller et al. (2004) it was proposed that a delay in cell division by SulA, may prevent recruitment of peptidoglycan synthase at the septum (FtsI), conferring more tolerance to ampicillin. This interpretation is not entirely consistent with our observations from single-cells under chronic DSBs. We do observe a significant fraction of cells not growing and dividing, however, they appear to be non viable (see section 4.4.2). Conversely, we do not observe a large frequency of normally dividing cells delaying cell division, enough to explain of the population surviving in the presence of ampicillin (data not shown). Consistent with this discrepancy, reports indicate that β-lactam preferentially targets FtsI (cephalexin) is only bacteriostatic in minimal media (Chung et al., 2009). We can confirm that we were unable to kill *E. coli* in slow-growing conditions using cephalexin (data not shown). An alternative explanation is that the effect of *sulA* mutation is indirect, for example, deleting *sulA* may free Lon protease to degrade other targets. This scenario may be plausible, considering the reports indicating that *lon* deletion increases the frequency of persistent cells (Goormaghtigh et al., 2018).

4.7 Discussion

4.7.1 Growth may influence the success of DSB repair

We have discovered that single-cell variability in SOS induction by chronic DSBs is very sensitive to growth conditions. In particular, we observed bi-modal distribution of SOS induction in slow-growing conditions, whereas SOS-expression distributions were uni-modal in fast-growing conditions. Cells with very high SOS induction in slow-growing conditions were characterised by an arrest in cell division, reduction in cell growth and gene expression, which is most likely irreversible.

Quantification of RecA enrichment induced by chronic DSBs across the genome revealed that DSB repair may depend on the growth condition, in particular that RecA is loaded further from the break site, suggesting multiple events of RecBCD processing, possibly from failed repair attempts. These events could be the cause for the observed reduction in growth and gene expression in single-cells, as degradation of DNA surrounding the break site could half the dosage of essential genes. This effect may trigger additional cellular responses like the general stress response, which ultimately would result in a reduction of gene expression and growth.

One main limitation for the interpretation of the observations in RecA enrichment is that the mechanism leading to higher levels of SOS induction remains unknown. For example, it is concealable that palindromes can be cleaved post-replication on both strands, albeit with a low probability. This would lead to non-reparable DSBs in slow-growing cells, whereas the probability of cleaving all copies would be lower for fast-growing cells. This hypothesis could explain why some cells induce very high levels of SOS, it would predict that this conversion is irreversible, and one may argue that RecA is enriched further from the break-site in slow-growing conditions because of successive failed attempts at finding an homologous partner for repair. Coming with methods for disproving this hypothesis is challenging. We believe that marker frequency analysis using deep-sequencing in cells sorted by SOS-induction levels could provide useful insights (Hasan et al., 2018), as we should expect a complete loss of reads near the break site in cells with very high SOS, and a perfect palindrome that is known to cleave both strands could be used a positive control (Azeroglu et al., 2014). The palindromes used in this study contain a 24bp interruption to prevent hairpin formation. An interesting possibility could be evaluate if by increasing the size of the

interruption it is possible to reduce the frequency of cells with very high SOS induction, but still generate chronic DSBs.

4.7.2 Cells with very high SOS induction reduce growth

The observation that cells with very high SOS-induction reduce growth is somewhat unique, as to our knowledge it has not been reported for other sources of DNA damage. As stated above, it is difficult to speculate whether this is specific to chronic DSBs induced by palindromes (e.g. due to un-repairable DSBs) or generic to DSBs induced by other means. Preliminary observations of cells under ciprofloxacin treatment using time-lapse microscopy using agar-pads shows that some cells with very high-SOS induction also appear to grow slower, but further characterisation is required to confirm this (data not shown). Recent reports confirms that moderately higher concentration of ciprofloxacin than those used in this thesis (4-8 ng/ml) induce the general stress response (RpoS) (Pribis et al., 2018), and that RpoS induction correlated with oxidative damage via an unknown mechanism. Therefore we can expect that some cells will also reduce cellular growth under quinolone treatment correlated with RpoS induction. The fact that there is a high variability in division times have important consequences when interpreting steady state distributions of gene expression, which will be discussed in more detail in section 5.4.

4.7.3 Physiological consequences of chronic DSBs depend on the genomic locus

Another novel finding we have uncovered is that both the amount of SOS induced by chronic DSBs, and the physiological consequence resulting in phenotypes like antibiotic tolerance, may depend on the break site location in the genome. The first observation pertaining the differences in SOS induction we believe can be explained the χ-site distribution surrounding the break site. χ-site enrichment is biased towards the origin proximal side (Halpern et al., 2007), so we can expect higher variability between locus in the enrichment towards the terminus side. Indeed, the locus with more χ-sites towards the terminus (left-palindrome) correlates with higher SOS induction in slow-growing conditions. It has been speculated that RecBCD may collide with the replisome moving towards terminus and fall off before loading RecA (Cockram et al., 2015).

Regarding the effect on persistence to ampicilin, it is interesting that persistence was found only with the palindrome locus that showed less SOS induction (right-palindrome). Induction of SOS is required for persistence in this strain, as it can be abolished by deletion of *sulA*, but the level of SOS is not predictive of persistence. Instead, we believe degradation of relevant genes surrounding the break site may reduce their expression, and eventually induce a sub-population of persistence cells, in the case of *lacZ* a reasonable candidate is the *lon* gene. This is in agreement with other studies that have shown an increase in antibiotic tolerance in the absence of Lon protease (Harms et al., 2017). Finally, our observations on locus specific effects may be relevant beyond the study of DSBs repair, as targeted DSBs has been proposed as a strategy for killing cells, such as CRISPR-Cas delivered by phages proposed in Bikard et al. (2014). The functionality of surrounding genes should be considered when deciding potential targets for these applications.

Chapter 5

Conclusions

5.1 Influence of growth in the DNA damage response as a scalling problem

Exponential cellular and population growth imply a partial auto-catalytic process, however not every cellular process may contribute to growth equally. Therefore, it is not surprising that the cellular composition changes by increasing growth-rate, resulting for example in increasing the concentration of ribosomes and reducing the concentration of proteins not directly related to growth.

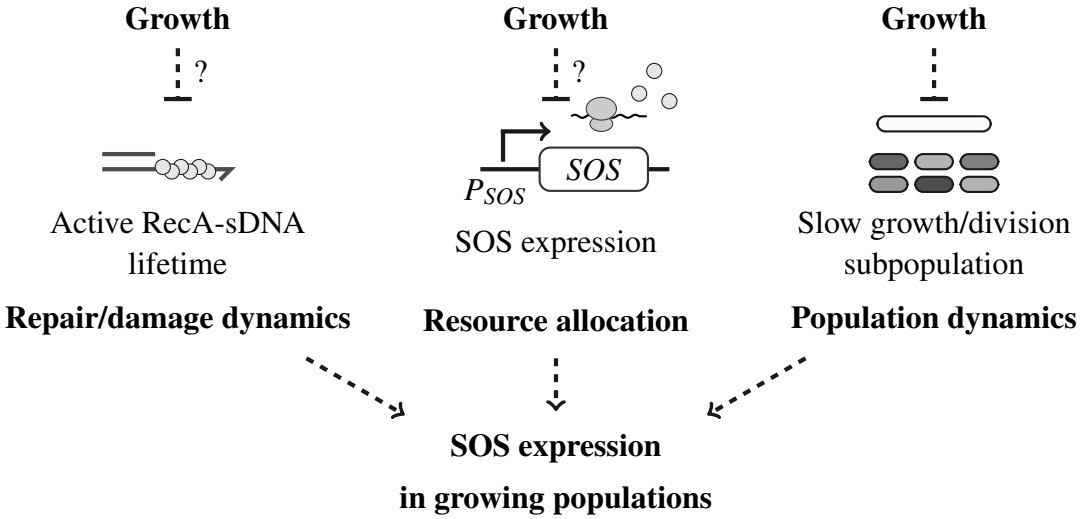

Figure 5.1: **Multiple factors influence the distribution of SOS-induction in single cells**. The distribution of SOS-induction in single cells is a combination of several processes that can be affected by growth conditions. Changes in the frequency of DNA-replication could affect the rate of DNA damage, however, we have not found direct evidence for this under moderate damage conditions. Changes in copy numbers per cell could influence the relevance of fluctuations inherent to biochemical reactions, such as homology search by RecA, which could be consistent with our observations. We have not found direct evidence that expression of SOS genes is limited by resource allocation. Finally, we have found that very high levels of SOS correlate with reduced growth in addition to delaying cell division in single cells. This introduces a sampling bias towards faster dividing cells (with low SOS), which is expected to increase when cells are in fast-growing conditions.

The frequency of DNA-replication, which may influence the frequency of DSBs. However we found that for chronic DSBs that are replication-dependent, this does not

translate necessarily into higher SOS-induction, at least within the moderate levels of DNA damage used in this study. Instead, we found that the biggest influence of growth-conditions is in the frequency of cells with very high SOS-induction. Unexpectedly we found that SOS distributions have a very long-tail; and that cells with very high SOS-induction are over-represented in slow-growing conditions.

Qualitatively, higher single-cell variability in slow-growing conditions could be a consequence of at least three different processes: higher SOS expression in slow growing conditions, for which our results argue against; fluctuations in the levels of SOS-signal (RecA-ssDNA) which could be higher in slow-growing cells; and population dynamics, because of the observed correlation between SOS-induction and long division times.

5.2 Is the maximum SOS-expression growth invariant?

Our results from deleting *lexA* suggest that the maximum expression from promoters is not limited by resource allocation in the same way constitutive genes are (Scott et al., 2010; Klumpp and Hwa, 2014). However further studies would need to verify this indeed a property of SOS genes *recA*, *sulA*, and *recN*, and not an artifact from using a GFP reporter. In case our observations are not artifacts, it would indicate additional regulation acting on these promoters. For example, repression of SOS promoters by an additional factor could explain invariant expression by changes in growth, however, despite decades of studies, none additional regulation has been described for these three promoters. This may not be entirely surprising, as the use of *lexA* deletions is not common in studies of the SOS-induction. The possibility of additional regulation on SOS promoters appears as an interesting evolutionary strategy to overcome limitations by resource allocation. One interesting thought is that for evolution, the maximum SOS expression may have been tuned to set the rate at which SOS is induced after DNA damage, meaning whether cells reach or not that maximum level may not be that relevant.

Recently it has been proposed that the *recN* promoter could be moderately repressed by DnaA binding (Wurihan et al., 2018). However, the mutations used in the aforementioned study to support regulation by DnaA could also impact growth and constitutive expression, but not control was added to account for this possibility, in order to make sure the effect on *recN* is indeed specific, and not just a global change in

gene-expression. For this reason, we advise the use of constitutive reporters which can reveal the global impact of perturbations on gene expression, particularly when the effects in question are relatively small.

5.3 Copy numbers and variability in DSB repair

Given that SOS expression results from repairing DSBs and these are discrete events, we can expect some single-cell variability in the SOS signal (RecA-ssDNA) because of biochemical fluctuations. Theoretically, fluctuations in the duration of molecular events can be averaged when molecules are in higher numbers and are more predominant when copy numbers are low. Slow-growing cells are smaller in size, thus having fewer repair molecules per cell (*e.g.* RecA and LexA) could increase the relevance of fluctuations and translate into higher variability in SOS induction. An interesting perspective for future studies could be to increase ectopically the expression of some repair enzymes, and evaluate whether variability in SOS-induction is reduced. The high degree of variability in SOS induction under chronic DSBs appears to be consistent with the idea that some cells may have trouble repairing, which may lead to long-lived SOS-signal (RecA-ssDNA), and thus very high levels of SOS-induction. It is not entirely impossible that repair by homologous recombination may fail with a certain low probability, however, we cannot exclude the possibility that the palindromes used to induce chronic DSBs may be cleaved on both strands with a low probability, thus leading to non-repairable breaks. Indeed we observed that most very high-SOS cells appear to be unable to recover. We can expect also single-cell variability in the amount of damage experienced under ciprofloxacin treatment, which is not surprising given breaks induced in this condition are probably random. Although it is difficult to discuss their origin as the mechanism leading to DSBs is not well understood (Drlica et al., 2008).

In order to evaluate the role of DSB repair in SOS induction, some estimation of the lifetime in different growth conditions is required. The only approach we see possible is to optimize RecA fluorescent labeling to observe DSB repair in single cells, which is complicated because of the tendency of RecA protein to form aggregates. Very recently a new method based on a fluorescently-labeled truncation of the λ-repressor has been reported, which could be a valuable tool for studying the repair process in single-cells (Ghodke et al., 2019).

5.4 Cell division and sampling bias in growing populations

Recent advances in time-lapse microscopy have renewed the interest in cell cycle variability in single-cells (Powell, 1956; Rosenthal et al., 2017; Potvin-Trottier et al., 2018). Theoretical work has shown that in growing populations, cell lineages with shorter cell cycles will be over-represented as a consequence of population dynamics (Thomas, 2017). This is relevant in the context of the DNA damage response because of SOS induction delays cell division. Furthermore, we have found evidence that in some cases high levels of SOS induction can also correlate with a reduction in single-cell growth, which can delay even further the division time of cells with elevated levels of SOS. Because cells with high levels of SOS take longer to divide, they will be less represented than low-SOS cells that divide faster. If the difference in division times between each sub-population is high enough, then the fraction of slow-dividing cells will decrease in fast-growing conditions (Patra and Klumpp, 2013). Thus, in this light, it is not entirely surprising that cells with very high SOS induction are over-represented in slow-growing conditions.

A key question is how to distinguish the influence of growth in SOS-induction variability at single cells, from the influence it has in population dynamics. Unfortunately, we are not aware of any simple method to isolate these effects from the distributions at steady-state alone, and the problem can be theoretically challenging (Patra and Klumpp, 2013; Thomas, 2017). Careful quantification of SOS induction in single-cells, how this affects the cell cycle, and subsequent quantitative modelling would be required to disentangle molecular single-cell variability from population dynamics. The difference in cell cycles demands the use of micro-chambers to avoid competition and filamentation due to the DNA damage response can become quite problematic in mother-machine like devices, particularly in fast-growing conditions where cells become very long.

These observations may have further consequences for the mathematical models used to estimate mutagenesis rates (Foster, 2005, 2006; Kussell, 2013). In addition to single cell variability in SOS induction, as shown in this thesis and in other reports (Uphoff, 2018; Patange et al., 2018), the fact that high SOS induction correlates with a reduction of single cell growth may result in under-estimating the real value of mu-

tation rates. Interestingly, mutation rates for cultures grown in chemostat have been shown to increase by decreasing the growth rate (Maharjan and Ferenci, 2018). For the future would be necessary to establish the contribution of molecular mechanisms (e.g. SOS induction and general stress response) and population dynamics (subpopulation with reduced growth) to the mutagenesis process, in order to develop a more quantitative understanding of the consequences that antibiotic treatment has for bacteria growing at different rates.

5.5 General lessons for studying the response to stress in different growth conditions

Studying quantitatively the influence of growth-conditions in the response(s) to stress should be seen as solving three related problems: 1) how the relevant molecular processes scale with growth? (*e.g.* resource allocation constraints); 2) what is the cell cycle variability under the stress conditions? (population dynamics); and 3) how variability in molecular processes correlates with cell cycle variability? We believe these considerations to be very important in the study of sub-lethal doses of antibiotics, as cell cycle variability has been observed for antibiotics inhibiting cell wall synthesis (Lambert and Kussell, 2015) and for those inhibiting translation (Deris et al., 2013). Additionally, heterogeneity in the cell cycle can be expected when the general stress response is induced (Patange et al., 2018), which has been reported to be induced by different bactericidal antibiotics (Laureti et al., 2013). Addressing these questions requires to observe cells growing and responding in real-time, which highlights the need for advancing microfluidics and microscopy technologies.

Appendix A

List of plasmids, strains, and primers

Table A.1: **List of plasmids**.

Plasmid	**Purpose**	**Source**
pSJR015	Source sequence for P_{recA}-*mGFP*	Zaslaver et al. (2006)
pSJR016	Source sequence for P_{recA}-*mGFP*	Zaslaver et al. (2006)
pSJR017	Clone-integration marker excision	pE-FLP (St-Pierre et al., 2013)
pSJR021	Clone-integration at HK022 site	pOSIP-KH (St-Pierre et al., 2013)
pSJR025	Clone-integration at P21 site	pOSIP-KT (St-Pierre et al., 2013)
pSJR028	P_{recA}-*mGFP* insertion by CLI	This study
pSJR030	P_{recN}-*mGFP* insertion by CLI	This study
pSJR035	Source sequence for P*sulA-mGFP*	DL4847
pSJR036	P_{sulA}-*mGFP* insertion by CLI	This study
pSJR046	P_{tetO1}-*mKate2* insertion by CLI	This study
pSJR047	*recA-mCherry* insertion by PMGR	DL5196 (Amarh et al., 2018)
pSJR052	*sulA* deletion by PMGR	DL1573 (Darmon et al., 2014)
pSJR054	*sbcDC* deletion by PMGR	DL1628 (Darmon et al., 2007)
pSJR055	P_{BAD}-*sbcDC* replacement by PMGR	DL1779 (Eykelenboom et al., 2008)
pSJR067	*lexA* deletion by PMGR	DL2741 (D. Leach lab, unpublished)
pSJR071	pTOF24 vector	Merlin et al. (2002)
pSJR073	*symE* deletion by PMGR	This study
pSJR074	*yafNOP* deletion by PMGR	This study
pSJR077	*dinQ* deletion by PMGR	This study
pSJR096	*recA-mGFP* insertion by PMGR	This study
pSJR097	*recA-ypet* insertion by PMGR	This study

Table A.2: **Plasmid construction**. List of plasmids constructed in this study. For the first seven plasmids, the vector was digested with restriction enzymes, the insert(s) were amplified by PCR, and finally the plasmid ligated using Gibson assembly. For the last two plasmids, the vector was amplified directly by PCR. When two inserts were used, PCR primer pairs are separated with a semicolon.

Plasmid		**Backbone**	**Digestion**	**PCR template(s)**	**primer pair(s)**
pSJR028	*HK022::*P_{recA}*-mGFP*	pSJR021	EcoRI, PstI	pSJR015	oSJR036, oSJR054
pSJR030	*HK022::*P_{recN}*-mGFP*	pSJR021	EcoRI, PstI	pSJR016	oSJR036, oSJR054
pSJR036	*HK022::*P_{sulA}*-mGFP*	pSJR021	EcoRI, PstI	pSJR035	oSJR084, oSJR085
pSJR046	*P21::*P_{tetO1}*-mKate2*	pSJR025	EcoRI, PstI	eSJR017	oSJR066, oSJR098
pSJR072	Δ*tisAB*	pSJR075	XhoI, BamHI	eSJR048	oSJR183, oSJR184; oSJR185, oSJR186
pSJR073	Δ*symE*	pSJR075	XhoI, BamHI	eSJR048	oSJR189, oSJR190; oSJR191, oSJR192
pSJR074	Δ*yafNOP*	pSJR075	XhoI, BamHI	eSJR048	oSJR195, oSJR196; oSJR197, oSJR198
pSJR077	Δ*dinQ*	pSJR075	XhoI, BamHI	eSJR048	oSJR212, oSJR213; oSJR214, oSJR215
pSJR096	*recA-mGFP*			pSJR047; pSJR035	oSJR330, oSJR333; oSJR331, oSJR332
pSJR097	*recA-ypet*			pSJR047; eSJR036	oSJR340, oSJR343; oSJR341, oSJR342

Table A.3: **List of strains**. CLI stands for clone-integration; PMGR for plasmid mediated gene replacement, and P1 for phage transduction.

Strain	Background	Genotype	Source/Construction
eSJR001	BW27783		Gift from Raul Fernandez Lopez
eSJR017	MG1655	*seqA::mGFP* P_{rna1}*-mKate2*	Gift from Raul Fernandez Lopez (RFL84). mKate2 construct built by Nathan Lord.
eSJR036	BW27784	*ssb-Ypet*	Gift from David Leach (DL5251)
eSJR048	MG1655	*rph-1* λ^-	Genomic Stock Center (CGSC7740)
eSJR059	MG1655	*lacI*^{q} *lacZ::pal246 cynX::Gm*^{R}	Gift from David Leach (DL2859)
eSJR070	MG1655	Δ*recA::Cm*^{R}	eSJR048 P1 using DL0654 (strain carrying Δ*recA::Cm*^{R}, gift from David Leach)
eSJR079	BW27784	ΔP_{sbcDC} P_{BAD}*-sbcDC* *lacI*^{q} *lacZ::pal246 cynX::Gm*^{R}	Gift from David Leach (DL2005)
eSJR123	MG1655	*HK022:*P_{recA}*-mGFP*	eSJR048 CLI using pSJR028
eSJR125	MG1655	*HK022:*P_{recA}*-mGFP*	eSJR048 CLI using pSJR030
eSJR130	BW27784	*asbB::pal246 ascF::Kn*^{R}	Gift from David Leach (DL4212)
eSJR145	MG1655	*HK022:*P_{sulA}*-mGFP*	eSJR048 CLI using pSJR036
eSJR203	MG1655	*HK022:*P_{recA}*-mGFP* *P21:*P_{tet01}*-mKate2*	eSJR123 CLI using pSJR046
eSJR205	MG1655	*HK022:*P_{recN}*-mGFP* *P21:*P_{tet01}*-mKate2*	eSJR125 CLI using pSJR046
eSJR206	MG1655	*HK022:*P_{sulA}*-mGFP* *P21:*P_{tet01}*-mKate2*	eSJR145 CLI using pSJR046
eSJR214	MG1655	eSJR206 *asbB::pal246 ascF::Kn*^{R}	eSJR206 P1 using eSJR130
eSJR225	BW27783	*HK022:*P_{sulA}*-mGFP*	eSJR001 CLI using pSJR036
eSJR232	BW27783	*HK022:*P_{sulA}*-mGFP* *P21:*P_{tet01}*-mKate2*	eSJR225 CLI using pSJR046
eSJR235	MG1655	*recA-recX::recAmwg-mCherry*	eSJR048 PMGR using pSJR047
eSJR246	MG1655	eSJR206 Δ*sulA*	eSJR206 PMGR using pSJR052
eSJR262	BW27783	eSJR232 Δ*sbcDC*	eSJR232 PMGR using pSJR054
eSJR265	BW27783	eSJR232 ΔP_{sbcDC} P_{BAD}*-sbcDC*	eSJR232 PMGR using pSJR055

Strain	Background	Genotype	Source/Construction
eSJR268	BW27783	eSJR265 *lacI^q lacZ::pal246 cynX::Gm^R*	
eSJR270	BW27783	eSJR265 *asbB::pal246 ascF::Kn^R*	
eSJR272	BW27783	eSJR262 *lacI^q lacZ::pal246 cynX::Gm^R*	eSJR262 P1 using eSJR079
eSJR273	BW27783	eSJR262 *asbB::pal246 ascF::Kn^R*	eSJR262 P1 using eSJR130
eSJR274	BW27783	eSJR265 *lacI^q lacZ::pal246 cynX::Gm^R asbB::pal246 ascF::Kn^R*	
eSJR276	BW27783	eSJR262 *lacI^q lacZ::pal246 cynX::Gm^R asbB::pal246 ascF::Kn^R*	eSJR272 P1 using eSJR130
eSJR301	MG1655	eSJR206 *lacI^q lacZ::pal246 cynX::Gm^R*	eSJR206 P1 using eSJR059
eSJR302	MG1655	eSJR206 *lacI^q lacZ::pal246 cynX::Gm^R asbB::pal246 ascF::Kn^R*	eSJR301 P1 using eSJR130
eSJR326	MG1655	eSJR206 Δ*tisAB*	eSJR206 PMGR using pSJR072
eSJR327	MG1655	eSJR206 Δ*symE*	eSJR206 PMGR using pSJR072
eSJR328	MG1655	eSJR206 Δ*yafNOP*	eSJR206 PMGR using pSJR072
eSJR329	MG1655	eSJR302 Δ*tisAB*	eSJR302 PMGR using pSJR072
eSJR330	MG1655	eSJR302 Δ*symE*	eSJR302 PMGR using pSJR072
eSJR331	MG1655	eSJR302 Δ*yafNOP*	eSJR302 PMGR using pSJR072
eSJR332	MG1655	eSJR206 Δ*tisAB* Δ*symE*	eSJR326 PMGR using pSJR073
eSJR333	MG1655	eSJR206 Δ*symE* Δ*yafNOP*	eSJR327 PMGR using pSJR074
eSJR334	MG1655	eSJR206 Δ*yafNOP* Δ*tisAB*	eSJR328 PMGR using pSJR072
eSJR335	MG1655	eSJR302 Δ*tisAB* Δ*symE*	eSJR329 PMGR using pSJR073
eSJR336	MG1655	eSJR302 Δ*symE* Δ*yafNOP*	eSJR330 PMGR using pSJR074
eSJR337	MG1655	eSJR302 Δ*yafNOP* Δ*tisAB*	eSJR331 PMGR using pSJR072
eSJR338	MG1655	eSJR206 Δ*tisAB* Δ*symE* Δ*yafNOP*	eSJR333 PMGR using pSJR072
eSJR339	MG1655	eSJR302 Δ*tisAB* Δ*symE* Δ*yafNOP*	eSJR336 PMGR using pSJR072
eSJR341	MG1655	eSJR206 Δ*dinQ*	eSJR206 PMGR using pSJR077
eSJR342	MG1655	eSJR302 Δ*dinQ*	eSJR302 PMGR using pSJR077

Strain	Background	Genotype	Source/Construction
eSJR343	MG1655	eSJR206 Δ*tisAB* Δ*symE* Δ*yafNOP* Δ*dinQ*	eSJR338 PMGR using pSJR077
eSJR344	MG1655	eSJR302 Δ*tisAB* Δ*symE* Δ*yafNOP* Δ*dinQ*	eSJR339 PMGR using pSJR077
eSJR395	MG1655	eSJR206 Δ*sulA asbB::pal246 ascF::Kn^R*	eSJR246 P1 using eSJR130
eSJR396	MG1655	eSJR204 Δ*sulA*	eSJR204 PMGR using pSJR052
eSJR397	MG1655	eSJR205 Δ*sulA*	eSJR205 PMGR using pSJR052
eSJR399	MG1655	eSJR206 Δ*sulA lacI^q lacZ::pal246 cynX::Gm^R asbB::pal246 ascF::Kn^R*	eSJR395 P1 using eSJR059
eSJR400	MG1655	eSJR206 Δ*sulA* Δ*lexA*	eSJR246 PMGR using pSJR067
eSJR401	MG1655	eSJR204 Δ*sulA* Δ*lexA*	eSJR396 PMGR using pSJR067
eSJR402	MG1655	eSJR205 Δ*sulA* Δ*lexA*	eSJR397 PMGR using pSJR067
eSJR431	MG1655	*recA-recX::recAmwg-mGFP*	eSJR048 PMGR using pSJR096
eSJR432	MG1655	*recA-recX::recAmwg-ypet*	eSJR048 PMGR using pSJR097

Table A.4: **List of primers**. For plasmids constructed with two different inserts, primer pairs are identified by “arm-1” and “arm-2”.FW and RV straind for forward and rever primers.

Primer	5′-3′ Sequence	Purpose
oSJR036	TAGGTTAGGCGCCATGCATCTCGAGGCATG	pSJR028 and pSJR030 construction
	CCTGCAGTTATTTGTATAGTTCATCCATGC	
oSJR054	GGACGCCCGCCATAAACTGCCAGGAATTGG	pSJR028 and pSJR030 construction
	GGATCGGAATTCCGACGTCTAAGAAACCAT	
oSJR084	GGACGCCCGCCATAAACTGCCAGGAATTGG	pSJR036 construction
	GGATCGGAATTCAGGGTTGATCTTTGTTGT	
oSJR085	TTAGGTTAGGCGCCATGCATCTCGAGGCAT	pSJR036 construction
	GCCTGCAGTTATTTGTATAGTTCATCCATG	
oSJR066	ACGCCCGCCATAAACTGCCAGGAATTGGGG	pSJR046 construction
	ATCGGAATTCTTATCTGTGCCCCAGTTTGC	
oSJR098	ATGAATTCAAATACTGTCCTTCCGGTCAGT	pSJR046 construction
	GCGTCCTGCTGATGTGCTCAGTATCTCTAT	
	CACTGATAGGGATGTCAATCTCTATCACTG	
	ATAGGGACTCGACTGCAGGCATGCCTCGAG	
	ATGCATGGCGCCTAACCTAAACTGACA	
oSJR058	GGAATCAATGCCTGAGTG	HK022 insertion verification
oSJR059	ACTTAACGGCTGACATGG	HK022 insertion verification
oSJR060	ACGAGTATCGAGATGGCA	HK022 insertion verification
oSJR061	GGCATCAACAGCACATTC	HK022 insertion verification
oSJR092	ATCGCCTGTATGAACCTG	P21 insertion verification
oSJR093	ACTTAACGGCTGACATGG	P21 insertion verification
oSJR094	GGGAATTAATTCTTGAAGACG	P21 insertion verification
oSJR095	TAGAACTACCACCTGACC	P21 insertion verification
oSJR183	TGTTATGAGCCATATTCAACGGGAAACGTC	pSJR072 construction arm-1 FW
	TTGCTCGAGCGGGGTTTTGGAATCGTGTGT	
oSJR184	CGTCAGCATCGCATCCGACACCAACCCGCA	pSJR072 construction arm-1 RV
	CGCTAAATACCCGCATAACACATTGCGTAC	
oSJR185	AACTTCTATAATATCACTGTACGCAATGTG	pSJR072 construction arm-2 FW
	TTATGCGGGTATTTAGCGTGCGGGTTGGTG	
oSJR186	ACCGGTCGACTCTAGAGGATCGCGGCCGCT	pSJR072 construction arm-2 RV
	CTAGAGGATCCCGCGACCAGCGTTGCCAGC	

Primer	5′-3′ Sequence	Purpose
oSJR189	ATGAGCCATATTCAACGGGAAACGTCTTGC TCGAGAATCAATACCCTGTGAGACTTTTTG	pSJR073 construction arm-1 FW
oSJR190	AATCACTATTCCTGGAGAATAGCAGTTATG ACTTCAGTAAATATTTACCAGTCTGATTTT	pSJR073 construction arm-1 RV
oSJR191	TTTTTACTGCAAAATCAGACTGGTAAATAT TTACTGAAGTCATAACTGCTATTCTCCAGG	pSJR073 construction arm-2 FW
oSJR192	CGGTCGACTCTAGAGGATCGCGGCCGCTCT AGAGGATCCGAACAAGCCGAAATCGTTCGC	pSJR073 construction arm-2 RV
oSJR195	TTATGAGCCATATTCAACGGGAAACGTCTT GCTCGAGTACAAAAGTGTGATCTGGTGATG	pSJR074 construction arm-1 FW
oSJR196	ATACCAGGCGGGCGTTATTTTCATTGCAAG CTGGATACAGTGATACCCTCATAATAATGC	pSJR074 construction arm-1 RV
oSJR197	TATATTCTGGTGTGCATTATTATGAGGGTA TCACTGTATCCAGCTTGCAATGAAAATAAC	pSJR074 construction arm-2 FW
oSJR198	CCGGTCGACTCTAGAGGATCGCGGCCGCTC TAGAGGATCCGAAGAACGCTGCGCCAATCG	pSJR074 construction arm-2 RV
oSJR212	GTGTTATGAGCCATATTCAACGGGAAACGT CTTGCTCGAGGATAACACGGGTGCAGTGGA	pSJR077 construction arm-1 FW
oSJR213	GGTTTTATAACCTGCATGTACTGTATGATT ATCCAGTTTAGCGGAAACGTAATTAAGGGC	pSJR077 construction arm-1 RV
oSJR214	TAGTGTGCTCTTAGCCCTTAATTACGTTTC CGCTAAACTGGATAATCATACAGTACATGC	pSJR077 construction arm-2 FW
oSJR215	CGACTCTAGAGGATCGCGGCCGCTCTAGAG GATCCGTCAAAAACATATATGACTTAACGA	pSJR077 construction arm-2 RV
oSJR120	TCAACGGTCAGGCTGTAACT	*sulA* deletion verification FW
oSJR121	GGTGTTATCTTTCGGAGCGG	*sulA* deletion verification RV
oSJR124	TCTCGGCCAGAACTTCTACA	*sbcDC* deletion verification FW
oSJR125	TCACTGCAAACGTACTTTCCA	*sbcDC* deletion verification RV
oSJR126	CGTCGCACATATCTTCAGGT	P_{BAD}-*sbcDC* insertion verification FW
oSJR127	TCACCGGCAACAATAATCGC	P_{BAD}-*sbcDC* insertion verification RV
oSJR176	CAGTTTATGGTTCCAAAATCGCC	*lexA* deletion verification FW
oSJR177	TGAAGTGAGGAATGCCATGC	*lexA* deletion verification RV
oSJR142	CGTTGAGCATGGAAGTAGTCA	*tisAB* deletion verification FW
oSJR145	TTGAGATCGCGCGCCATAT	*tisAB* deletion verification RV

Primer	5′-3′ Sequence	Purpose
oSJR193	ACCATAAGCCAAAACCAACTCA	*symE* deletion verification FW
oSJR194	CACGCCAATCATAACCCACA	*symE* deletion verification RV
oSJR199	GTATCCGGAACTTGAACGCC	*yafNOP* deletion verification FW
oSJR200	GCCTTCCTGCAACTCGAATT	*yafNOP* deletion verification RV
oSJR218	GAAGGTATTTACGCGGTGGG	*dinQ* deletion verification FW
oSJR219	GCAGGTAGTGTCTCTCTTCGA	*dinQ* deletion verification RV
oSJR330	GAATTGGGACAACTCCAGTGAAAAGTTCTT CTCCTTTACTGATGCTCCCAAAGTCCTCGT	pSJR096 vector amplification FW
oSJR333	TGGGATTACACATGGCATGGATGAACTATA CAAATAATCGTCTTGTTTGATACACAAGGG	pSJR096 vector amplification RV
oSJR331	TGTAGCCGAAACCAACGAGGACTTTGGGAG CATCAGTAAAGGAGAAGAACTTTTCACTGG	pSJR096 insert amplification FW
oSJR332	CCGCAGATGCGACCCTTGTGTATCAAACAA GACGATTATTTGTATAGTTCATCCATGCCA	pSJR096 insert amplification RV
oSJR340	TTGGGACAACACCAGTGAATAATTCTTCAC CTTTAGACATGATGCTCCCAAAGTCCTCGT	pSJR097 vector amplification FW
oSJR343	TGCTGGTATTACCGAGGGTATGAATGAATT GTACAAATCGTCTTGTTTGATACACAAGGG	pSJR097 vector amplification RV
oSJR341	AGCCGAAACCAACGAGGACTTTGGGAGCAT CATGTCTAAAGGTGAAGAATTATTCACTGG	pSJR097 insert amplification FW
oSJR342	CGCAGATGCGACCCTTGTGTATCAAACAAG ACGATTTGTACAATTCATTCATACCCTCGG	pSJR097 insert amplification RV
oSJR027	TGCCCGCGGTGAAGGCATTACC	*recA* fusion insertion verification FW
oSJR106	TTTTGCCCATAATCGGTGCC	*recA* fusion insertion verification RV
oSJR072	TTATGCTTCCGGCTCGTATG	*lacZ::pal246* verification FW
oSJR073	GGCGATTAAGTTGGGTAACG	*lacZ::pal246* verification RV
oSJR080	CCAACCAGTCTGAAGGTGCG	*ascB::pal246* verification FW
oSJR081	CCAGCGGTTCGATACCGTAC	*ascB::pal246* verification RV

Appendix B

Mathematical modelling

B.1 Introduction

The aim of this section is to serve as theoretical support for some of the arguments developed within the main text. In the first part, we will revisit the Cooper and Helmstetter model of DNA-replication (Helmstetter and Cooper, 1968; Cooper and Helmstetter, 1968), and provide an alternative derivation for gene-dosage at different growth-rates. These equations were used to estimate the number of replication forks per cell passing through the palindrome regions in chapter 4. Next, we derive a simpler version of the model presented in (Patra and Klumpp, 2013). This model was used in chapter 4 to partially explain why we may expect high-SOS cells to be over-represented in slow-growing conditions. Finally, we utilise the coarse-grained cell model developed in Weiße et al. (2015) to show why a decrease in growth due to metabolic burden from protein over-expression, is expected to correlate with a reduction in constitutive expression. This result is used in chapter 3 to argue that the decrease in growth observed for the Δ*lexA* Δ*sulA* is unlikely to result from metabolic burden due to over-expressing SOS genes.

B.2 Cooper and Helmstetter model revisited

Cooper and Helmstetter original model was developed to explain changes in total DNA synthesis as function of growth rate (Helmstetter and Cooper, 1968; Cooper and Helmstetter, 1968), but did not included explicitly gene copy numbers per cell (gene dosage). Since then, others have extended their derivation to account for individual location within the chromosome (Bremer and Churchward, 1977; Bremer et al., 1979), and they have been used over the years to account for growth dependent changes in gene dosage (*e.g.* Tadmor and Tlusty (2008); Rudolph et al. (2013); Si et al. (2017)). As we will see, the derivation in (Bremer and Churchward, 1977; Bremer et al., 1979) does not model DNA replication directly, but utilises consequences that follow from balanced growth conditions. Therefore, we decided to re-derive their model from explicit assumptions, which will see generate the same results.

B.2.1 Original balanced growth derivation

It is worth beginning with the original derivation in Bremer and Churchward (1977). Conceptually the argument is an extension from Cooper and Helmstetter model (C&H

model), with constraints imposed by assuming balanced growth conditions.

To beging with, let's call $N(t)$ the number of cells growing exponentially over time. Assuming exponential growth, we have

$$N(t) = N_0 2^{\mu t}$$

Now, from C&H model, we assume a fixed delay between division and replication denoted by D. Then, the total number of chromosomal terminus T in the population is related to the total number of cells by $T(t-D) = N(t)$, or to say $T(t) = N(t+D) \propto 2^{\mu(t+D)}$. Then, the number of terminus per cell is given by

$$\frac{T}{N} = 2^{\mu D}$$

Now, we shall introduce the second assumption from C&H model, that is it takes C to replicate the chromosome. Then, the total number of origins I in the population should satisfy the following relations $I(t-D-C) = T(t-C) = N(t)$ because of the delays. In other words, $I(t) = N(t+C+D) \propto 2^{\mu(t+C+D)}$. Meaning that the number of origins per cell is given by

$$\frac{I}{N} = 2^{\mu(C+D)}$$

Finally, we need to relate these relation to the copies per cell in between origin and terminus. Let's call $m \in [0,1]$ the genomic location, with $m(ori) = 1$ and $m(ter) = 0$. Given DNA replication is bi-directional, gene copy numbers can be assumed to be symmetric between both replicative arms. Assuming replication speed is constant, it takes Cm for the replication fork to travel from m to the terminus. So the total the total number of copies of location m ($X(t)$) should follow $X(t-Cm-D) = T(t-Cm) = N(t)$. In order words $X(t) = N(t+Cm+D) \propto 2^{\mu(Cm+D)}$. Then, the dosage of location m per cell is given by

$$\frac{X}{N} = 2^{\mu(Cm+D)} \tag{B.1}$$

B.2.2 Deterministic model of DNA replication at steady state

We will provide an alternative derivation for gene-dosage beginning explicitly from C&H assumptions, and arrive to the same equation as in Bremer and Churchward (1977). This derivation was made in collaboration with Vincent Danos.

We shall begin with a few definitions. Let's call m the relative position on the chromosome, $m_{ter} = 0$, $m_{ori} = 1$, $m \in [0,1]$. Let's call t the time within the cell cycle of

period τ, $t \in [0,\tau]$. Let's call $\mathsf{r}_i(t)$ the position of the ith replication fork (counting from the terminus) $\mathsf{r}_i \in [0,1], \mathsf{r}_i(t) \leq \mathsf{r}_{i+1}(t)$. Also, let's call $\iota(m,t)$ the number of replication forks between the terminus and location m, defined as

$$\iota(m,t) = j, \quad \mathsf{r}_j(t) \leq m < \mathsf{r}_{j+1}(t) \tag{B.2}$$

with this, we can define explicitly gene-dosage $\mathcal{D}(m,t)$ as

$$\mathcal{D}(m,t) = 2^{\iota(m,t)} \tag{B.3}$$

Notice gene-dosage now depends on the genomic locus m and time of the cell cycle t. What is left to do is to identify the function $\iota(m,t)$, which will see can be derived from C&H assumtions.

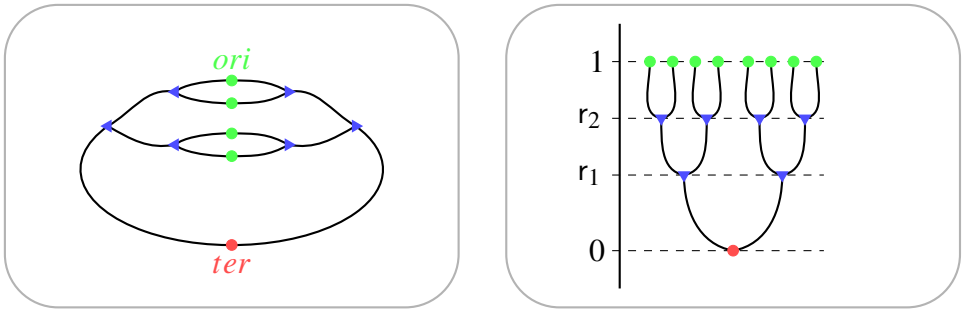

Figure B.1: **Representation of replicating chromosome**. Diagram showing the equivalence between chromosome replication (left) and our mathematical representation (right). The positions of the replication forks are r_i.

Following Cooper and Helmstetter (Cooper and Helmstetter, 1968), we will assume that: 1) the chromosome is replicated at a constant speed, 2) the location of a replication fork is the same as the next fork after one division time, 3) and that there is a fixed delay between the end of chromosome replication and cell division. These assumptions can be formaly written as follow

$$\begin{aligned} \mathsf{r}_i(t) &= -\tfrac{t}{C} + \gamma_i \quad (1) \\ \mathsf{r}_i(t) &= \mathsf{r}_{i+1}(t+\tau) \quad (2) \\ C\,\mathsf{r}_1(0) &= \tau - D \quad (3) \end{aligned} \tag{B.4}$$

where $\frac{1}{C}$ is the speed of DNA replication, and D is the delay period bewteen replication forks reaching terminus and cell division. Remember cell division occurs withing a period τ. We will see these equations are enough to obtain an explicit expression for the positions of the replication forks $\mathsf{r}_i(t)$.

From (1) and (2) we can obtain a relation for the initial position of the replication forks

$$\gamma_{i+n} = n\frac{\tau}{C} + \gamma_i$$

From (3) and (1) we can obtain an explicit expression for the initial position of the replication fork closer to terminus

$$\gamma_1 = \frac{\tau - D}{C}$$

Then combining both relations, we obtain an explicit expression for the initial position of the replication forks

$$\gamma_i = \frac{i\tau - D}{C}$$

Then, we can replace this expression in (1), and obtain the position of DNA replication forks in time

$$\mathsf{r}_i(t) = \frac{i\tau - D - t}{C} = \frac{1}{\mu C}\left(i - \mu(D+t)\right)$$

where μ is the doubling rate, $\mu = 1/\tau$. Notice some correction is needed, as the domain of replication fork position is bounded between 0 and 1, $\mathsf{r}_i(t) \in [0,1]$. To be precise, the position of DNA replication forks is given by

$$\mathsf{r}_i(t) = \begin{array}{ll} 0 & t \geq i\tau - D \\ \nexists & i\tau - (C+D) > t \\ \frac{1}{\mu C}\left(i - \mu(D+t)\right) & else \end{array} \tag{B.5}$$

The first case accounts for replication forks that have reached terminus, as values less than 0 have no physical meaning. The second case accounts for DNA replication forks before initiating a new round of replication. That is because our derivation assumed "virtual" DNA replication forks with position bigger than one ($m > 1$). The time for initiating a new round of DNA replication is precisely that at which the position of the "virtual" DNA replication forks is one ($m = 1$). Finally, the last case represent the position of forks travelling towards terminus.

Now we can return the question of gene-dosage. The number of replication forks between the terminus and location m ($\iota(m,t)$) is defined as $\iota(m,t) = j$, given that $\mathsf{r}_j(t) \leq m < \mathsf{r}_{j+1}(t)$. Then using the expression for the position of DNA replication forks $\mathsf{r}_i(t)$ we obtained

$$\begin{array}{rcccl} \frac{\iota(m,t)\tau - D - t}{C} & \leq & m & < & \frac{(\iota(m,t)+1)\tau - D - t}{C} \\ \iota(m,t) & \leq & \mu(Cm + D + t) & < & \iota(m,t) + 1 \end{array}$$

that is to say

$$\mathfrak{u}(m,t) = \lfloor \mu(Cm+D+t) \rfloor \tag{B.6}$$

Notice that the integer part operator $\lfloor \rfloor$ makes irrelevant our previous distinction of different cases for $\mathsf{r}_i(t)$. With this, we finally obtained a closed expression for gene-dosage over the cell cycle

$$\mathcal{D}(m,t) = 2^{\lfloor \mu(Cm+D+t) \rfloor} \tag{B.7}$$

This expression properly accounts for the fact DNA replication is discrete, in line with the original derivation in (Cooper and Helmstetter, 1968).

B.2.3 Gene-dosage in exponentially growing population

In order to relate gene-dosage over the cell cycle (equation B.7) to population measurements, we need to integrate over the cell cycle. However, a simple integration would be wrong, as not all cell ages are equally represented in balanced growth populations. In particular, newly born cells are represented twice more than just dividing cells. Assuming constant division time, the stationary distribution of cell age as $\mathsf{f}_a(t)$ has a precise expression (Powell, 1956)

$$\mathsf{f}_a(t) = \ln(2)\, \mu 2^{1-\mu t}$$

This distribution was also used in the original derivation in Cooper and Helmstetter (1968). We this, we can weight cell age by its density function, and calculate the expected value of gene-dosage in growing populations by integrating

$$\hat{\mathcal{D}}_\phi(m) = \int_0^\tau \mathsf{f}_a(t) 2^{\lfloor \mu(Cm+D+t) \rfloor} dt$$

Unfortunately, at present we have not solved this integral explicitly[1]. Instead, we have compared numerical integrations to the expected expression from Bremer et al. (1979), and found them to be equivalent, regardless of doubling rate and parameters for C and D. Therefore, we can conclude that

$$\hat{\mathcal{D}}_\phi(m) = 2^{\mu(Cm+D)} \tag{B.8}$$

[1] The presence of the integer part operator demands to divide the integral by intervals. Depending on the relative position of DNA replication initiation and termination in the cell cycle, the integral should be divided differently. The time of initiation of DNA replication is given by $t_{ori} = \tau\left(1 - \left\{\mu(C+D)\right\}\right)$, and the time at which DNA replication reaches terminus is given by $t_{ter} = \tau\left(1 - \left\{\mu D\right\}\right)$. We have not evaluated for all possible cases, but in principle this integral should be solvable.

B.2.4 Alternative derivation for cell age distribution

Powell appears to the first that tried to take into account the statistics of single cell growth into the typical average measurements (Powell, 1956; Koch and Schaechter, 1962). In the words of K. Powell: *"The age distribution in a growing culture has a curious and interesting property which is not generally known; roughly speaking, the youngest organisms are present in greatest number"*

Defining age of a cell the time which has elapsed since its inception, Powell found that the distribution of cell ages $\mathsf{f}_a(a)$ in an exponentially growing culture should follow

$$\mathsf{f}_a(a) = 2\lambda e^{-\lambda a} \int_a^\infty \mathsf{f}_\tau(s) ds$$

where λ is the growth rate of the culture, and $\mathsf{f}_\tau(s)$ is the distribution division times. To reach this conclusion, powell assumed that (1) cell population are homogeneous (one type of cells), (2) cultures have been in continous growth long enough such that age distribution becomes constant (convergence), (3) number of organism is so large, that can be treated as a continous variable.

B.2.4.1 Discrete derivation at constant doubling time

Here we will try to derive an expression for the stationary age distribution $\mathsf{f}_a(a)$, but instead taking division as a discrete process, as our gene-dosage derivation is also modelled as a discrete process. We will focus exclusively in the case cell division is assumed to be deterministic.

To begin with, we will answer the question: what is the age of a cell after a given time Δt? Let's name the age of a given cell by $a(t)$. The exact number of division it has gone thought after Δt is clearly $\lfloor \mu(\Delta t + a(t)) \rfloor$. Then, the answer to our question is

$$a(t+\Delta t) = a(t) + \Delta t - \tau \lfloor \mu(\Delta t + a(t)) \rfloor \tag{B.9}$$

We simply have stated the increase in cell age, minus the reversal to "new born" by the number of division events.

Notice that after each division a new cell is introduced to the population. What consequence does this have? As the number of division after Δt is $\lfloor \mu(\Delta t + a(t)) \rfloor$, we will we will have $2^{\lfloor \mu(\Delta t + a(t)) \rfloor}$ copies of cells with the same age $a(t+\Delta t)$. We can

exploit this fact to obtain some conditions on the stationary distributions of cell ages. Call $\mathsf{f}_a(a(t))$ the age distribution at time t. For $\mathsf{f}_a(a(t))$ to be stationary, then it must satisfy

$$\mathsf{f}_a(a(t+\Delta t)) = 2^{\lfloor \mu(\Delta t + a(t))\rfloor}\mathsf{f}_a(a(t))$$

which together with the expresion for $a(t+\Delta t)$ (equation B.9), can be rewritten as

$$\mathsf{f}_a(a) = 2^{-\lfloor \mu(\Delta t + a)\rfloor}\mathsf{f}_a(\Delta t + a - \tau\lfloor \mu(\Delta t + a)\rfloor) \tag{B.10}$$

This establishes a periodic condition for $\mathsf{f}_a(a)$ to be stationary, with regard to any increase in time Δt.

In principle, it would appear we can't solve $\mathsf{f}_a(a)$, but a pattern emerges when we manipulate somewhat the periodic condition. Let's name $s = \Delta t + a$. Then we can rewrite equation B.10 as

$$\mathsf{f}_a(s - \Delta t) = 2^{-\lfloor \mu s\rfloor}\mathsf{f}_a(s - \tau\lfloor \mu s\rfloor)$$

In order to simplify the integer and fractional part operators, we can separate the expression by intervals

$$\begin{aligned}
\mathsf{f}_a(s-\Delta t) &= \mathsf{f}_a(s), & s \in [0,\tau]\\
\mathsf{f}_a(s-\Delta t) &= 2^{-1}\mathsf{f}_a(s-\tau), & s \in [\tau,2\tau]\\
\mathsf{f}_a(s-\Delta t) &= 2^{-2}\mathsf{f}_a(s-2\tau), & s \in [2\tau,3\tau]\\
&\dots
\end{aligned}$$

in other words,

$$\mathsf{f}_a(s) = 2^{-1}\mathsf{f}_a(s-\tau) = 2^{-2}\mathsf{f}_a(s-2\tau) = \dots$$

Clearly, the solution must be a function of the kind

$$\mathsf{f}_a(s) = k2^{-\mu s}$$

otherwise it could not satisfy the periodic condition. As $\mathsf{f}_a(a)$ is defined as a probability density function, all is left is to find a suitable k such that

$$\int_0^\tau k2^{-\mu a}da = 1$$

which implies that $k = ln(2)\ \mu 2$. Finally, we obtain the stationary distribution of cell age, defined as

$$\mathsf{f}_a(a) = ln(2)\ \mu 2^{1-\mu a} \tag{B.11}$$

where $a \in [0,\tau]$. This expression is the same as the one found in Powell (1956) by assuming constant division time, meaning that assuming cell division to be discrete does not influences the result.

B.2.5 DNA replication initiation mass

Finally, we will like to revisit the controversial concept of mass at initiation of DNA replication. In Donachie (1968) was suggested suggesting that the mass at initiation of DNA replication ("initiation mass") was proportional to the number of origins per cell, leading to the so called constant "initiation mass" model (CITE). His argument was based on C&H model Cooper and Helmstetter (1968), together with observations in (Schaechter et al., 1958) on average cell mass at different growth conditions, in particular suggesting that the average cell mass increases exponentially with growth rate. This hypothesis has been controversial over the years, but recent evidence appear to indicate that is valid for a large number of growing conditions(Si et al., 2017). Therefore, we thought worthwhile to re-derive the mass at initiation of DNA replication, as it does not follow explicitly from Donachie's assumptions.

First, let's begin with how to describe cell mass over the cell cycle. It is now established that cell size increases exponentially (Taheri-Araghi et al., 2015). It what follows we will assume that cell mass is proportional to the size (constant density). Then, we can write the mass of cells over the cell cycle as

$$m(t) = m_0 2^{\mu t}$$

where m_0 is the mass at birth, and μ is the doubling rate constant. If the average cell mass increases exponentially with growth rate (Schaechter et al., 1958; Si et al., 2017), then the mass at birth must also increase exponentially (Koch and Schaechter, 1962). In other words, we can write the mass at birth as

$$m_0 = m_m 2^{k\mu}$$

where m_m and k are some constants. Then combining both expressions, we can rewrite the cell mass over the cell cycle as

$$m(t) = m_m 2^{\mu(k+t)} \tag{B.12}$$

What is the mass at initiation of DNA replication? First, we need to find the time at which initiation of DNA replication takes place, t_{ori}. The time of DNA replication initiation is exactly the when origin gene-dosage doubles. From C&H model we know that replication origin dosage is given by $2^{\lfloor \mu(C+D+t) \rfloor}$. Then, the transition point of the integer operator $\lfloor\rfloor$ will be given by

$$\mu(C+D+t_{ori}) = \lfloor \mu(C+D+t_{ori}) \rfloor$$

Or equivalently

$$\Big\{\mu(C+D+t_{ori})\Big\} = 0$$

We know that $\Big\{\mu(C+D+t)\Big\}$ completes one period in τ time, then it must also be true that $\Big\{\mu(C+D)\Big\} + \mu t_{ori} = 0$[2]. So, the time at initiation of DNA replication is

$$t_{ori} = \tau\left(1 - \Big\{\mu(C+D)\Big\}\right) \tag{B.13}$$

This expression is consistent with the original arguments by C&H (see figure 4 in Helmstetter and Cooper (1968)).

Now, we can express the mass of cells at initiation of DNA replication from the expression for $m(t)$ (equation B.12) and the value of t_{ori} (equation B.13). After some rearrangements, we find that

$$m(t_{ori}) = m_m 2^{\mu(k+t_{ori})} = 2m_m 2^{\mu(k-(C+D))+\lfloor\mu(C+D)\rfloor} \tag{B.14}$$

Notice that the factor $2^{\lfloor\mu(C+D)\rfloor}$ happens to be the number of origins per cell, similarly to Donachie's argument. However the proportionality bewteen $m(t_{ori})$ and $2^{\lfloor\mu(C+D)\rfloor}$ depends on the value of constant k. For example, the mass at initiation is exactly proportional to the number of origins per cell only when k is equal to $(C+D)$. The value of k is not explicit in Donachie's argument, as instead he argues in the opposite direction. He claims that if mass at initiation is "constant", then we should observe an exponential increase in cell mass with growth rate (Donachie, 1968). As we have seen, one does not exactly imply the other.

This apparent contradiction can be resolved by measuring directly exponential constant k, as it has been done in a recent publication with measurements of single-cell size under many kinds of growing conditions (Si et al., 2017). It appears that $k \approx 2\,(C+D)$ (Figure S5 in that publication), which would imply that mass at initiation is not exactly proportional to the number of origins per cell. However, it is possible to do an approximation which reveals that the initiation mass is closely proportional. Before doing so, let's generalise the finding in Si et al. (2017) by saying that k is proportional to $C+D$. Then we can rewrite equation B.14 as

$$m(t_{ori}) = 2m_m 2^{\mu(\theta-1)(C+D)+\lfloor\mu(C+D)\rfloor} \approx m_m 2^{\mu(C+D)+\theta+1} \tag{B.15}$$

[2] As a matter of fact, the argument could be generalised for any location of the chromosome, where the equation to satisfy is $\Big\{\mu(Cm+D)\Big\} + \mu t_m = 0$

where $k = \theta\,(C+D)$, and we have done the approximation $\lfloor \mu(C+D) \rfloor \approx \mu(C+D)$. Notice that now the mass at initiation is approximately proportional to $2^{\mu(C+D)}$, that is the population average origins per cell. More generally, we can replace $k = \theta\,(C+D)$ in the expression for the cell mass over the cell cycle $m(t)$ (equation B.12)

$$m(t) = m_m 2^{\mu(C+D+t)+\theta}$$

This last equation can be interpret as an "universal" law for cell mass for any doubling rate, and is not an approximation as equation B.15.

It is worth mentioning that these expressions are granted for any conditions such that $C+D$ is independent of growth rate, as we can always find a suitable θ such that $k = \theta\,(C+D)$. This implies that stating approximately "constant initiation mass" in conditions when $C+D$ is invariant has no additional meaning, beyond exponential increase in cell mass with growth rate, and C&H model of DNA replication. The surprising fact is that the approximation $k \approx \theta\,(C+D)$ appears to be valid in cases where $C+D$ changes, as shown in Si et al. (2017). The underlaying mechanism appears to be linked to the mass gained or lost while waiting for the next initiation of replication, but it is beyond the scope of this section.

In conclusion, we have shown that the conditions for constant mass at initiation of DNA replication per the average number of origins are: (1) C&H model of DNA replication, (2) exponential increase in cell mass with growth rate, and (3) exponential constant k is proportional to $C+D$. We hope that the criterion of k as function of $C+D$ clarifies the concept of "constant initiation mass" and could be of use to other studies.

B.3 Population bias against non-dividing cells

We have observed that in conditions of chronic double-strand breaks, a non-dividing sub-population emerges. This non-dividing state appears to be irreversible, or at least conversion to normal dividing state is very slow. We wondered how the growth rate of dividing cells could impact the fraction of non-dividing cell within the population. In the following, we will present a simple deterministic model using differential equations, that establish a population bias against non-dividing cells.

Call n_1 and n_0 two populations. n_1 grows exponentially with rate λ, n_0 does not grow. n_1 converts into n_0 with rate β, and n_0 into n_1 with rate α. The dynamics of the

two populations are defined by the following equations

$$\begin{aligned} \frac{dn_1}{dt} &= \lambda n_1 - \beta n_1 + \alpha n_0 \\ \frac{dn_0}{dt} &= \beta n_1 - \alpha n_0 \end{aligned}$$

We are not interested in the absolute values of the populations (as they grow exponentially), but rather the population fractions. Let's define population fractions as $f_1 = \frac{n_1}{n_1+n_0} \in [0,1]$, and $f_0 = \frac{n_0}{n_1+n_0} \in [0,1]$. By using the rules of derivatives, and the fact that $\frac{d(n_1+n_0)}{dt} = \lambda n_1$, we get the following equations for the dynamics of population fractions

$$\begin{aligned} \frac{df_1}{dt} &= \lambda f_1 - \beta f_1 + \alpha f_0 - \lambda f_1^2 \\ \frac{df_0}{dt} &= \beta f_1 - \alpha f_0 - \lambda f_1 f_0 \end{aligned}$$

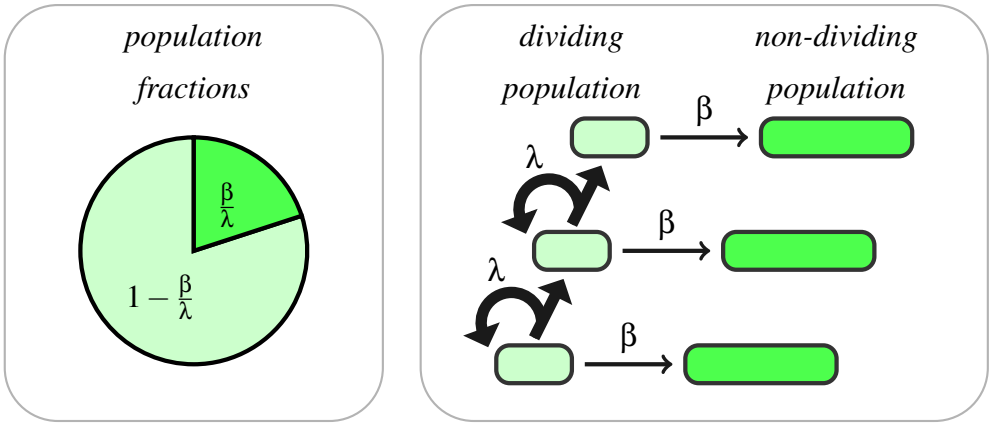

Figure B.2: **Population growth rate bias against a non-dividing sub-population**. In case there two sub-populations, one dividing and another non-dividing, and conversion from dividing to non-dividing is irreversible, the fraction of non-dividing cells is inversely proportional to population growth rate at steady state.

We are interested in the value of populations fractions at steady state. For calculating the steady state, we can take $\frac{df_1}{dt} - \frac{df_0}{dt} = 0$, together with $f_1 + f_0 = 1$, and find that f_0 is equal to

$$f_0 = \frac{1}{2\lambda}\left(\lambda + \beta + \alpha \pm \sqrt{(\lambda+\beta+\alpha)^2 - 4\lambda\beta}\right) \tag{B.16}$$

With this, we now have an explicit expression for the fraction of non-dividing population, f_0, at steady state.

The expression for f_0 can be simplified for some extreme conditions. For example, when conversion from n_1 to n_0 is irreversible, meaning $\alpha = 0$, $f_0 = \{\frac{\beta}{\lambda}, 1\}$. Or

more generally, in case $\beta \gg \alpha$, $f_0 \approx \{\frac{\beta}{\lambda}, 1\}$. In order words, when conversion from non-dividing to dividing state is very slow, the fraction of non-dividing cells will be inversely proportional to the growth rate of dividing cells (illustrated in figure B.2). This reasoning could also be extended more generally to any condition where a sub-population does not growth and divide, such as those that are persistent to antibiotic treatment (Patra and Klumpp, 2013; Brauner et al., 2016).

B.4 Coarse grained kinetic model of translational limitations

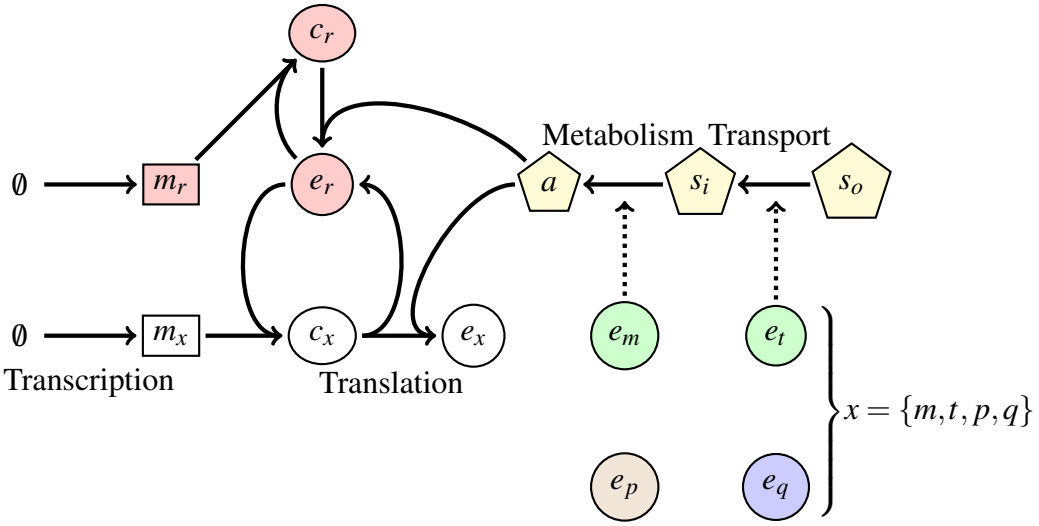

Figure B.3: **Schematic of coarse-grained model of growth and gene expression**. Solid arrows represent mass relations, whereas dotted arrows represent catalytic functions. The classes of chemical species are: external nutrient s_o, high energy molecules a, ribosomes e_r, metabolic enzymes e_m, transporter proteins e_t, other proteins (growth variant) e_p, other proteins (growth invariant) e_q, and their correspondent mRNAs m_m, m_p, m_q, m_r, and m_t. For simplicity, all classes other than ribosomes are collected as x. The concomitant production of mRNA from the production of proteins is not drawn, nor decay and dilution reactions (Weiße et al., 2015).

Many models have been developed attempting to represent cell growth, togethwer with constraints in gene expression by translational resource allocation. Among them, the model presented in Weiße et al. (2015) does a serious attempt to provide a coarse-

grained description cell growth and gene expression that is mechanistic. In particular, the model from Weiße et al. (2015) describes the coarse-grained average dynamics of exponentially growing *E. coli*, using diferential equations. There main classes of chemical species are: nutrient s_i, high energy molecules a, ribosomes r, metabolic enzymes e_m, transporter proteins e_t, other proteins (growth variant) e_p, other proteins (growth invariant) e_q, and mRNAs m_m, m_p, m_q, m_r, and m_t (see diagram in figure B.3). The model accounts for processes of import of nutrients, conversion of nutrients to high energy metabolites, transcription and translation. Cellular growth is represented as the rate of protein accumulation, and changes in nutrient chemical composition are represented by an stochiometric factor between nutrients and high energy metabolite a.

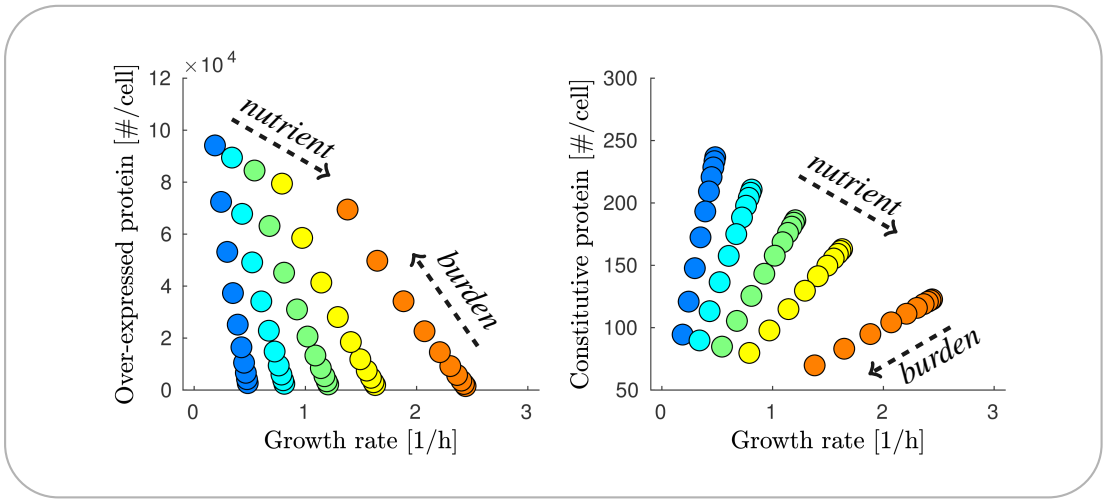

Figure B.4: **Over-expression burden decreases constitutive gene-expression**. Effect of over-expression burden on growth and constitutive expression at steady-state. Each color represent media with different nutrient quality. Default parameter values from (Weiße et al., 2015) were used for numerical simulations. For over-expression maximum transcription rate constant was varied between 0 and 20, in order to simulate the effect of over-expression.

We have used this model to evaluate the effect of burden by gene over-expression, into the expression of a constitutive gene. The motivation is to ask whether over-expression burden, for example from full SOS induction, could influence the expression of a constitutive gene. Given the mechanistic description of the model, it is relatively straight forward to incorporate new classes of genes. In particular, we have

added two new classes of constitutive expressed genes, and varied the maximum transcription rate of one of them, while monitoring the expression from the other gene[3]. We can observe that at steady state, changes in nutrient quality decrease constitutive expression as expected from constraints by resource allocation (see figure B.4). On the other hand, burden by over-expression results in decreasing both growth rate and constitutive expression. In conclusion, decrease of growth by over-expression burden should correlate with a reduction in constitutive gene-expression.

[3]Code for numerical simulations can be found at `https://gitlab.com/MEKlab/sjr_thesis/tree/master/simulations/ws_model/wsoverexpr`

Bibliography

Aagaard, J., Gasser, T., Rhodes, P., and Madsen, P. O. (1991). MICs of ciprofloxacin and trimethoprim for *Escherichia coli*: influence of pH, inoculum size and various body fluids. *Infection*, 19 Suppl 3:S167–9.

Aksenov, S. V. (1999). Dynamics of the inducing signal for the SOS regulatory system in *Escherichia coli* after ultraviolet irradiation. *Math Biosci*, 157(1-2):269–286.

Aldred, K. J., Kerns, R. J., and Osheroff, N. (2014). Mechanism of quinolone action and resistance. *Biochemistry*, 53(10):1565–1574.

Amarh, V., White, M. A., and Leach, D. R. F. (2018). Dynamics of RecA-mediated repair of replication-dependent DNA breaks. *J Cell Biol*, 217(7):2299–2307.

Amundsen, S. K., Taylor, A. F., and Smith, G. R. (2000). The RecD subunit of the *Escherichia coli* RecBCD enzyme inhibits RecA loading, homologous recombination, and DNA repair. *Proc Natl Acad Sci USA*, 97(13):7399–7404.

Andersen, J. B., Sternberg, C., Poulsen, L. K., Bjorn, S. P., Givskov, M., and Molin, S. (1998). New unstable variants of green fluorescent protein for studies of transient gene expression in bacteria. *Appl Environ Microbiol*, 64(6):2240–2246.

Andersson, D. I. and Hughes, D. (2011). Persistence of antibiotic resistance in bacterial populations. *FEMS Microbiol Rev*, 35(5):901–911.

Andersson, D. I., Koskiniemi, S., and Hughes, D. (2010). Biological roles of translesion synthesis DNA polymerases in eubacteria. *Mol Microbiol*, 77(3):540–548.

Ashley, R. E., Dittmore, A., McPherson, S. A., Turnbough, C. L., Neuman, K. C., and Osheroff, N. (2017). Activities of gyrase and topoisomerase IV on positively supercoiled DNA. *Nucleic Acids Res*, 45(16):9611–9624.

Azeroglu, B. and Leach, D. R. F. (2017). RecG controls DNA amplification at double-strand breaks and arrested replication forks. *FEBS Lett*, 591(8):1101–1113.

Azeroglu, B., Lincker, F., White, M. A., Jain, D., and Leach, D. R. F. (2014). A perfect palindrome in the *Escherichia coli* chromosome forms DNA hairpins on both leading- and lagging-strands. *Nucleic Acids Res*, 42(21):13206–13213.

Bachmann, B. J. (1972). Pedigrees of some mutant strains of *Escherichia coli* K-12. *Bacteriol Rev*, 36(4):525–557.

Baharoglu, Z., Bikard, D., and Mazel, D. (2010). Conjugative DNA transfer induces the bacterial SOS response and promotes antibiotic resistance development through integron activation. *PLoS Genet*, 6(10):e1001165.

Baharoglu, Z. and Mazel, D. (2014). SOS, the formidable strategy of bacteria against aggressions. *FEMS Microbiology Reviews*, 38(6):1126–1145.

Baralla, A. (2008). Modeling and parameter estimation of the sos response network in e. coli. Master's thesis, University of Trento, Trento, Italy.

Barbé, J., Villaverde, A., Cairo, J., and Guerrero, R. (1986). ATP hydrolysis during SOS induction in *Escherichia coli*. *J Bacteriol*, 167(3):1055–1057.

Barker, M. M., Gaal, T., Josaitis, C. A., and Gourse, R. L. (2001). Mechanism of regulation of transcription initiation by ppGpp. i. effects of ppGpp on transcription initiation in vivo and in vitro. *J Mol Biol*, 305(4):673–688.

Basan, M., Hui, S., Okano, H., Zhang, Z., Shen, Y., Williamson, J. R., and Hwa, T. (2015a). Overflow metabolism in *Escherichia coli* results from efficient proteome allocation. *Nature*, 528(7580):99–104.

Basan, M., Zhu, M., Dai, X., Warren, M., Sévin, D., Wang, Y.-P., and Hwa, T. (2015b). Inflating bacterial cells by increased protein synthesis. *Mol Syst Biol*, 11(10):836.

Basu, A., Parente, A. C., and Bryant, Z. (2016). Structural dynamics and mechanochemical coupling in DNA gyrase. *J Mol Biol*, 428(9 Pt B):1833–1845.

Battesti, A., Majdalani, N., and Gottesman, S. (2011). The RpoS-mediated general stress response in escherichia coli. *Annu Rev Microbiol*, 65:189–213.

Battesti, A., Tsegaye, Y. M., Packer, D. G., Majdalani, N., and Gottesman, S. (2012). H-NS regulation of IraD and IraM antiadaptors for control of RpoS degradation. *J Bacteriol*, 194(10):2470–2478.

Beaber, J. W., Hochhut, B., and Waldor, M. K. (2004). SOS response promotes horizontal dissemination of antibiotic resistance genes. *Nature*, 427(6969):72–74.

Bell, J. C. and Kowalczykowski, S. C. (2016). Mechanics and single-molecule interrogation of DNA recombination. *Annu Rev Biochem*, 85:193–226.

Belov, O. V. (2011). Modeling ultraviolet-induced SOS response in translesion synthesis-deficient cells of Escherichia coli bacteria. *Phys. Part. Nuclei Lett.*, 8(1):61–66.

Belov, O. V., Krasavin, E. A., and Parkhomenko, A. Y. (2009). Model of SOS-induced mutagenesis in bacteria *Escherichia coli* under ultraviolet irradiation. *J Theor Biol*, 261(3):388–395.

Bentley, W. E., Mirjalili, N., Andersen, D. C., Davis, R. H., and Kompala, D. S. (1990). Plasmid-encoded protein: the principal factor in the "metabolic burden" associated with recombinant bacteria. *Biotechnol Bioeng*, 35(7):668–681.

Berghoff, B. A., Hoekzema, M., Aulbach, L., and Wagner, E. G. H. (2017). Two regulatory RNA elements affect TisB-dependent depolarization and persister formation. *Mol Microbiol*, 103(6):1020–1033.

Bernhardt, T. G. and de Boer, P. A. J. (2005). SlmA, a nucleoid-associated, FtsZ binding protein required for blocking septal ring assembly over chromosomes in e. coli. *Mol Cell*, 18(5):555–564.

Bi, E. and Lutkenhaus, J. (1993). Cell division inhibitors SulA and MinCD prevent formation of the FtsZ ring. *J Bacteriol*, 175(4):1118–1125.

Bichara, M., Meier, M., Wagner, J., Cordonnier, A., and Lambert, I. B. (2011). Postreplication repair mechanisms in the presence of DNA adducts in *Escherichia coli*. *Mutat Res*, 727(3):104–122.

Bidnenko, V., Ehrlich, S. D., and Michel, B. (2002). Replication fork collapse at replication terminator sequences. *EMBO J*, 21(14):3898–3907.

Bikard, D., Euler, C. W., Jiang, W., Nussenzweig, P. M., Goldberg, G. W., Duportet, X., Fischetti, V. A., and Marraffini, L. A. (2014). Exploiting CRISPR-cas nucleases to produce sequence-specific antimicrobials. *Nat Biotechnol*, 32(11):1146–1150.

Bollenbach, T., Quan, S., Chait, R., and Kishony, R. (2014). Nonoptimal Microbial Response to Antibiotics Underlies Suppressive Drug Interactions. *Cell*, 139(4):707–718.

Boubakri, H., de Septenville, A. L., Viguera, E., and Michel, B. (2010). The helicases DinG, rep and UvrD cooperate to promote replication across transcription units in vivo. *EMBO J*, 29(1):145–157.

Bougdour, A., Cunning, C., Baptiste, P. J., Elliott, T., and Gottesman, S. (2008). Multiple pathways for regulation of sigmaS (RpoS) stability in *Escherichia coli* via the action of multiple anti-adaptors. *Mol Microbiol*, 68(2):298–313.

Bouveret, E. and Battesti, A. (2011). The stringent response. In Hengge, R. and Storz, G., editors, *Bacterial stress responses, second edition*, pages 231–250. American Society of Microbiology.

Brauner, A., Fridman, O., Gefen, O., and Balaban, N. Q. (2016). Distinguishing between resistance, tolerance and persistence to antibiotic treatment. *Nat Rev Microbiol*, 14(5):320–330.

Bremer, H. and Churchward, G. (1977). An Examination of the Cooper-Helmstetter Theory of DNA Replication in Bacteria and its Underlying Assumptions. *J. theor. Biol.*, 69:645–654.

Bremer, H. and Churchward, G. (1991). Control of cyclic chromosome replication in *Escherichia coli*. *Microbiol Rev*, 55(3):459–475.

Bremer, H., Churchward, G., and Young, R. (1979). Relation Between Growth and Replication in Bacteria. *J. theor. Biol.*, 81:533–545.

Bremer, H. and Dennis, P. (2008a). Feedback control of ribosome function in *Escherichia coli*. *Biochimie*, 90(3):493–499.

Bremer, H. and Dennis, P. P. (2008b). Modulation of chemical composition and other parameters of the cell at different exponential growth rates. *Ecosal Plus*, 3(1).

Browning, D. F. and Busby, S. J. W. (2016). Local and global regulation of transcription initiation in bacteria. *Nat Rev Microbiol*, 14(10):638–650.

Bryce, A., Hay, A. D., Lane, I. F., Thornton, H. V., Wootton, M., and Costelloe, C. (2016). Global prevalence of antibiotic resistance in paediatric urinary tract infections caused by *Escherichia coli* and association with routine use of antibiotics in primary care: systematic review and meta-analysis. *BMJ*, 352:i939.

Bush, N. G., Evans-Roberts, K., and Maxwell, A. (2015). DNA topoisomerases. *Ecosal Plus*, 6(2).

Butala, M., Klose, D., Hodnik, V., Rems, A., Podlesek, Z., Klare, J. P., Anderluh, G., Busby, S. J. W., Steinhoff, H.-J., and Zgur-Bertok, D. (2011). Interconversion between bound and free conformations of LexA orchestrates the bacterial SOS response. *Nucleic Acids Res*, 39(15):6546–6557.

Butala, M., Zgur-Bertok, D., and Busby, S. J. W. (2009). The bacterial LexA transcriptional repressor. *Cell Mol Life Sci*, 66(1):82–93.

Cambridge, J., Blinkova, A., Magnan, D., Bates, D., and Walker, J. R. (2014). A Replication-Inhibited Unsegregated Nucleoid at Mid-Cell Blocks Z-Ring Formation and Cell Division Independently of SOS and the SlmA Nucleoid Occlusion Protein in *Escherichia coli*. *Journal of Bacteriology*, 196(1):36–49.

Campbell, A. (1957). Synchronization of cell division. *Bacteriol Rev*, 21(4):263–272.

Centore, R. C. and Sandler, S. J. (2007). UvrD limits the number and intensities of RecA-green fluorescent protein structures in *Escherichia coli* K-12. *J Bacteriol*, 189(7):2915–2920.

Ceroni, F., Boo, A., Furini, S., Gorochowski, T. E., Borkowski, O., Ladak, Y. N., Awan, A. R., Gilbert, C., Stan, G.-B., and Ellis, T. (2018). Burden-driven feedback control of gene expression. *Nat Methods*, 15(5):387–393.

Chandler, M. G. and Pritchard, R. H. (1975). The effect of gene concentration and relative gene dosage on gene output in *Escherichia coli*. *Mol Gen Genet*, 138(2):127–141.

Chapman, J. S. and Georgopapadakou, N. H. (1988). Routes of quinolone permeation in *Escherichia coli*. *Antimicrob Agents Chemother*, 32(4):438–442.

Chatterji, M. and Nagaraja, V. (2002). GyrI: a counter-defensive strategy against proteinaceous inhibitors of DNA gyrase. *EMBO Rep*, 3(3):261–267.

Chatterji, M., Sengupta, S., and Nagaraja, V. (2003). Chromosomally encoded gyrase inhibitor GyrI protects *Escherichia coli* against DNA-damaging agents. *Arch Microbiol*, 180(5):339–346.

Chen, J. C. and Beckwith, J. (2001). FtsQ, FtsL and FtsI require FtsK, but not FtsN, for co-localization with FtsZ during *Escherichia coli* cell division. *Mol Microbiol*, 42(2):395–413.

Chen, Y., Milam, S. L., and Erickson, H. P. (2012). SulA inhibits assembly of FtsZ by a simple sequestration mechanism. *Biochemistry*, 51(14):3100–3109.

Chen, Z., Yang, H., and Pavletich, N. P. (2008). Mechanism of homologous recombination from the RecA-ssDNA/dsDNA structures. *Nature*, 453(7194):489–484.

Cheng, G., Hao, H., Dai, M., Liu, Z., and Yuan, Z. (2013). Antibacterial action of quinolones: from target to network. *Eur J Med Chem*, 66:555–562.

Chevereau, G. and Bollenbach, T. (2015). Systematic discovery of drug interaction mechanisms. *Mol Syst Biol*, 11(4):807.

Chiang, S. M. and Schellhorn, H. E. (2012). Regulators of oxidative stress response genes in escherichia coli and their functional conservation in bacteria. *Arch Biochem Biophys*, 525(2):161–169.

Cho, H., McManus, H. R., Dove, S. L., and Bernhardt, T. G. (2011). Nucleoid occlusion factor SlmA is a DNA-activated FtsZ polymerization antagonist. *Proc Natl Acad Sci USA*, 108(9):3773–3778.

Christensen-Dalsgaard, M., Jørgensen, M. G., and Gerdes, K. (2010). Three new RelE-homologous mRNA interferases of *Escherichia coli* differentially induced by environmental stresses. *Mol Microbiol*, 75(2):333–348.

Chubukov, V., Gerosa, L., Kochanowski, K., and Sauer, U. (2014). Coordination of microbial metabolism. *Nat Rev Microbiol*, 12(5):327–340.

Chung, H. S., Yao, Z., Goehring, N. W., Kishony, R., Beckwith, J., and Kahne, D. (2009). Rapid beta-lactam-induced lysis requires successful assembly of the cell division machinery. *Proc Natl Acad Sci USA*, 106(51):21872–21877.

Cockram, C. A. (2013). *Genomic Analysis of RecA-DNA Interactions During Double-Strand Break Repair in* Escherichia coli. PhD thesis, The University of Edinburgh.

Cockram, C. A., Filatenkova, M., Danos, V., El Karoui, M., and Leach, D. R. F. (2015). Quantitative genomic analysis of RecA protein binding during DNA double-strand break repair reveals RecBCD action in vivo. *Proc Natl Acad Sci USA*, 112(34):E4735–42.

Cooper, S. (1969). Cell division and DNA replication following a shift to a richer medium. *J Mol Biol*, 43(1):1–11.

Cooper, S. and Helmstetter, C. E. (1968). Chromosome replication and the division cycle of *Escherichia coli* B/r. *Journal of Molecular Biology*, 31(3):519 – 540.

Cromie, G. A., Connelly, J. C., and Leach, D. R. (2001). Recombination at double-strand breaks and DNA ends. *Molecular cell*, 8(6):1163–1174.

Culyba, M. J., Kubiak, J. M., Mo, C. Y., Goulian, M., and Kohli, R. M. (2018). Non-equilibrium repressor binding kinetics link DNA damage dose to transcriptional timing within the SOS gene network. *PLoS Genet*, 14(6):e1007405.

Dahan-Grobgeld, E., Livneh, Z., Maretzek, A. F., Polak-Charcon, S., Eichenbaum, Z., and Degani, H. (1998). Reversible induction of ATP synthesis by DNA damage and repair in *Escherichia coli*. in vivo NMR studies. *J Biol Chem*, 273(46):30232–30238.

Dai, X., Zhu, M., Warren, M., Balakrishnan, R., Okano, H., Williamson, J. R., Fredrick, K., and Hwa, T. (2018). Slowdown of translational elongation in *Escherichia coli* under hyperosmotic stress. *MBio*, 9(1).

Dajkovic, A., Mukherjee, A., and Lutkenhaus, J. (2008). Investigation of regulation of FtsZ assembly by SulA and development of a model for FtsZ polymerization. *J Bacteriol*, 190(7):2513–2526.

Danilowicz, C., Hermans, L., Coljee, V., Prévost, C., and Prentiss, M. (2017). ATP hydrolysis provides functions that promote rejection of pairings between different copies of long repeated sequences. *Nucleic Acids Res*, 45(14):8448–8462.

Dapa, T., Fleurier, S., Bredeche, M.-F., and Matic, I. (2017). The SOS and rpos regulons contribute to bacterial cell robustness to genotoxic stress by synergistically regulating DNA polymerase pol II. *Genetics*, 206(3):1349–1360.

Darfeuille, F., Unoson, C., Vogel, J., and Wagner, E. G. H. (2007). An antisense RNA inhibits translation by competing with standby ribosomes. *Mol Cell*, 26(3):381–392.

d'Ari, R. (1985). The SOS system. *Biochimie*, 67(3-4):343–347.

Darmon, E., Eykelenboom, J. K., Lopez-Vernaza, M. A., White, M. A., and Leach, D. R. F. (2014). Repair on the Go: *E. coli* Maintains a High Proliferation Rate while Repairing a Chronic DNA Double-Strand Break. *PLoS ONE*, 9(10):e110784.

Darmon, E. and Leach, D. R. F. (2014). Bacterial Genome Instability. *Microbiology and Molecular Biology Reviews*, 78(1):1–39.

Darmon, E., Lopez-Vernaza, M. A., Helness, A. C., Borking, A., Wilson, E., Thacker, Z., Wardrope, L., and Leach, D. R. F. (2007). SbcCD Regulation and Localization in *Escherichia coli*. *Journal of Bacteriology*, 189(18):6686–6694.

Deitz, W. H., Cook, T. M., and Goss, W. A. (1966). Mechanism of action of nalidixic acid on escherichia coli. 3. conditions required for lethality. *J Bacteriol*, 91(2):768–773.

Demirel, Y. (2014). Chapter 11 - thermodynamics and biological systems. In Demirel, Y., editor, *Nonequilibrium Thermodynamics (Third Edition)*, pages 485 – 562. Elsevier, Amsterdam, third edition edition.

Deris, J. B., Kim, M., Zhang, Z., Okano, H., Hermsen, R., Groisman, A., and Hwa, T. (2013). The innate growth bistability and fitness landscapes of antibiotic-resistant bacteria. *Science*, 342(6162).

Donachie, W. D. (1968). Relationship between cell size and time of initiation of DNA replication. *Nature*.

Donachie, W. D. and Blakely, G. W. (2003). Coupling the initiation of chromosome replication to cell size in *Escherichia coli*. *Curr Opin Microbiol*, 6(2):146–150.

Draper, G. C., McLennan, N., Begg, K., Masters, M., and Donachie, W. D. (1998). Only the n-terminal domain of FtsK functions in cell division. *J Bacteriol*, 180(17):4621–4627.

Drees, J. C., Lusetti, S. L., and Cox, M. M. (2004). Inhibition of RecA protein by the *Escherichia coli* RecX protein: modulation by the RecA c terminus and filament functional state. *J Biol Chem*, 279(51):52991–52997.

Drlica, K., Malik, M., Kerns, R. J., and Zhao, X. (2008). Quinolone-mediated bacterial death. *Antimicrob Agents Chemother*, 52(2):385–392.

Dubreuil, J. D., Isaacson, R. E., and Schifferli, D. M. (2016). Animal enterotoxigenic *Escherichia coli*. *Ecosal Plus*, 7(1).

Duval, M., Simonetti, A., Caldelari, I., and Marzi, S. (2015). Multiple ways to regulate translation initiation in bacteria: Mechanisms, regulatory circuits, dynamics. *Biochimie*, 114:18–29.

Duval, V. and Lister, I. M. (2013). MarA, SoxS and rob of *Escherichia coli* - global regulators of multidrug resistance, virulence and stress response. *Int J Biotechnol Wellness Ind*, 2(3):101–124.

Dwyer, D. J., Collins, J. J., and Walker, G. C. (2015). Unraveling the physiological complexities of antibiotic lethality. *Annu Rev Pharmacol Toxicol*, 55(1):313–332.

Dwyer, D. J., Kohanski, M. A., Hayete, B., and Collins, J. J. (2007). Gyrase inhibitors induce an oxidative damage cellular death pathway in *Escherichia coli*. *Mol Syst Biol*, 3:91.

Eckburg, P. B., Bik, E. M., Bernstein, C. N., Purdom, E., Dethlefsen, L., Sargent, M., Gill, S. R., Nelson, K. E., and Relman, D. A. (2005). Diversity of the human intestinal microbial flora. *Science*, 308(5728):1635–1638.

Edelstein, A., Amodaj, N., Hoover, K., Vale, R., and Stuurman, N. (2010). Computer control of microscopes using μmanager. *Curr Protoc Mol Biol*, Chapter 14:Unit14.20.

El Sayyed, H., Le Chat, L., Lebailly, E., Vickridge, E., Pages, C., Cornet, F., Cosentino Lagomarsino, M., and Espéli, O. (2016). Mapping topoisomerase IV binding and activity sites on the e. coli genome. *PLoS Genet*, 12(5):e1006025.

Eliopoulos, G. M. and Huovinen, P. (2001). Resistance to trimethoprim-sulfamethoxazole. *Clin Infect Dis*, 32(11):1608–1614.

Erickson, D. W., Schink, S. J., Patsalo, V., Williamson, J. R., Gerland, U., and Hwa, T. (2017a). A global resource allocation strategy governs growth transition kinetics of *Escherichia coli*. *Nature*, 551(7678):119–123.

Erickson, K. E., Winkler, J. D., Nguyen, D. T., Gill, R. T., and Chatterjee, A. (2017b). The tolerome: A database of transcriptome-level contributions to diverse *Escherichia coli* resistance and tolerance phenotypes. *ACS Synth Biol*, 6(12):2302–2315.

Erill, I., Campoy, S., and Barbé, J. (2007). Aeons of distress: an evolutionary perspective on the bacterial SOS response. *FEMS Microbiol Rev*, 31(6):637–656.

Eykelenboom, J. K., Blackwood, J. K., Okely, E., and Leach, D. R. (2008). SbcCD Causes a Double-Strand Break at a DNA Palindrome in the Escherichia coli Chromosome. *Molecular Cell*, 29(5):644–651.

Fernández De Henestrosa, A. R., Ogi, T., Aoyagi, S., Chafin, D., Hayes, J. J., Ohmori, H., and Woodgate, R. (2000). Identification of additional genes belonging to the LexA regulon in *Escherichia coli*. *Mol Microbiol*, 35(6):1560–1572.

Ferrell, J. E. (2002). Self-perpetuating states in signal transduction: positive feedback, double-negative feedback and bistability. *Curr Opin Cell Biol*, 14(2):140–148.

Finn, K., Lowndes, N. F., and Grenon, M. (2012). Eukaryotic DNA damage checkpoint activation in response to double-strand breaks. *Cell Mol Life Sci*, 69(9):1447–1473.

Florés, M.-J., Sanchez, N., and Michel, B. (2005). A fork-clearing role for UvrD. *Mol Microbiol*, 57(6):1664–1675.

Fornelos, N., Browning, D. F., and Butala, M. (2016). The use and abuse of lexa by mobile genetic elements. *Trends Microbiol*, 24(5):391–401.

Forsyth, V. S., Armbruster, C. E., Smith, S. N., Pirani, A., Springman, A. C., Walters, M. S., Nielubowicz, G. R., Himpsl, S. D., Snitkin, E. S., and Mobley, H. L. T. (2018). Rapid growth of uropathogenic *Escherichia coli* during human urinary tract infection. *MBio*, 9(2).

Foster, P. L. (2005). Stress responses and genetic variation in bacteria. *Mutat Res*, 569(1-2):3–11.

Foster, P. L. (2006). Methods for determining spontaneous mutation rates. *Meth Enzymol*, 409:195–213.

Friedman, N., Vardi, S., Ronen, M., Alon, U., and Stavans, J. (2005). Precise Temporal Modulation in the Response of the SOS DNA Repair Network in Individual Bacteria. *PLoS Biol*, 3(7):e238.

Friedmann, H. (2014). Escherich and Escherichia. *EcoSal Plus*.

Gama-Castro, S., Salgado, H., Santos-Zavaleta, A., Ledezma-Tejeida, D., Muñiz Rascado, L., García-Sotelo, J. S., Alquicira-Hernández, K., Martínez-Flores, I., Pannier, L., Castro-Mondragón, J. A., Medina-Rivera, A., Solano-Lira, H., Bonavides-Martínez, C., Pérez-Rueda, E., Alquicira-Hernández, S., Porrón-Sotelo, L., López-Fuentes, A., Hernández-Koutoucheva, A., Del Moral-Chávez, V., Rinaldi, F., and Collado-Vides, J. (2016). RegulonDB version 9.0: high-level integration of gene regulation, coexpression, motif clustering and beyond. *Nucleic Acids Res*, 44(D1):D133–43.

Ganti, T. (2003). *The Principles of Life*. Oxford University Press UK.

Ghodke, H., Paudel, B. P., Lewis, J. S., Jergic, S., Gopal, K., Romero, Z. J., Wood, E. A., Woodgate, R., Cox, M. M., and van Oijen, A. M. (2019). Spatial and temporal organization of reca in the *Escherichia coli* dna-damage response. *eLife*, 8:e42761.

Gibson, D. G., Young, L., Chuang, R.-Y., Venter, J. C., Hutchison, C. A., and Smith, H. O. (2009). Enzymatic assembly of DNA molecules up to several hundred kilobases. *Nat Methods*, 6(5):343–345.

Gibson, J. L., Lombardo, M.-J., Thornton, P. C., Hu, K. H., Galhardo, R. S., Beadle, B., Habib, A., Magner, D. B., Frost, L. S., Herman, C., Hastings, P. J., and Rosenberg, S. M. (2010). The sigma(e) stress response is required for stress-induced mutation and amplification in escherichia coli. *Mol Microbiol*, 77(2):415–430.

Giroux, X., Su, W.-L., Bredeche, M.-F., and Matic, I. (2017). Maladaptive DNA repair is the ultimate contributor to the death of trimethoprim-treated cells under aerobic and anaerobic conditions. *Proc Natl Acad Sci USA*, 114(43):11512–11517.

Goodman, M. F., McDonald, J. P., Jaszczur, M. M., and Woodgate, R. (2016). Insights into the complex levels of regulation imposed on *Escherichia coli* DNA polymerase v. *DNA Repair (Amst)*, 44:42–50.

Goormaghtigh, F., Fraikin, N., Putrinš, M., Hallaert, T., Hauryliuk, V., Garcia-Pino, A., Sjödin, A., Kasvandik, S., Udekwu, K., Tenson, T., Kaldalu, N., and Van Melderen, L. (2018). Reassessing the role of type II toxin-antitoxin systems in formation of *Escherichia coli* type II persister cells. *MBio*, 9(3).

Gore, J., Bryant, Z., Stone, M. D., Nöllmann, M., Cozzarelli, N. R., and Bustamante, C. (2006). Mechanochemical analysis of DNA gyrase using rotor bead tracking. *Nature*, 439(7072):100–104.

Grant, M., Saggioro, C., Ferrari, U., Bassetti, B., Sclavi, B., and Lagomarsino, M. C. (2011). DnaA and the timing of chromosome replication in *Escherichia coli* as a function of growth rate. *BMC Systems Biology*, 5(1):201.

Green, J. M. and Matthews, R. G. (2007). Folate biosynthesis, reduction, and polyglutamylation and the interconversion of folate derivatives. *Ecosal Plus*, 2(2).

Grenga, L., Luzi, G., Paolozzi, L., and Ghelardini, P. (2008). The *Escherichia coli* FtsK functional domains involved in its interaction with its divisome protein partners. *FEMS Microbiol Lett*, 287(2):163–167.

Greulich, P., Scott, M., Evans, M. R., and Allen, R. J. (2015). Growth-dependent bacterial susceptibility to ribosome-targeting antibiotics. *Mol Syst Biol*, 11(3):796.

Grudniak, A. M., Markowska, K., and Wolska, K. I. (2015). Interactions of *Escherichia coli* molecular chaperone HtpG with DnaA replication initiator DNA. *Cell Stress Chaperones*, 20(6):951–957.

Guo, M. S. and Gross, C. A. (2014). Stress-induced remodeling of the bacterial proteome. *Curr Biol*, 24(10):R424–34.

Haeusser, D. P. and Levin, P. A. (2008). The great divide: coordinating cell cycle events during bacterial growth and division. *Curr Opin Microbiol*, 11(2):94–99.

Haldane, J. B. S. (1941). *New Paths in Genetics*. Allen & Unwin. London, UK.

Halpern, D., Chiapello, H., Schbath, S., Robin, S., Hennequet-Antier, C., Gruss, A., and El Karoui, M. (2007). Identification of DNA motifs implicated in maintenance of bacterial core genomes by predictive modeling. *PLoS Genet*, 3(9):1614–1621.

Hansen, F., Christensen, B., and Atlung, T. (1991). The initiator titration model: computer simulation of chromosome and minichromosome control. *Res Microbiol*, 142(2-3):161–167.

Hansen, F. G. and Atlung, T. (2018). The DnaA tale. *Front Microbiol*, 9:319.

Harmon, F. G., Rehrauer, W. M., and Kowalczykowski, S. C. (1996). Interaction of *Escherichia coli* RecA protein with LexA repressor. II. inhibition of DNA strand exchange by the uncleavable LexA S119A repressor argues that recombination and SOS induction are competitive processes. *J Biol Chem*, 271(39):23874–23883.

Harms, A., Brodersen, D. E., Mitarai, N., and Gerdes, K. (2018). Toxins, targets, and triggers: An overview of toxin-antitoxin biology. *Mol Cell*, 70(5):768–784.

Harms, A., Fino, C., Sørensen, M. A., Semsey, S., and Gerdes, K. (2017). Prophages and growth dynamics confound experimental results with antibiotic-tolerant persister cells. *MBio*, 8(6).

Harrison, J. J., Wade, W. D., Akierman, S., Vacchi-Suzzi, C., Stremick, C. A., Turner, R. J., and Ceri, H. (2009). The chromosomal toxin gene yafQ is a determinant of multidrug tolerance for *Escherichia coli* growing in a biofilm. *Antimicrob Agents Chemother*, 53(6):2253–2258.

Hasan, A. M., Azeroglu, B., and Leach, D. R. (2018). Chapter twenty-two - genomic analysis of dna double-strand break repair in escherichia coli. In Carpousis, A. J., editor, *High-Density Sequencing Applications in Microbial Molecular Genetics*, volume 612 of *Methods in Enzymology*, pages 523 – 554. Academic Press.

Hauryliuk, V., Atkinson, G. C., Murakami, K. S., Tenson, T., and Gerdes, K. (2015). Recent functional insights into the role of (p)ppGpp in bacterial physiology. *Nat Rev Microbiol*, 13(5):298–309.

Helmstetter, C. E. (1967). Rate of DNA synthesis during the division cycle of *Escherichia coli* B/r. *Journal of Molecular Biology*, 24(3):417 – 427.

Helmstetter, C. E. (1996). Timing of synthetic activities in the cell cycle. In Neidhardt, F. C., Curtiss III, R., Ingraham, J. L., Lin, E. C. C., Low, K. B., Magasanik, B., Reznikoff, W. S., Riley, M., Schaechter, M., and Umbarger, H. E., editors, *Escherichia coli and Salmonella. Cellular and Molecular Biology. Second edition.*, pages 1627–1639. ASM Press.

Helmstetter, C. E. and Cooper, S. (1968). DNA synthesis during the division cycle of rapidly growing *Escherichia coli* B/r. *Journal of Molecular Biology*, 31(3):507 – 518.

Helmstetter, C. E., Eenhuis, C., Theisen, P., Grimwade, J., and Leonard, A. C. (1992). Improved bacterial baby machine: application to *Escherichia coli* K-12. *J Bacteriol*, 174(11):3445–3449.

Hilbert, L., Albrecht, D., and Mackey, M. C. (2011). Small delay, big waves: a minimal delayed negative feedback model captures *Escherichia coli* single cell SOS kinetics. *Mol Biosyst*, 7(9):2599–2607.

Hishida, T., Han, Y.-W., Shibata, T., Kubota, Y., Ishino, Y., Iwasaki, H., and Shinagawa, H. (2004). Role of the *Escherichia coli* RecQ DNA helicase in SOS signaling and genome stabilization at stalled replication forks. *Genes Dev*, 18(15):1886–1897.

Hsieh, P., Camerini-Otero, C. S., and Camerini-Otero, R. D. (1992). The synapsis event in the homologous pairing of DNAs: RecA recognizes and pairs less than one helical repeat of DNA. *Proc Natl Acad Sci USA*, 89(14):6492–6496.

Hu, Y., Kwan, B. W., Osbourne, D. O., Benedik, M. J., and Wood, T. K. (2015). Toxin YafQ increases persister cell formation by reducing indole signalling. *Environ Microbiol*, 17(4):1275–1285.

Hui, M. P., Foley, P. L., and Belasco, J. G. (2014). Messenger RNA degradation in bacterial cells. *Annu Rev Genet*, 48(1):537–559.

Hui, S., Silverman, J. M., Chen, S. S., Erickson, D. W., Basan, M., Wang, J., Hwa, T., and Williamson, J. R. (2015). Quantitative proteomic analysis reveals a simple strategy of global resource allocation in bacteria. *Mol Syst Biol*, 11(1):784.

Huisman, O., D'Ari, R., and Casaregola, S. (1982). How *Escherichia coli* sets different basal levels in SOS operons. *Biochimie*, 64(8-9):709–712.

Huisman, O., D'Ari, R., and Gottesman, S. (1984). Cell-division control in *Escherichia coli*: specific induction of the SOS function SfiA protein is sufficient to block septation. *Proc Natl Acad Sci USA*, 81(14):4490–4494.

Iyer-Biswas, S. and Zilman, A. (2016). First-passage processes in cellular biology. In Rice, S. A. and Dinner, A. R., editors, *Advances in chemical physics*, Advances in chemical physics, pages 261–306. John Wiley & Sons, Inc, Hoboken, NJ.

Janion, C. (2008). Inducible SOS response system of DNA repair and mutagenesis in *Escherichia coli*. *Int J Biol Sci*, 4(6):338–344.

Jeong, K. S., Ahn, J., and Khodursky, A. B. (2004). Spatial patterns of transcriptional activity in the chromosome of *Escherichia coli*. *Genome Biol*, 5(11):R86.

Jiang, Q., Karata, K., Woodgate, R., Cox, M. M., and Goodman, M. F. (2009). The active form of DNA polymerase v is UmuD'(2)c-RecA-ATP. *Nature*, 460(7253):359–363.

Jun, S., Si, F., Pugatch, R., and Scott, M. (2018). Fundamental principles in bacterial physiology-history, recent progress, and the future with focus on cell size control: a review. *Rep Prog Phys*, 81(5):056601.

Kamenšek, S., Podlesek, Z., Gillor, O., and Zgur-Bertok, D. (2010). Genes regulated by the *Escherichia coli* SOS repressor LexA exhibit heterogeneous expression. *BMC microbiology*, 10(1):283.

Kawano, M., Aravind, L., and Storz, G. (2007). An antisense RNA controls synthesis of an SOS-induced toxin evolved from an antitoxin. *Mol Microbiol*, 64(3):738–754.

Keren, L., Zackay, O., Lotan-Pompan, M., Barenholz, U., Dekel, E., Sasson, V., Aidelberg, G., Bren, A., Zeevi, D., Weinberger, A., Alon, U., Milo, R., and Segal, E. (2013). Promoters maintain their relative activity levels under different growth conditions. *Mol Syst Biol*, 9:701.

Keseler, I. M., Mackie, A., Santos-Zavaleta, A., Billington, R., Bonavides-Martínez, C., Caspi, R., Fulcher, C., Gama-Castro, S., Kothari, A., Krummenacker, M., Latendresse, M., Muñiz-Rascado, L., Ong, Q., Paley, S., Peralta-Gil, M., Subhraveti, P., Velázquez-Ramírez, D. A., Weaver, D., Collado-Vides, J., Paulsen, I., and Karp, P. D. (2017). The EcoCyc database: reflecting new knowledge about *Escherichia coli* K-12. *Nucleic Acids Res*, 45(D1):D543–D550.

Keyamura, K., Sakaguchi, C., Kubota, Y., Niki, H., and Hishida, T. (2013). RecA protein recruits structural maintenance of chromosomes (SMC)-like RecN protein to DNA double-strand breaks. *J Biol Chem*, 288(41):29229–29237.

Khil, P. P. and Camerini-Otero, R. D. (2002). Over 1000 genes are involved in the DNA damage response of *Escherichia coli*. *Mol Microbiol*, 44(1):89–105.

Kirkpatrick, C. L., Martins, D., Redder, P., Frandi, A., Mignolet, J., Chapalay, J. B., Chambon, M., Turcatti, G., and Viollier, P. H. (2016). Growth control switch by a

DNA-damage-inducible toxin-antitoxin system in caulobacter crescentus. *Nat Microbiol*, 1:16008.

Klumpp, S. and Hwa, T. (2014). Bacterial growth: global effects on gene expression, growth feedback and proteome partition. *Curr Opin Biotechnol*, 28:96–102.

Klumpp, S., Zhang, Z., and Hwa, T. (2009). Growth rate-dependent global effects on gene expression in bacteria. *Cell*, 139(7):1366–1375.

Koch, A. L. and Schaechter, M. (1962). A model for statistics of the cell division process. *J Gen Microbiol*, 29:435–454.

Kohanski, M. A., Dwyer, D. J., and Collins, J. J. (2010). How antibiotics kill bacteria: from targets to networks. *Nat Rev Microbiol*, 8(6):423–435.

Kolodkin-Gal, I., Verdiger, R., Shlosberg-Fedida, A., and Engelberg-Kulka, H. (2009). A differential effect of e. coli toxin-antitoxin systems on cell death in liquid media and biofilm formation. *PLoS ONE*, 4(8):e6785.

Korem Kohanim, Y., Levi, D., Jona, G., Towbin, B. D., Bren, A., and Alon, U. (2018). A bacterial growth law out of steady state. *Cell Rep*, 23(10):2891–2900.

Kovačič, L., Paulič, N., Leonardi, A., Hodnik, V., Anderluh, G., Podlesek, Z., Žgur Bertok, D., Kriăj, I., and Butala, M. (2013). Structural insight into LexA-RecA* interaction. *Nucleic Acids Res*, 41(21):9901–9910.

Kreuzer, K. N. (2005). Interplay between DNA replication and recombination in prokaryotes. *Annu Rev Microbiol*, 59:43–67.

Kreuzer, K. N. (2013). DNA Damage Responses in Prokaryotes: Regulating Gene Expression, Modulating Growth Patterns, and Manipulating Replication Forks. *Cold Spring Harbor Perspectives in Biology*, 5(11).

Krishna, S., Maslov, S., and Sneppen, K. (2007). UV-induced mutagenesis in *Escherichia coli* SOS response: a quantitative model. *PLoS Comput Biol*, 3(3):e41.

Kurth, I. and O'Donnell, M. (2009). Replisome dynamics during chromosome duplication. *Ecosal Plus*, 2009.

Kussell, E. (2013). Evolution in microbes. *Annu Rev Biophys*, 42:493–514.

Kuzminov, A. (1999). Recombinational repair of DNA damage in *Escherichia coli* and bacteriophage lambda. *Microbiol Mol Biol Rev*, 63(4):751–813, table of contents.

Kuzminov, A. (2001). Single-strand interruptions in replicating chromosomes cause double-strand breaks. *Proc Natl Acad Sci USA*, 98(15):8241–8246.

Lambert, G. and Kussell, E. (2015). Quantifying selective pressures driving bacterial evolution using lineage analysis. *Phys. Rev. X*, 5:011016.

Laureti, L., Matic, I., and Gutierrez, A. (2013). Bacterial responses and genome instability induced by subinhibitory concentrations of antibiotics. *Antibiotics*, 2(1):100–114.

Lee, T. S. (1996). Image representation using 2D gabor wavelets. *IEEE Trans Pattern Anal Mach Intell*, 18(10):959–971.

Lemke, J. J., Sanchez-Vazquez, P., Burgos, H. L., Hedberg, G., Ross, W., and Gourse, R. L. (2011). Direct regulation of *Escherichia coli* ribosomal protein promoters by the transcription factors ppGpp and DksA. *Proc Natl Acad Sci USA*, 108(14):5712–5717.

Lesterlin, C., Ball, G., Schermelleh, L., and Sherratt, D. J. (2014). RecA bundles mediate homology pairing between distant sisters during DNA break repair. *Nature*, 506(7487):249–253.

Levin-Reisman, I., Ronin, I., Gefen, O., Braniss, I., Shoresh, N., and Balaban, N. Q. (2017). Antibiotic tolerance facilitates the evolution of resistance. *Science*, 355(6327):826–830.

Levy, S. B. and Marshall, B. (2004). Antibacterial resistance worldwide: causes, challenges and responses. *Nat Med*, 10(12 Suppl):S122–9.

Lewin, C. S. and Amyes, S. G. (1991). The role of the SOS response in bacteria exposed to zidovudine or trimethoprim. *J Med Microbiol*, 34(6):329–332.

Li, G.-W., Burkhardt, D., Gross, C., and Weissman, J. S. (2014). Quantifying absolute protein synthesis rates reveals principles underlying allocation of cellular resources. *Cell*, 157(3):624–635.

Lin, L. L. and Little, J. W. (1988). Isolation and characterization of noncleavable (ind-) mutants of the LexA repressor of *Escherichia coli* K-12. *J Bacteriol*, 170(5):2163–2173.

Little, J. W. (1991). Mechanism of specific LexA cleavage: autodigestion and the role of RecA coprotease. *Biochimie*, 73(4):411–421.

Little, J. W., Edmiston, S. H., Pacelli, L. Z., and Mount, D. W. (1980). Cleavage of the *Escherichia coli* lexA protein by the recA protease. *Proc Natl Acad Sci USA*, 77(6):3225–3229.

Liu, J., Gefen, O., and Balaban, N. Q. (2017). Tackling antibiotic resistance with systems-level perspective. *Cell Syst*, 5(6):546–548.

Liu, Y. and Imlay, J. A. (2013). Cell death from antibiotics without the involvement of reactive oxygen species. *Science*, 339(6124):1210–1213.

Lloyd, R. G. and Buckman, C. (1991). Genetic analysis of the recG locus of *Escherichia coli* K-12 and of its role in recombination and DNA repair. *J Bacteriol*, 173(3):1004–1011.

Lucarelli, D., Wang, Y. A., Galkin, V. E., Yu, X., Wigley, D. B., and Egelman, E. H. (2009). The RecB nuclease domain binds to RecA-DNA filaments: implications for filament loading. *J Mol Biol*, 391(2):269–274.

Lusetti, S. L., Drees, J. C., Stohl, E. A., Seifert, H. S., and Cox, M. M. (2004). The DinI and RecX proteins are competing modulators of RecA function. *J Biol Chem*, 279(53):55073–55079.

Lynch, M. and Marinov, G. K. (2015). The bioenergetic costs of a gene. *Proc Natl Acad Sci USA*, 112(51):15690–15695.

Maaløe, O. (1979). Regulation of the protein-synthesizing Machinery —Ribosomes, tRNA, factors, and so on. In Goldberger, R. F., editor, *Biological regulation and development*, pages 487–542. Springer US, Boston, MA.

Machuca, J., Recacha, E., Briales, A., Díaz-de Alba, P., Blazquez, J., Pascual, A., and Rodríguez-Martínez, J.-M. (2017). Cellular response to ciprofloxacin in low-level quinolone-resistant *Escherichia coli*. *Front Microbiol*, 8:1370.

Maharjan, R. P. and Ferenci, T. (2018). The impact of growth rate and environmental factors on mutation rates and spectra in escherichia coli. *Environ Microbiol Rep*, 10(6):626–633.

Markham, B. E., Harper, J. E., and Mount, D. W. (1985). Physiology of the SOS response: kinetics of lexA and recA transcriptional activity following induction. *Mol Gen Genet*, 198(2):207–212.

Marr, A. G. (1991). Growth rate of *Escherichia coli*. *Microbiol Rev*, 55(2):316–333.

Massoni, S. C., Leeson, M. C., Long, J. E., Gemme, K., Mui, A., and Sandler, S. J. (2012). Factors limiting SOS expression in log-phase cells of escherichia coli. *J Bacteriol*, 194(19):5325–5333.

Matic, I. (2017). Molecular mechanisms involved in the regulation of mutation rates in bacteria. *Period Biol*, 118(4):363–372.

Maturana, H. R. and Varela, F. J. (1980). On machines, living and otherwise. In Cohen, R. S. and Wartofsky, M. W., editors, *Autopoiesis and Cognition*, volume 42 of *Boston studies in the philosophy of science*, pages 77–84. Springer Netherlands, Dordrecht.

Mazin, A. V. and Kowalczykowski, S. C. (1996). The specificity of the secondary DNA binding site of RecA protein defines its role in DNA strand exchange. *Proc Natl Acad Sci USA*, 93(20):10673–10678.

Medawar, P. B. (1952). *An Unsolved Problem of Biology*. H. K. Lewis. London, UK.

Menetski, J. P., Bear, D. G., and Kowalczykowski, S. C. (1990). Stable DNA heteroduplex formation catalyzed by the *Escherichia coli* RecA protein in the absence of ATP hydrolysis. *Proc Natl Acad Sci USA*, 87(1):21–25.

Merlin, C., McAteer, S., and Masters, M. (2002). Tools for characterization of *Escherichia coli* genes of unknown function. *J Bacteriol*, 184(16):4573–4581.

Merrikh, H., Ferrazzoli, A. E., Bougdour, A., Olivier-Mason, A., and Lovett, S. T. (2009a). A DNA damage response in *Escherichia coli* involving the alternative sigma factor, RpoS. *Proc Natl Acad Sci USA*, 106(2):611–616.

Merrikh, H., Ferrazzoli, A. E., and Lovett, S. T. (2009b). Growth phase and (p)ppGpp control of IraD, a regulator of RpoS stability, in *Escherichia coli*. *J Bacteriol*, 191(24):7436–7446.

Micevski, D., Zammit, J. E., Truscott, K. N., and Dougan, D. A. (2015). Anti-adaptors use distinct modes of binding to inhibit the RssB-dependent turnover of RpoS (σ(s)) by ClpXP. *Front Mol Biosci*, 2:15.

Michel, B., Grompone, G., Florès, M.-J., and Bidnenko, V. (2004). Multiple pathways process stalled replication forks. *Proc Natl Acad Sci USA*, 101(35):12783–12788.

Michel, B. and Leach, D. (2012). Homologous recombination-enzymes and pathways. *Ecosal Plus*, 5(1).

Michel, B., Sinha, A. K., and Leach, D. R. F. (2018). Replication fork breakage and restart in *Escherichia coli*. *Microbiol Mol Biol Rev*, 82(3).

Michelsen, O., Teixeira de Mattos, M. J., Jensen, P. R., and Hansen, F. G. (2003). Precise determinations of c and d periods by flow cytometry in *Escherichia coli* K-12 and B/r. *Microbiology (Reading, Engl)*, 149(Pt 4):1001–1010.

Miller, C., Ingmer, H., Thomsen, L. E., Skarstad, K., and Cohen, S. N. (2003). DpiA binding to the replication origin of *Escherichia coli* plasmids and chromosomes destabilizes plasmid inheritance and induces the bacterial SOS response. *J Bacteriol*, 185(20):6025–6031.

Miller, C., Thomsen, L. E., Gaggero, C., Mosseri, R., Ingmer, H., and Cohen, S. N. (2004). SOS response induction by beta-lactams and bacterial defense against antibiotic lethality. *Science*, 305(5690):1629–1631.

Mitosch, K., Rieckh, G., and Bollenbach, T. (2017). Noisy response to antibiotic stress predicts subsequent single-cell survival in an acidic environment. *Cell Syst*, 4(4):393–403.e5.

Mo, C. Y., Manning, S. A., Roggiani, M., Culyba, M. J., Samuels, A. N., Sniegowski, P. D., Goulian, M., and Kohli, R. M. (2016). Systematically altering bacterial SOS activity under stress reveals therapeutic strategies for potentiating antibiotics. *mSphere*, 1(4).

Monod, J. (1949). The Growth of Bacterial Cultures. *Annual Review of Microbiology*, 3(1):371–394.

Mount, D. W., Low, K. B., and Edmiston, S. J. (1972). Dominant mutations (lex) in *Escherichia coli* K-12 which affect radiation sensitivity and frequency of ultraviolet lght-induced mutations. *J Bacteriol*, 112(2):886–893.

Murray, K. D. and Bremer, H. (1996). Control of spoT-dependent ppGpp synthesis and degradation in *Escherichia coli*. *J Mol Biol*, 259(1):41–57.

Myhrvold, C., Kotula, J. W., Hicks, W. M., Conway, N. J., and Silver, P. A. (2015). A distributed cell division counter reveals growth dynamics in the gut microbiota. *Nat Commun*, 6:10039.

Nazir, A. and Harinarayanan, R. (2015). Inactivation of cell division protein FtsZ by SulA makes lon indispensable for the viability of a ppGpp0 strain of *Escherichia coli*. *J Bacteriol*, 198(4):688–700.

Ni, M., Yang, L., Liu, X.-L., and Qi, O. (2008). Fluence-response dynamics of the UV-induced SOS response in *Escherichia coli*. *Curr Microbiol*, 57(6):521–526.

Nichols, R. J., Sen, S., Choo, Y. J., Beltrao, P., Zietek, M., Chaba, R., Lee, S., Kazmierczak, K. M., Lee, K. J., Wong, A., Shales, M., Lovett, S., Winkler, M. E., Krogan, N. J., Typas, A., and Gross, C. A. (2011). Phenotypic landscape of a bacterial cell. *Cell*, 144(1):143–156.

Odsbu, I. and Skarstad, K. (2014). DNA compaction in the early part of the SOS response is dependent on RecN and RecA. *Microbiology (Reading, Engl)*, 160(Pt 5):872–882.

Okumus, B., Baker, C. J., Arias-Castro, J. C., Lai, G. C., Leoncini, E., Bakshi, S., Luro, S., Landgraf, D., and Paulsson, J. (2018). Single-cell microscopy of suspension cultures using a microfluidics-assisted cell screening platform. *Nat Protoc*, 13(1):170–194.

Okumus, B., Landgraf, D., Lai, G. C., Bakhsi, S., Arias-Castro, J. C., Yildiz, S., Huh, D., Fernandez-Lopez, R., Peterson, C. N., Toprak, E., El Karoui, M., and Paulsson, J. (2016). Mechanical slowing-down of cytoplasmic diffusion allows in vivo counting of proteins in individual cells. *Nat Commun*, 7:11641.

Painter, P. R. and Marr, A. G. (1968). Mathematics of microbial populations. *Annu Rev Microbiol*, 22:519–548.

Patange, O., Schwall, C., Jones, M., Villava, C., Griffith, D. A., Phillips, A., and Locke, J. C. W. (2018). Escherichia coli can survive stress by noisy growth modulation. *Nat Commun*, 9(1):5333.

Patra, P. and Klumpp, S. (2013). Population dynamics of bacterial persistence. *PLoS ONE*, 8(5):e62814.

Paul, B. J., Berkmen, M. B., and Gourse, R. L. (2005). DksA potentiates direct activation of amino acid promoters by ppGpp. *Proc Natl Acad Sci USA*, 102(22):7823–7828.

Paul, B. J., Ross, W., Gaal, T., and Gourse, R. L. (2004). rRNA transcription in *Escherichia coli*. *Annu Rev Genet*, 38:749–770.

Pennington, J. M. and Rosenberg, S. M. (2007). Spontaneous DNA breakage in single living escherichia coli cells. *Nat Genet*, 39(6):797–802.

Petrova, V., Chitteni-Pattu, S., Drees, J. C., Inman, R. B., and Cox, M. M. (2009). An SOS inhibitor that binds to free RecA protein: the PsiB protein. *Mol Cell*, 36(1):121–130.

Piddock, L. J., Jin, Y. F., Ricci, V., and Asuquo, A. E. (1999). Quinolone accumulation by *Pseudomonas aeruginosa*, *Staphylococcus aureus* and *Escherichia coli*. *J Antimicrob Chemother*, 43(1):61–70.

Pohlhaus, J. R. and Kreuzer, K. N. (2005). Norfloxacin-induced DNA gyrase cleavage complexes block *Escherichia coli* replication forks, causing double-stranded breaks in vivo. *Mol Microbiol*, 56(6):1416–1429.

Potrykus, K., Murphy, H., Philippe, N., and Cashel, M. (2011). ppGpp is the major source of growth rate control in e. coli. *Environ Microbiol*, 13(3):563–575.

Potvin-Trottier, L., Luro, S., and Paulsson, J. (2018). Microfluidics and single-cell microscopy to study stochastic processes in bacteria. *Current Opinion in Microbiology*, 43:186–192.

Powell, E. O. (1956). Growth Rate and Generation Time of Bacteria, with Special Reference to Continuous Culture. *Microbiology*, 15:492–511.

Pribis, J. P., Garcia-Villada, L., Zhai, Y., Lewin-Epstein, O., Wang, A., Liu, J., Xia, J., Mei, Q., Fitzgerald, D. M., Bos, J., Austin, R., Herman, C., Bates, D., Hadany, L., Hastings, P., and Rosenberg, S. M. (2018). Gamblers: an antibiotic-induced evolvable cell subpopulation differentiated by reactive-oxygen-induced general stress response. *bioRxiv*.

Prysak, M. H., Mozdzierz, C. J., Cook, A. M., Zhu, L., Zhang, Y., Inouye, M., and Woychik, N. A. (2009). Bacterial toxin YafQ is an endoribonuclease that associates with the ribosome and blocks translation elongation through sequence-specific and frame-dependent mRNA cleavage. *Mol Microbiol*, 71(5):1071–1087.

Pugatch, R. (2015). Greedy scheduling of cellular self-replication leads to optimal doubling times with a log-frechet distribution. *Proc Natl Acad Sci USA*, 112(8):2611–2616.

Radman, M. (1975). SOS repair hypothesis: phenomenology of an inducible DNA repair which is accompanied by mutagenesis. In Hanawalt, P. C. and Setlow, R. B., editors, *Molecular mechanisms for repair of DNA*, pages 355–367. Springer US, Boston, MA.

Radzikowski, J. L., Schramke, H., and Heinemann, M. (2017). Bacterial persistence from a system-level perspective. *Curr Opin Biotechnol*, 46:98–105.

Ragone, S., Maman, J. D., Furnham, N., and Pellegrini, L. (2008). Structural basis for inhibition of homologous recombination by the RecX protein. *EMBO J*, 27(16):2259–2269.

Rang, C. U., Proenca, A., Buetz, C., Shi, C., and Chao, L. (2018). Minicells as a damage disposal mechanism in escherichia coli. *mSphere*, 3(5).

Rao, P., Rozgaja, T. A., Alqahtani, A., Grimwade, J. E., and Leonard, A. C. (2018). Low affinity DnaA-ATP recognition sites in e. coli oriC make non-equivalent and growth rate-dependent contributions to the regulated timing of chromosome replication. *Front Microbiol*, 9:1673.

Raser, J. M. and O'Shea, E. K. (2005). Noise in gene expression: origins, consequences, and control. *Science*, 309(5743):2010–2013.

Rehrauer, W. M., Lavery, P. E., Palmer, E. L., Singh, R. N., and Kowalczykowski, S. C. (1996). Interaction of *Escherichia coli* RecA protein with LexA repressor. i. LexA repressor cleavage is competitive with binding of a secondary DNA molecule. *J Biol Chem*, 271(39):23865–23873.

Renzette, N., Gumlaw, N., Nordman, J. T., Krieger, M., Yeh, S.-P., Long, E., Centore, R., Boonsombat, R., and Sandler, S. J. (2005). Localization of RecA in *Escherichia coli* K-12 using RecA-GFP. *Mol Microbiol*, 57(4):1074–1085.

Renzette, N., Gumlaw, N., and Sandler, S. J. (2007). DinI and RecX modulate RecA-DNA structures in *Escherichia coli* K-12. *Mol Microbiol*, 63(1):103–115.

Renzette, N. and Sandler, S. J. (2008). Requirements for ATP binding and hydrolysis in RecA function in *Escherichia coli*. *Mol Microbiol*, 67(6):1347–1359.

Reyes-Lamothe, R., Nicolas, E., and Sherratt, D. J. (2012). Chromosome replication and segregation in bacteria. *Annu Rev Genet*, 46:121–143.

Robert, L., Ollion, J., Robert, J., Song, X., Matic, I., and Elez, M. (2018). Mutation dynamics and fitness effects followed in single cells. *Science*, 359(6381):1283–1286.

Robinson, A., McDonald, J. P., Caldas, V. E. A., Patel, M., Wood, E. A., Punter, C. M., Ghodke, H., Cox, M. M., Woodgate, R., Goodman, M. F., and van Oijen, A. M. (2015). Regulation of mutagenic DNA polymerase v activation in space and time. *PLoS Genet*, 11(8):e1005482.

Rocha, E. P. (2008). The Organization of the Bacterial Genome. *Annual Review of Genetics*, 42(1):211–233. PMID: 18605898.

Rocha, E. P. C., Cornet, E., and Michel, B. (2005). Comparative and evolutionary analysis of the bacterial homologous recombination systems. *PLoS Genet*, 1(2):e15.

Rodnina, M. V. (2018). Translation in prokaryotes. *Cold Spring Harb Perspect Biol*.

Rodríguez-Beltrán, J., Rodríguez-Rojas, A., Guelfo, J. R., Couce, A., and Blázquez, J. (2012). The *Escherichia coli* SOS gene dinF protects against oxidative stress and bile salts. *PLoS ONE*, 7(4):e34791.

Roncarati, D. and Scarlato, V. (2017). Regulation of heat-shock genes in bacteria: from signal sensing to gene expression output. *FEMS Microbiol Rev*, 41(4):549–574.

Rooney, J. P., George, A. D., Patil, A., Begley, U., Bessette, E., Zappala, M. R., Huang, X., Conklin, D. S., Cunningham, R. P., and Begley, T. J. (2009). Systems based mapping demonstrates that recovery from alkylation damage requires DNA repair, RNA processing, and translation associated networks. *Genomics*, 93(1):42–51.

Rosenfeld, N., Elowitz, M. B., and Alon, U. (2002). Negative autoregulation speeds the response times of transcription networks. *J Mol Biol*, 323(5):785–793.

Rosenthal, K., Oehling, V., Dusny, C., and Schmid, A. (2017). Beyond the bulk: disclosing the life of single microbial cells. *FEMS Microbiol Rev*, 41(6):751–780.

Rotman, E., Amado, L., and Kuzminov, A. (2010). Unauthorized horizontal spread in the laboratory environment: the tactics of lula, a temperate lambdoid bacteriophage of *Escherichia coli*. *PLoS ONE*, 5(6):e11106.

Rovinskiy, N., Agbleke, A. A., Chesnokova, O., Pang, Z., and Higgins, N. P. (2012). Rates of gyrase supercoiling and transcription elongation control supercoil density in a bacterial chromosome. *PLoS Genet*, 8(8):e1002845.

Ruangprasert, A., Maehigashi, T., Miles, S. J., Giridharan, N., Liu, J. X., and Dunham, C. M. (2014). Mechanisms of toxin inhibition and transcriptional repression by *Escherichia coli* DinJ-YafQ. *J Biol Chem*, 289(30):20559–20569.

Rudolph, C. J., Upton, A. L., Stockum, A., Nieduszynski, C. A., and Lloyd, R. G. (2013). Avoiding chromosome pathology when replication forks collide. *Nature*, 500(7464):608–611.

Sahu, S. N., Acharya, S., Tuminaro, H., Patel, I., Dudley, K., LeClerc, J. E., Cebula, T. A., and Mukhopadhyay, S. (2003). The bacterial adaptive response gene, barA, encodes a novel conserved histidine kinase regulatory switch for adaptation and modulation of metabolism in *Escherichia coli*. *Mol Cell Biochem*, 253(1-2):167–177.

Saier, M. H., Reddy, V. S., Tsu, B. V., Ahmed, M. S., Li, C., and Moreno-Hagelsieb, G. (2016). The transporter classification database (TCDB): recent advances. *Nucleic Acids Res*, 44(D1):D372–9.

Sakai, A. and Cox, M. M. (2009). RecFOR and RecOR as distinct RecA loading pathways. *J Biol Chem*, 284(5):3264–3272.

Schaechter, M. (2006). From growth physiology to systems biology. *Int Microbiol*, 9(3):157–161.

Schaechter, M., Maaloe, O., and Kjeldgaard, N. O. (1958). Dependency on medium and temperature of cell size and chemical composition during balanced grown of *Salmonella typhimurium*. *J Gen Microbiol*, 19(3):592–606.

Schneider, D. A. and Gourse, R. L. (2003). Changes in *Escherichia coli* rRNA promoter activity correlate with changes in initiating nucleoside triphosphate and guanosine 5' diphosphate 3'-diphosphate concentrations after induction of feedback control of ribosome synthesis. *J Bacteriol*, 185(20):6185–6191.

Schneider, D. A. and Gourse, R. L. (2004). Relationship between growth rate and ATP concentration in *Escherichia coli*: a bioassay for available cellular ATP. *J Biol Chem*, 279(9):8262–8268.

Schroeder, J. W., Yeesin, P., Simmons, L. A., and Wang, J. D. (2018). Sources of spontaneous mutagenesis in bacteria. *Crit Rev Biochem Mol Biol*, 53(1):29–48.

Scott, M., Gunderson, C. W., Mateescu, E. M., Zhang, Z., and Hwa, T. (2010). Interdependence of cell growth and gene expression: Origins and consequences. *Science*, 330(6007):1099–1102.

Shereda, R. D., Kozlov, A. G., Lohman, T. M., Cox, M. M., and Keck, J. L. (2008). SSB as an organizer/mobilizer of genome maintenance complexes. *Crit Rev Biochem Mol Biol*, 43(5):289–318.

Shimoni, Y., Altuvia, S., Margalit, H., and Biham, O. (2009). Stochastic analysis of the SOS response in *Escherichia coli*. *PLoS ONE*, 4(5):e5363.

Shinar, G., Milo, R., Martínez, M. R., and Alon, U. (2007). Input output robustness in simple bacterial signaling systems. *Proc Natl Acad Sci USA*, 104(50):19931–19935.

Shun-Mei, E., Zeng, J.-M., Yuan, H., Lu, Y., Cai, R.-X., and Chen, C. (2017). Sub-inhibitory concentrations of fluoroquinolones increase conjugation frequency. *Microb Pathog*, 114:57–62.

Si, F., Li, D., Cox, S. E., Sauls, J. T., Azizi, O., Sou, C., Schwartz, A. B., Erickstad, M. J., Jun, Y., Li, X., and Jun, S. (2017). Invariance of initiation mass and predictability of cell size in *Escherichia coli*. *Curr Biol*, 27(9):1278–1287.

Sinha, A. K., Durand, A., Desfontaines, J.-M., Iurchenko, I., Auger, H., Leach, D. R. F., Barre, F.-X., and Michel, B. (2017). Division-induced DNA double strand breaks in the chromosome terminus region of *Escherichia coli* lacking RecBCD DNA repair enzyme. *PLoS Genet*, 13(10):e1006895.

Skarstad, K. and Katayama, T. (2013). Regulating DNA Replication in Bacteria. *Cold Spring Harbor Perspectives in Biology*, 5(4).

Smith, G. R. (2012). How RecBCD enzyme and chi promote DNA break repair and recombination: a molecular biologist's view. *Microbiol Mol Biol Rev*, 76(2):217–228.

St-Pierre, F., Cui, L., Priest, D. G., Endy, D., Dodd, I. B., and Shearwin, K. E. (2013). One-Step Cloning and Chromosomal Integration of DNA. *ACS Synthetic Biology*, 2(9):537–541. PMID: 24050148.

Stevenson, K., McVey, A. F., Clark, I. B. N., Swain, P. S., and Pilizota, T. (2016). General calibration of microbial growth in microplate readers. *Sci Rep*, 6:38828.

Stohl, E. A., Brockman, J. P., Burkle, K. L., Morimatsu, K., Kowalczykowski, S. C., and Seifert, H. S. (2003). *Escherichia coli* RecX inhibits RecA recombinase and coprotease activities in vitro and in vivo. *J Biol Chem*, 278(4):2278–2285.

Stokke, C., Flåtten, I., and Skarstad, K. (2012). An easy-to-use simulation program demonstrates variations in bacterial cell cycle parameters depending on medium and temperature. *PLoS ONE*, 7(2):e30981.

Storvik, K. A. M. and Foster, P. L. (2010). RpoS, the stress response sigma factor, plays a dual role in the regulation of *Escherichia coli*'s error-prone DNA polymerase IV. *J Bacteriol*, 192(14):3639–3644.

Stouf, M., Meile, J.-C., and Cornet, F. (2013). FtsK actively segregates sister chromosomes in *Escherichia coli*. *Proc Natl Acad Sci USA*, 110(27):11157–11162.

Sufya, N., Allison, D. G., and Gilbert, P. (2003). Clonal variation in maximum specific growth rate and susceptibility towards antimicrobials. *J Appl Microbiol*, 95(6):1261–1267.

Sutera, V. A. and Lovett, S. T. (2006). The role of replication initiation control in promoting survival of replication fork damage. *Mol Microbiol*, 60(1):229–239.

Suzuki, K., Wang, X., Weilbacher, T., Pernestig, A.-K., Melefors, O., Georgellis, D., Babitzke, P., and Romeo, T. (2002). Regulatory circuitry of the CsrA/CsrB and BarA/UvrY systems of *Escherichia coli*. *J Bacteriol*, 184(18):5130–5140.

Szekely, P., Sheftel, H., Mayo, A., and Alon, U. (2013). Evolutionary tradeoffs between economy and effectiveness in biological homeostasis systems. *PLoS Comput Biol*, 9(8):e1003163.

Tadmor, A. D. and Tlusty, T. (2008). A Coarse-Grained Biophysical Model of *E. coli* and its Application to Perturbation of the rRNA Operon Copy Number. *PLoS Comput Biol*, 4(5):e1000038.

Taheri-Araghi, S., Brown, S. D., Sauls, J. T., McIntosh, D. B., and Jun, S. (2015). Single-Cell Physiology. *Annual Review of Biophysics*, 44(1):123–142. PMID: 25747591.

Tan, C., Marguet, P., and You, L. (2009). Emergent bistability by a growth-modulating positive feedback circuit. *Nat Chem Biol*, 5(11):842–848.

Thomas, P. (2017). Making sense of snapshot data: ergodic principle for clonal cell populations. *J R Soc Interface*, 14(136).

Thomas, P. (2019). Intrinsic and extrinsic noise of gene expression in lineage trees. *Sci Rep*, 9(1):474.

Tonthat, N. K., Arold, S. T., Pickering, B. F., Van Dyke, M. W., Liang, S., Lu, Y., Beuria, T. K., Margolin, W., and Schumacher, M. A. (2011). Molecular mechanism by which the nucleoid occlusion factor, SlmA, keeps cytokinesis in check. *EMBO J*, 30(1):154–164.

Touchon, M., Hoede, C., Tenaillon, O., Barbe, V., Baeriswyl, S., Bidet, P., Bingen, E., Bonacorsi, S., Bouchier, C., Bouvet, O., Calteau, A., Chiapello, H., Clermont, O., Cruveiller, S., Danchin, A., Diard, M., Dossat, C., Karoui, M. E., Frapy, E., Garry, L., Ghigo, J. M., Gilles, A. M., Johnson, J., Le Bouguénec, C., Lescat, M., Mangenot, S., Martinez-Jéhanne, V., Matic, I., Nassif, X., Oztas, S., Petit, M. A., Pichon, C., Rouy, Z., Ruf, C. S., Schneider, D., Tourret, J., Vacherie, B., Vallenet, D., Médigue, C., Rocha, E. P. C., and Denamur, E. (2009). Organised genome dynamics in the *Escherichia coli* species results in highly diverse adaptive paths. *PLoS Genet*, 5(1):e1000344.

Uphoff, S. (2018). Real-time dynamics of mutagenesis reveal the chronology of DNA repair and damage tolerance responses in single cells. *Proc Natl Acad Sci USA*, 115(28):E6516–E6525.

Uranga, L. A., Reyes, E. D., Patidar, P. L., Redman, L. N., and Lusetti, S. L. (2017). The cohesin-like RecN protein stimulates RecA-mediated recombinational repair of DNA double-strand breaks. *Nat Commun*, 8:15282.

Vaisman, A., McDonald, J. P., and Woodgate, R. (2012). Translesion DNA synthesis. *Ecosal Plus*, 5(1).

Van Kampen, N. (2007). CHEMICAL REACTIONS. In *Stochastic processes in physics and chemistry*, pages 166–192. Elsevier.

Veaute, X., Delmas, S., Selva, M., Jeusset, J., Le Cam, E., Matic, I., Fabre, F., and Petit, M.-A. (2005). UvrD helicase, unlike rep helicase, dismantles RecA nucleoprotein filaments in *Escherichia coli*. *EMBO J*, 24(1):180–189.

Veening, J.-W., Smits, W. K., and Kuipers, O. P. (2008). Bistability, epigenetics, and bet-hedging in bacteria. *Annu Rev Microbiol*, 62:193–210.

Vickridge, E., Planchenault, C., Cockram, C., Junceda, I. G., and Espéli, O. (2017). Management of e. coli sister chromatid cohesion in response to genotoxic stress. *Nat Commun*, 8:14618.

Voloshin, O. N., Vanevski, F., Khil, P. P., and Camerini-Otero, R. D. (2003). Characterization of the DNA damage-inducible helicase DinG from *Escherichia coli*. *J Biol Chem*, 278(30):28284–28293.

von Stockar, U. and Liu, J.-S. (1999). Does microbial life always feed on negative entropy? thermodynamic analysis of microbial growth. *Biochimica et Biophysica Acta (BBA) - Bioenergetics*, 1412(3):191–211.

Wade, J. T., Reppas, N. B., Church, G. M., and Struhl, K. (2005). Genomic analysis of LexA binding reveals the permissive nature of the *Escherichia coli* genome and identifies unconventional target sites. *Genes Dev*, 19(21):2619–2630.

Wang, L. and Lutkenhaus, J. (1998). FtsK is an essential cell division protein that is localized to the septum and induced as part of the SOS response. *Mol Microbiol*, 29(3):731–740.

Wang, P., Robert, L., Pelletier, J., Dang, W. L., Taddei, F., Wright, A., and Jun, S. (2010). Robust growth of *Escherichia coli*. *Current biology : CB*, 20(12):1099–1103.

Wang, Q. P. and Kaguni, J. M. (1989). dnaA protein regulates transcriptions of the rpoH gene of *Escherichia coli*. *J Biol Chem*, 264(13):7338–7344.

Washburn, R. S. and Gottesman, M. E. (2015). Regulation of transcription elongation and termination. *Biomolecules*, 5(2):1063–1078.

Webb, S., Hector, R. D., Kudla, G., and Granneman, S. (2014). PAR-CLIP data indicate that nrd1-nab3-dependent transcription termination regulates expression of hundreds of protein coding genes in yeast. *Genome Biol*, 15(1):R8.

Weber, H., Polen, T., Heuveling, J., Wendisch, V. F., and Hengge, R. (2005). Genome-wide analysis of the general stress response network in *Escherichia coli*: sigmaS-dependent genes, promoters, and sigma factor selectivity. *J Bacteriol*, 187(5):1591–1603.

Weel-Sneve, R., Kristiansen, K. I., Odsbu, I., Dalhus, B., Booth, J., Rognes, T., Skarstad, K., and Bjøråas, M. (2013). Single transmembrane peptide DinQ modulates membrane-dependent activities. *PLoS Genet*, 9(2):e1003260.

Wehrens, M., Ershov, D., Rozendaal, R., Walker, N., Schultz, D., Kishony, R., Levin, P. A., and Tans, S. J. (2018). Size laws and division ring dynamics in filamentous *Escherichia coli* cells. *Curr Biol*, 28(6):972–979.e5.

Weiße, A. Y., Oyarzún, D. A., Danos, V., and Swain, P. S. (2015). Mechanistic links between cellular trade-offs, gene expression, and growth. *Proceedings of the National Academy of Sciences*, 112(9):E1038–E1047.

Wentzell, L. M. and Maxwell, A. (2000). The complex of DNA gyrase and quinolone drugs on DNA forms a barrier to the t7 DNA polymerase replication complex. *J Mol Biol*, 304(5):779–791.

West, S. C. (1997). Processing of recombination intermediates by the RuvABC proteins. *Annu Rev Genet*, 31:213–244.

White, M. A., Azeroglu, B., Lopez-Vernaza, M. A., Hasan, A. M. M., and Leach, D. R. F. (2018). RecBCD coordinates repair of two ends at a DNA double-strand break, preventing aberrant chromosome amplification. *Nucleic Acids Res*, 46(13):6670–6682.

Willis, L. and Huang, K. C. (2017). Sizing up the bacterial cell cycle. *Nat Rev Microbiol*, 15(10):606–620.

Wimberly, H., Shee, C., Thornton, P. C., Sivaramakrishnan, P., Rosenberg, S. M., and Hastings, P. J. (2013). R-loops and nicks initiate DNA breakage and genome instability in non-growing escherichia coli. *Nat Commun*, 4:2115.

Wohlleben, W., Mast, Y., Stegmann, E., and Ziemert, N. (2016). Antibiotic drug discovery. *Microb Biotechnol*, 9(5):541–548.

Wu, N., He, L., Cui, P., Wang, W., Yuan, Y., Liu, S., Xu, T., Zhang, S., Wu, J., Zhang, W., and Zhang, Y. (2015). Ranking of persister genes in the same *Escherichia coli* genetic background demonstrates varying importance of individual persister genes in tolerance to different antibiotics. *Front Microbiol*, 6:1003.

Wu, W. F., Zhou, Y., and Gottesman, S. (1999). Redundant in vivo proteolytic activities of *Escherichia coli* lon and the ClpYQ (HslUV) protease. *J Bacteriol*, 181(12):3681–3687.

Wurihan, W., GeZi, G., Brambilla, E., Wang, S., Sun, H., Fan, L., Shi, Y., Sclavi, B., and Morigen, M. (2018). DnaA and LexA proteins regulate transcription of the uvrB gene in *Escherichia coli*: the role of DnaA in the control of the SOS regulon. *Frontiers in Microbiology*.

Xiao, H., Kalman, M., Ikehara, K., Zemel, S., Glaser, G., and Cashel, M. (1991). Residual guanosine 3',5'-bispyrophosphate synthetic activity of relA null mutants can be eliminated by spoT null mutations. *J Biol Chem*, 266(9):5980–5990.

Yasuda, T., Morimatsu, K., Horii, T., Nagata, T., and Ohmori, H. (1998). Inhibition of *Escherichia coli* RecA coprotease activities by DinI. *EMBO J*, 17(11):3207–3216.

Yasuda, T., Morimatsu, K., Kato, R., Usukura, J., Takahashi, M., and Ohmori, H. (2001). Physical interactions between DinI and RecA nucleoprotein filament for the regulation of SOS mutagenesis. *EMBO J*, 20(5):1192–1202.

Yoshimasu, M., Aihara, H., Ito, Y., Rajesh, S., Ishibe, S., Mikawa, T., Yokoyama, S., and Shibata, T. (2003). An NMR study on the interaction of *Escherichia coli* DinI with RecA-ssDNA complexes. *Nucleic Acids Res*, 31(6):1735–1743.

Yu, X. and Egelman, E. H. (1993). The LexA repressor binds within the deep helical groove of the activated RecA filament. *J Mol Biol*, 231(1):29–40.

Zaslaver, A., Bren, A., Ronen, M., Itzkovitz, S., Kikoin, I., Shavit, S., Liebermeister, W., Surette, M. G., and Alon, U. (2006). A comprehensive library of fluorescent transcriptional reporters for *Escherichia coli*. *Nat Meth*, 3(8):623–628.

Zhang, X., Liu, Y., Genereux, J. C., Nolan, C., Singh, M., and Kelly, J. W. (2014). Heat-shock response transcriptional program enables high-yield and high-quality recombinant protein production in *Escherichia coli*. *ACS Chem Biol*, 9(9):1945–1949.

Zhang, Y., Yamaguchi, Y., and Inouye, M. (2009). Characterization of YafO, an *Escherichia coli* toxin. *J Biol Chem*, 284(38):25522–25531.

Zhao, X., Malik, M., Chan, N., Drlica-Wagner, A., Wang, J.-Y., Li, X., and Drlica, K. (2006). Lethal action of quinolones against a temperature-sensitive dnaB replication mutant of *Escherichia coli*. *Antimicrob Agents Chemother*, 50(1):362–364.